The Contribution of Mitochondrial Calcium Homeostasis in Agonist-Induced Platelet Responses

By

DURRE SHEHWAR

Department of Biochemistry
Faculty of Biological Sciences
Quaid-i-Azam University

Islamabad, Pakistan

2024

The Contribution of Mitochondrial Calcium Homeostasis in Agonist-Induced Platelet Responses

A thesis submitted in partial fulfillment of the requirements for

the degree of

Doctorate of Philosophy

in

Biochemistry/Molecular Biology

By

DURRE SHEHWAR

Department of Biochemistry

Faculty of Biological Sciences

Quaid-i-Azam University

Islamabad, Pakistan

2024

Author's Declaration

I **Durre Shehwar** hereby state that my PhD thesis, *titled* "**The Contribution of Mitochondrial Calcium Homeostasis in Agonist-Induced Platelet Responses**" is my own work and has not been submitted previously by me for taking any degree from

Department of Biochemistry, Faculty of Biological Sciences, Quaid-i-Azam University, Islamabad, Pakistan.

Or anywhere else in the country/world.

At any time if my statement is found to be incorrect even after my graduation, the University has the right to withdraw my Ph.D degree.

Student/Author Signature: _____

Ms. Durre Shehwar
Date: *October 1, 2024*

Plagiarism Undertaking

I solemnly declare that research work presented in the PhD thesis, titled **"The Contribution of Mitochondrial Calcium Homeostasis in Agonist-Induced Platelet Responses"** is solely my research work with no significant contribution from any other person. Small contribution/help wherever taken has been duly acknowledged and that complete thesis has been written by me.

I understand the zero-tolerance policy of the HEC and **Quaid-i-Azam University, Islamabad,** towards the plagiarism. Therefore, I as an Author of the above titled thesis declare that no portion of my thesis has been plagiarized and any material used as reference is properly referred/cited.

I undertake that if I am found guilty of any formal plagiarism in the above titled thesis even after award of PhD degree, the University reserves the right to withdraw/revoke my PhD degree and that HEC and the University has the right to publish my name on the HEC/University website on which names of students are placed who submitted plagiarized thesis.

Student/Author Signature: _____

Ms. Durre Shehwar
Date: *October 1, 2024*

Certificate of Approval

This is to certify that the research work presented in this thesis, entitled: "The Contribution of Mitochondrial Calcium Homeostasis in Agonist-Induced Platelet Responses" was conducted by **Ms. Durre Shehwar** under the supervision of Dr. Muhammad Rizwan Alam.

No part of this thesis has been submitted anywhere else for any other degree. This thesis is submitted to the Department of Biochemistry, Faculty of Biological Sciences, Quaid-i-Azam University, Islamabad, Pakistan in partial fulfillment of the requirements for the **Degree of Doctor of Philosophy** in the field of Biochemistry from Department of Biochemistry, Faculty of Biological Sciences, Quaid-i-Azam University, Islamabad, Pakistan.

Ms. Durre Shehwar   Signature: _____

Examination Committee:

1. **External Examiner:**   Signature: _____
    Dr. Muhammad Sheeraz Ahmad
    Associate Professor
    Department of Biochemistry
    PMAS Arid Agriculture University, Rawalpindi

2. **External Examiner:**   Signature: _____
    Dr. Muhammad Jadoon Khan
    Associate Professor
    Department of Biosciences
    COMSATS University Islamabad

3. **Supervisor:**   Signature: _____
    Dr. M. Rizwan Alam

4. **Chairperson:**   Signature: _____
    Prof. Dr. Samina Shakeel

Dated: _____   01-10-2024

Dedicated

To

My forever loving

Parents

Acknowledgement

All praise and thanks to ALLAH, the most Merciful and Beneficent, Who has blessed me with courage and motivation to achieve my goals. He, who is the Creator of the universe has blessed the man with knowledge and wisdom to understand the laws of nature and to explore the beauty of life.

First of all, I am very obliged to my PhD advisor Dr Muhammad Rizwan Alam for giving me a chance to work in his lab. I would like to express my deepest gratitude for his mentorship, kindness, humanity, and immense knowledge and wisdom in the field of Cell Biology, which has always been an inspiration for me. His enthusiasm and curiosity of new findings has opened a new ways of motivation in the world of research. I am very obliged for his consistent support, guidance and giving me life time gifts for my professional career. It was a wonderful experience to work under Dr Rizwan's supervision and my PhD journey will always remain a golden period in my memory.

I am very grateful to Dr Muhammad Ansar for his continuous support and facilitating me for my research. I am very thankful to Chairperson Dr Iram Murtaza for extending research facility of the department to accomplish this research work.

I am very thankful to Higher Education Commission (HEC) Pakistan for providing me with International Research Support Initiative Programme (IRSIP) fellow to facilitate my visit to University of Lausanne (UNIL) in order to complete my research work.

I can't thank enough to my foreign supervisor Dr. Lorenzo Alberio from University Hospital Lausanne (CHUV), University of Lausanne (UNIL) Switzerland for accommodating me in his lab and providing me with the state of the art facilities for my research. His guidance and support has fine-tuned my research skills and his wide knowledge on platelets and hemostasis has greatly helped me in accomplishing my thesis. Thank you for providing me an opportunity to interact internationally. I pay my sincere gratitude to my foreign colleagues Debora, Alessandro, Lucas and Cindy for giving me conducive environment in their lab. Their suggestions and skillful opinions has always improved my knowledge and skills. Besides, their helping hands in my research I am very thankful for their kindness and warm welcome, thank you for all the good times, for accompanying me in exploring Switzerland, all the parties and dinners and also the endless laughter's.

TABLE OF CONTENTS

List of Figures

List of Tables

List of Abbreviations

AC	Adenylate cyclase
AD	Adrenaline
ADAP	Adaptor protein
ADP	Adenosine diphosphate
ATP	Adenosine triphosphate
Btk/Tec	Tec family kinase, bruton tyrosine kinase
Ca^{2+}	Calcium
CalDAG-GEFI	Ca2+ diacylglycerol guanine-nucleotide-exchange factor I
cAMP	Cyclic adenosine monophosphate
CRAC	Calcium release activating channel
CGP	CGP37157
CHE	Calcium hydrogen exchanger
COAGAPO	ProCOAGulant and APOptotic platelets
CRP	Collagen-related peptide
CVX	Convulxin
CyD	Cyclophilin D
DAG	Diacylglycerol
DMSO	Dimethyl sulfoxide
DTS	Dense tubular system
EC50	effective concentration
FcR-γ	γ-chain of Fc receptor
FIX	Factor IX
FV	Factor V
FVIII	Factor VIII
FX	Factor X
GP	Glycoprotein
GPCRs	G-protein couple receptors
GPVI	Glycoprotein VI
HCX	Hydrogen calcium exchanger
IBC	Institutional Bioethical Committee
IC50	Half-maximal inhibitory dose
Ig	Immunoglobulin
IMM	Inner mitochondrial membrane
IMS	Inter mitochondrial space
IP3	Inositol 1,4,5-trisphosphate
IP3-R	Inositol 1,4,5-trisphosphate receptor
ITAM	immunoreceptor tyrosine activation motif
K^+	Potassium
LAT	Linker activation for T cells
LDH	Lactate dehydrogenase

MAPK	Mitogen-activated protein kinase
MCU	Mitochondrial calcium uniporter
MCUC	Mitochondrial calcium uniporter complex
MCUR	Mitochondrial calcium uniporter regulator
MCV	Mean cell voiume
MFI	Mean fluorescence intensity
Mg^{2+}	Magnesium
MLC	Myosin light chain
MP	Microparticle
mPTP	Mitochondrial permeability transition pore
MTT	3-(4,5-dimethylthiazol-2-yl)-2,5-diphenyltetrazolium bromide
MTX	Mitoxantrone
NAADP	Nicotinic acid adenine dinucleotide phosphate
NaCL	Sodium choloride
NCLX	Sodium calcium lithium exchanger
NCX	Sodium calcium exchanger
NHE	Sodium hydrogen exchanger
NO	Nitric oxide
NSAID	Non-steroidal anti-inflammatory drugs
OCS	Open canalicular system
OMM	Outer mitochondrial membrane
PARs	Protease activating receptors
PCR	Polymerase chain reaction
PF-4	Platelet factor-4
PGI_2	Prostaglandin-2
PI3K	Phosphoinositide 3 kinase
PIP2	Phosphotidylinositol 4,5-biphosphate
PKA	Protein kinase A
PKC	Protein kinase C
PLC	Phospholipase C
PMCA	Plasma membrane calcium ATPase
PPP	Platelet poor plasma
PRP	Platelet rich plasma
PS	Phosphotidylserine
RBCs	Red blood cells
RIAM	Rap1-GTP-interating adaptor molecule
RIPA	radioimmunoprecipitation
ROCE	Receptor operated calcium entry
ROS	Reactive oxygen species
SCIP	sustained Ca2+-induced platelets
SER	Smooth endoplasmic recticulum

SERCA	Saro-endoplasmic reticulum calcium ATPase
SOCE	Store operated calcium entry
Src	proto-oncogene tyrosine-protein kinase
STIM1	stromal interaction molecule 1
SyK	Spleen tyrosine kinase
TBHQ	2,5-di-(t-butyl)-1,4-hydroquinone
TF	Tissue factor
THR	Thrombin
TMBIM5	Transmembrane BAX inhibitor motif containing protein 5
TMEM65	Transmembrane protein 65
TRPC	Transient receptor potential channel
TXA2	Thromboxane A2
VASP	Vasodilator stimulator protein
vWF	Von Willibrand factor
Ψm	Mitochondrial membrane potential

ABSTRACT

Platelet agonists initiate a signaling cascade that leads to platelet activation, essential for thrombosis and hemostasis. Agonist-induced Ca^{2+} mobilization from intracellular stores contributes to platelet shape change, thromboxane A2 generation, platelet aggregation, granule secretion, and $\alpha IIb\beta 3$ integrin activation. Besides its role in platelet function, cytosolic Ca^{2+} is also taken up by mitochondria. The influx of mitochondrial Ca^{2+} is strongly regulated by MCU whereas the efflux of matrix Ca^{2+} is carried out by NCLX. The role of cytosolic Ca^{2+} in platelet function is a well-known phenomenon. However, the contribution of mitochondrial Ca^{2+} transport in agonist-induced platelet responses is poorly explored. In this study we aimed to investigate the role of mitochondrial Ca^{2+} in agonist-evoked platelet activation and aggregation. Presence of MCU and NCLX was confirmed by mRNA expression showing relatively lower level of NCLX in platelets. MCU and NCLX was blocked by their pharmacological inhibitors MTX and CGP respectively. Cell death assays including Annexin V assay, LDH release and trypan blue exclusion assay were performed to exclude the cytotoxic effect and preactivation of platelets in the presence of MTX and CGP. Platelet aggregation was measured by time-lapsed spectrophotometric assay and aggregometer. Platelet activation markers including PAC-1 binding and p-selectin expression and procoagulant platelets using Annexin V were measured by employing flow cytometry. Interestingly, our data revealed a promising inhibitory effect of MTX showing a remarkable decrease on ADP-induced platelet aggregation. Moreover, it significantly reduced platelet activation endpoints measured by p-selectin and PAC-1. On the contrary, we observed a striking result by inhibition of NCLX with CGP, which markedly enhanced ADP-mediated platelet aggregation and activation. Furthermore, in line with ADP-induced platelet response MTX exhibited a remarkable decrease on THR/CVX-stimulated platelet aggregation and activation. On the contrary, THR/CVX-induced platelet activation remained unaltered in the presence of CGP. In addition to this, MTX exhibited a significant effect on THR/CVX-induced procoagulant platelets. The effect of MTX on procoagulant platelets was further validated by Ru265 that is recently developed and more specific inhibitor of MCU. Altogether, the present study revealed a significant involvement of mitochondrial calcium fluxes in agonist-induced platelet responses.

Keywords: Mitochondrial Ca^{2+}, MCU, NCLX, procoagulant platelets, mitoxantrone, CGP37157.

1. INTRODUCTION

Platelets are the subcellular fragments of megakaryocytes and are the smallest of many types of cells circulating in blood. Platelets are anucleated discoid in shape ranging between 2 to 5 µm in diameter, 0.5µm in thickness with mean cell volume (MCV) of 6 to 10 fL (Palacios-Acedo et al. 2019). The normal platelet count in peripheral blood is $150x10^9/L$ to $400x10^{9/}/L$ having an average life span of 5 to 9 days (Ghoshal and Bhattacharyya 2014). Blood platelets, also known as thrombocytes, play a crucial role in hemostasis and blood clotting (Ribatti and Crivellato 2007). Besides, their critical role in thrombosis and hemostasis platelets are also recognized to play a key role in inflammation, atherogenesis, immunity, wound healing, haematological malignancies and metabolic disorders(Lindemann et al. 2007; Linden 2013). Guilio Bizzozero was the first to describe platelets in 1882 as a new blood component besides erythrocytes and leukocytes. The historical view of platelets is demonstrated in Fig 1.1 highlighting some key discoveries in platelet biology.
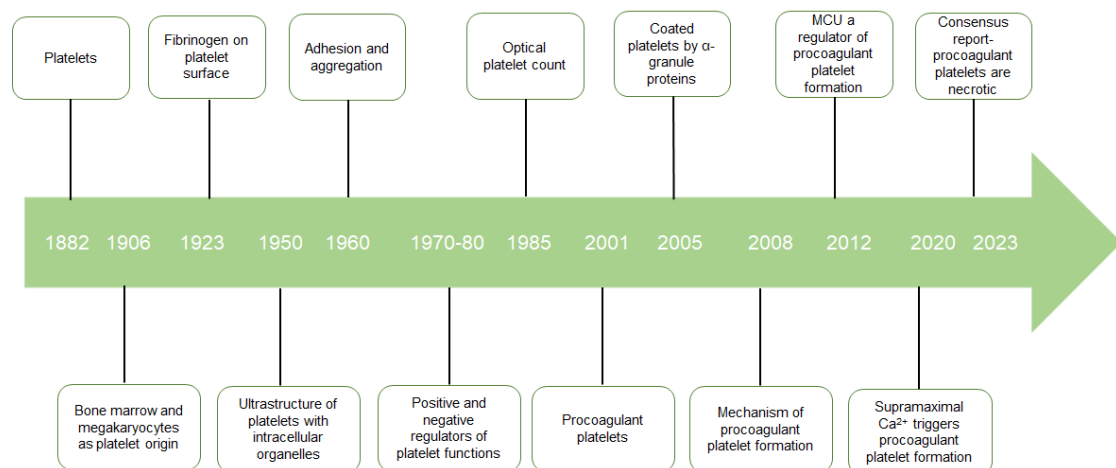
Figure 1.1 Historical timeline of platelets

1.1. Platelet Structure

Platelets are structurally divided into three zones shown in Fig 1.2.

1. Peripheral Zone

i. Plasma membrane

The outermost layer of platelet peripheral zone consists of plasma membrane which has thick glycocalyx, enriched with glycoproteins (GPs) receptors, and is necessary to

facilitate platelet interaction with surrounding milieu, platelet activation, adhesion and aggregation. Particularly, the mobile receptors of glycoprotein include complex of GP 1b-IX-V and integrin αIIbβ3, which are vital for platelet function (Gremmel, Frelinger III, and Michelson 2016).

ii. Open canalicular system (OCS)

The plasma membrane of the platelets invaginates interiorly forming twisting channels which makes up the open canalicular system (OCS). The OCS runs through the platelets and covers the surface area of about $14\mu m^2$. The chemical composition of OCS is similar to plasma membrane but it holds both extracellular and cytosolic faces (Fitch-Tewfik and Flaumenhaft 2013). OCS contributes to the transport of components such as plasma proteins including fibrinogen and tissue factors (TF). The OCS also plays an important role in the release of granular content during platelet activation (Selvadurai and Hamilton 2018). Moreover, it increases the surface area of the activated platelets as OCS can be everted, thereby providing parts of the membrane required for platelet spreading and platelet adhesion (Gremmel, Frelinger III, and Michelson 2016).

iii. Unit membrane

The middle layer of peripheral zone is the unit membrane, which lies under the glycocalyx and is incompressible and unstretchable. It is enriched with phospholipids that provide an essential surface for binding with blood coagulation proteins (Fritsma 2015). Anionic phospholipids and phosphatidylserine (PS) serve as a site for the formation of prothrombinase coagulation complex. Upon activation platelets release tissue factors (TF)-containing microparticles (MP) which facilitate the binding of coagulation factors to their surface PS (White and Michelson 2007).

2. Sol-Gel Zone

The sol-gel zone of platelet lies under the unit membrane, which is a matrix of platelet cytoplasm. It consists of a complex of microtubules and microfilaments.

i. Microtubules

Microtubules are encircled in the form of coils near the cell membrane with a diameter of 25nm. It helps to maintain the discoid shape of resting platelet along with cell integrity (Fritsma 2015).

ii. Microfilaments

It is a thick meshwork of microfilaments present in a narrow space between microtubules and plasma membrane. The cytoskeleton of platelet is a meshwork of spectrin protein (Hartwig 2006), which orients platelet organelles and also keep them apart from each other and from the plasma membrane in resting platelets (Gremmel, Frelinger III, and Michelson 2016). Upon activation, platelet undergoes reorganization of cytoskeleton accompanying with the assembly of new actin filaments. This actin-dependent reorganization of platelets facilitates platelet shape change, platelet adhesion and spreading (Linden 2013).

3. Organelle Zone

The organelle zone consists of secretory granules like α-granules and dense granule, lysosomes, peroxisomes and mitochondria. This part of platelet helps in metabolic processes and storage of enzymes, proteins, serotonin, calcium and non-metabolic adenine nucleotide (White 1987).

i. α-granules

α-granules are the most abundant organelle of platelet, typically 50-80 α-granules in average human platelets. It is round to oval in shape, expanded over $14\mu m^2$ surface area with a diameter of 200-500nm. α-granules contain variety of proteins including those involved in coagulation and fibrinolysis along with adhesion molecules, chemokines, growth factors and immunological molecules (Reed 2002). The common markers for α-granules are platelet factor (PF-4), von Willebrand factor (vWF) and p-selectin and they are mainly involved in processes like thrombosis, inflammation, cell adhesion, angiogenesis and host defense (Flaumenhaft and Sharda 2019).

ii. Dense granules

Dense granules are structurally spherical in shape, usually surrounded by an empty space or sometimes filled with granular substances (White and Michelson 2007). An average platelet contains 3-8 dense granules that cover an area of $<1\mu m^2$ with a diameter of 150nm. Common markers for dense granules are serotonin and ADP/ATP and they play a role in processes like inflammation and hemostasis (Flaumenhaft and Sharda 2019). Dense granules contain cations like calcium (Ca^{2+}), potassium (K^+), magnesium (Mg^{2+}), and small metabolites like pyrophosphates, ADP,ATP and serotonin (Fukami 1997).(Ebbeling et al. 1992)

iii. Dense Tubular System (DTS)

DTS represents the residual megakaryocyte smooth endoplasmic reticulum (SER), however, channels of DTS are randomly dispersed in cytoplasm (White 2002). DTS plays an integral part in regulation of platelet activation by Ca^{2+} sequestration and the release of Ca^{2+} through IP3-R present on its surface (Brass and Joseph 1985). At resting state, DTS of platelets is present in the form of thin elongated-stretched membranes. However, upon activation the elongated structure of DTS is converted to round vesicles (Ebbeling et al. 1992).

iv. Lysosomes

Platelets on average contain more than three lysosomes. They have a diameter of 200-500nm and are spread over more than $1\mu m^2$ surface area. Common markers of lysosomes in platelets are acid phosphatases and they play a role in endosomal digestion. Although few in number, platelet lysosomes have protein degrading enzymes such as elastase, cathepsins, and collagenase; carbohydrate degrading enzyme including galactosidase and glucosidase (Flaumenhaft and Sharda 2019).

v. Mitochondria

Although platelets are anucleated cells but they have functionally active mitochondria that are considered as fundamental organelles for producing ATP which is required for platelet activation and aggregation (Ma et al. 2023). Besides the energy production, mitochondria also serve as a Ca^{2+} sink and contributes to platelet Ca^{2+} homeostasis. Upon strong stimulation intra-mitochondrial Ca^{2+} rises followed by mitochondrial depolarization; which trigger changes in platelet subpopulation exhibiting PS exposure on platelets surface but not integrin activation and granule release (Choo et al. 2012).
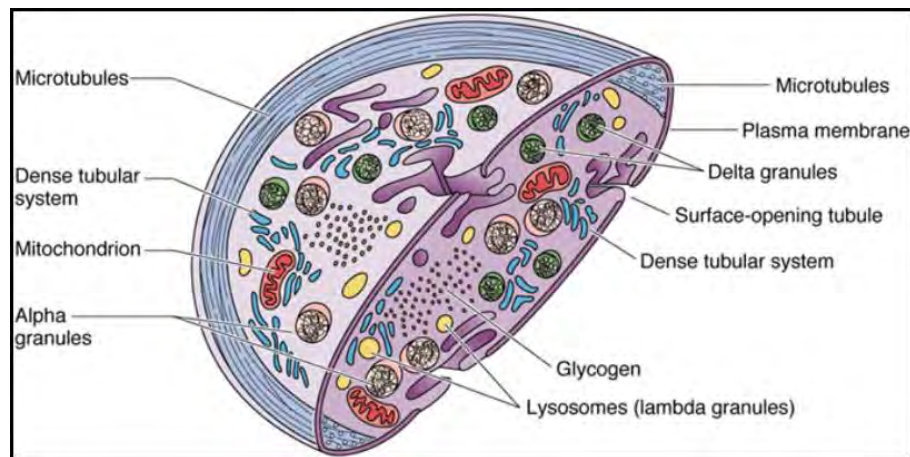
Figure 1.2 Ultrastructure of platelets: Platelets surface is covered with plasma membrane, which is invaginated to form open canalicualr system (OCS) or surface-opening tubules. It consists of several organelles including Dense tubular system (DTS), mitochondria, glycogen and lysosomes along with two major types of granules-alpha granules and dense granules. Platelets also contain a meshwork of microfilaments and microtubules to maintain its shape (Ordaz 2016).

1.2. Platelet Activation Pathways

Platelet exhibit a variety of receptors on their surface, which activate the platelets through several pathways by binding to their respective agonists (Jennings 2009). Platelet activation is directly involved in haemostasis and thrombus formation, providing a distinct role in physiology and pathophysiology (Janmey, McCulloch, and Miller 2016). Platelets are usually present in their resting state in blood circulation where they retain their inactive form by intact endothelium, production of prostaglandins (PGI_2) and nitric oxide (NO). Platelets are activated by endothelial damage upon tissue injury, loss of activation inhibitors and release of ADP (Van Geet et al. 2009). Agonist-induced platelet activation generates heterogeneous platelet responses with distinct platelet populations (van der Meijden and Heemskerk 2019). These distinct subtypes of platelets include procoagulant platelets, aggregatory platelets, COAT platelets and secretory platelets (Fig 1.3) (Hamad et al. 2022). Procoagulant platelets are generated by a high-sustained rise of cytosolic Ca^{2+} that leads to externalization of phosphatidylserine (PS) on the platelet surface, calpain-mediated integrin αIIbβ3 inactivation and ability to bind coagulation factors such as factor V (FV) and factor X (FX) (Mattheij et al. 2016) (Agbani et al. 2015). However, intermittent Ca^{2+} spikes are found in aggregatory platelets causing activation of integrin

αIIbβ3 on platelet surface, which is the main difference between procoagulant and aggregatory platelets (Heemskerk, Mattheij, and Cosemans 2013). A third kind of platelet population is also observed, which is obtained as a result of dual stimulation of platelets with collagen and thrombin and is known as COAT platelets. COAT platelets exhibit a high level of PS exposure along with α-granule proteins including fibrinogen, fibronectin, thrombospondin, FV and vWF that are irreversibly bound to the surface of COAT platelets (Veuthey et al. 2022). Another population of platelets, known as secretory platelets, mainly release their granules (α-granules, dense granules and lysosomes) upon activation (van der Meijden and Heemskerk 2019).
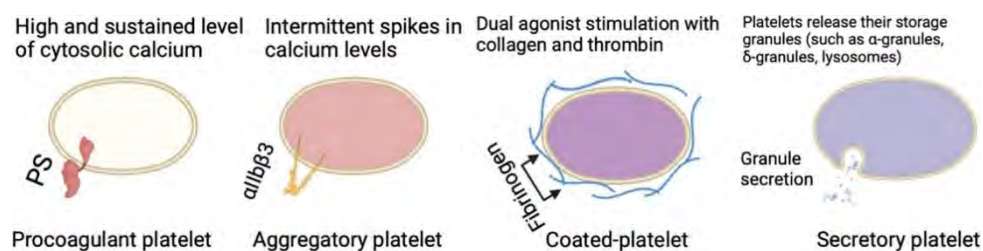
Figure 1.3 Subpopulations of platelets: *Platelets exhibit distinct subtypes upon activation based on their function. (1) Procoagulant platelets expose phosphatidylserine (PS) on their surface due to high and sustained cytosolic Ca^{2+} level (2) Aggregatory platelets have intermittent spikes of Ca^{2+} and express active integrin αIIbβ3 on their surface (3) Coated-platelets are generated by dual-stimulation of thrombin plus collagen and are coated with several procoagulant proteins such as fibrinogen (4) Secretory platelets release their storage granules form alpha-granules, dense granules and lysosomes (Hamad et al. 2022).*

1.2.1. Key regulators of platelet activation pathways

Platelet activation begins with the vascular injury by adhesive proteins such as vWF and collagen or by soluble platelet agonists like thrombin, thromboxane A_2 and ADP. Receptor-agonist interaction along with the adhesive proteins induce a signaling pathway that stimulates the platelets (Li et al. 2010). The characteristic features that leads to final endpoint activation of platelets involve platelet shape change (cytoskeleton rearrangement), granule release, integrin αIIbβ3 activation, sustained platelet aggregation and externalization of negatively charged phosphatidylserine (PS) that contributes to platelet procoagulant activity (Bye, Unsworth, and Gibbins 2016). The key regulators for platelet activation pathways are phospholipase C (PLCβ) and protein kinase C (PKC),

which are activated by Gq protein that leads to Ca^{2+} mobilization through inositole 1,4,5 triphosphate (IP3) and diacylglycerol (DAG) respectively. On the other hand Gi protein activates phosphoinositide 3 kinase (PI3K) that inhibits adenylate cyclase (AC), while G$_{12/13}$-dependent Rho kinase, which is the main contributor in platelet shape change (Fig 1.4) (Stegner and Nieswandt 2011). The two major activating signaling pathways that exist in platelets are triggered by GPVI/collagen receptors and G-protein-coupled receptors (GPCRs).
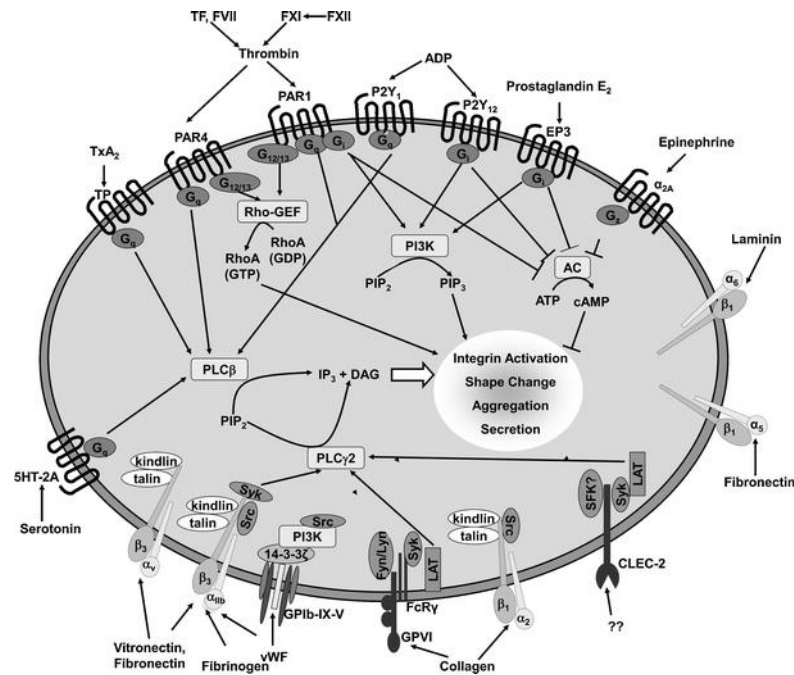
Figure 1.4 Platelet activation pathways: *Soluble agonist of platelets stimulate their respective receptors, many of which converge on IP3 and DAG.. Collagen and Fibrinogen receptors activate the phospholipase C (PLC) pathway. Rho-GEF is activated by protease activating recepors (PARs), IP-3+DAG and PLCγ and PLCβ collectively contributes to integrin activation, platelet shape change, aggregtaion and secretion of granules (Stegner and Nieswandt 2011).*

1.2.1.1. GPVI/collagen receptors

Platelets express a variety of collagen receptors on their surface, but GPVI is the major signaling receptor for collagen mediated platelet activation. Structurally it contains two immunoglobulin (Ig) domains with mucin-rich domain and a cytosolic tail of 51 amino acids in humans. GPVI forms a complex with γ-chain of Fc receptor (FcR- γ), each (FcR-γ) contains a copy of immunoreceptor tyrosine activation motif (ITAM) (Lecut et al.

2004). Upon activation with collagen, collagen-related peptide (CRP) or convulxin (snake venom protein) GPVI phosphorylates tyrosine residues of ITAM by recruiting two proto-oncogene tyrosine-protein kinase (Src-kinases) (Fyn and Lyn). This leads to the phosphorylation/activation of spleen tyrosine kinase (Syk) which in turn phosphorylates linker activation for T cells (LAT) (Poddar and Banerjee 2020). Phosphorylation of LAT initiates the formation of LAT signalosome with the help of two adaptor proteins (SLP-76 and Gads) and recruitment of a PI3K. The complex of kinases including Tec family kinase, bruton tyrosine kinase (Btk/Tec) and PI3K facilitates the recruitment of major effector in GPVI signaling that is phospholipase C (PLC)γ-2, which yields IP3 and DAG (Watson et al. 2005). IP3 induces Ca^{2+} mobilization from DTS and DAG activates PKC and Ca^{2+} diacylglycerol guanine-nucleotide-exchange factor I (CalDAG-GEFI). PKC, Ca^{2+} and CalDAG-GEFI altogether activate small GTPase Rap1, which results in granule release, TXA2 production and integrin activation (Fig 1.5) (Li et al. 2010).
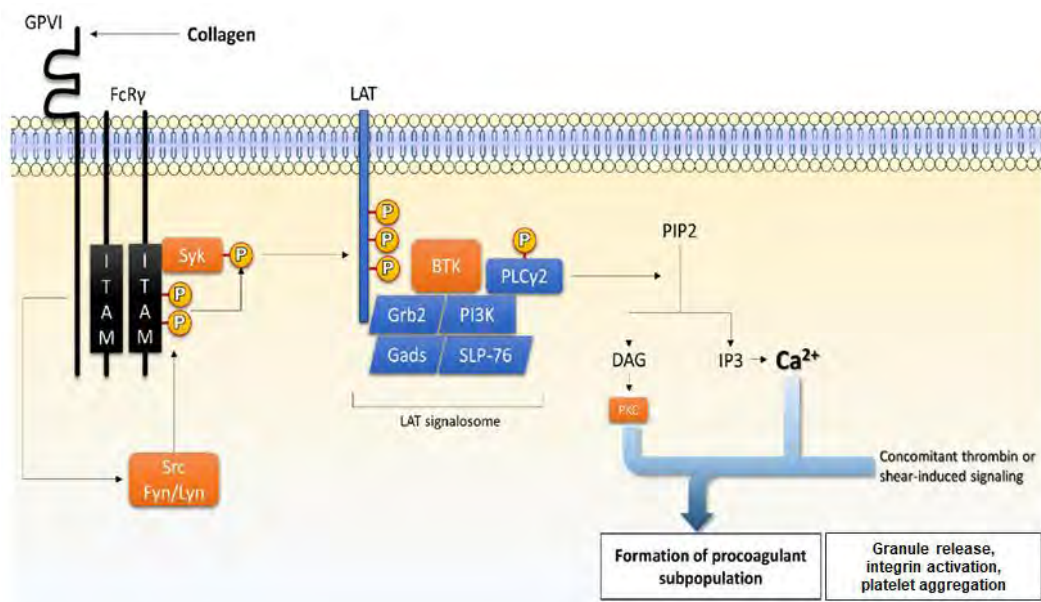
Figure 1.5 Collagen/GPVI receptor signaling: *Collagen binds to GPVI receptor resulting in the formation of LAT linker activation for T cells signalosome with the help of phosphorylation of Syk. LAT activates PLCγ2 (phospholipase C) resulting in the release of DAG and IP3, which subsequently helps in the formation of procoagulant platelet with the help of thrombin signaling along with triggering granule release, integrin activation and platelet aggregation. (Veuthey et al. 2022).*

1.2.1.2.G-protein coupled receptors

GPCRs contain a large family of proteins in humans and can be activated by a diverse variety of ligands including peptides, ions, nucleotides, and proteases. GPCRs specifically interact with heterodimeric guanine (G) nucleotide and can induce different signaling events to alter cellular function. However, in platelets GPCRs are primary mediators of second phase of platelet activation in thrombosis and hemostasis (Gurbel, Kuliopulos, and Tantry 2015).

Thrombin receptors

Thrombin activates platelets through protease activating receptors; PAR1 and PAR4 in humans (Poddar and Banerjee 2020). The PARs belong to a superfamily of GPCRs with seven transmembrane α-helices, four extracellular and intracellular loops, and domains. PAR1 triggers platelet activation at low concentration while PAR4 is only sensitive to higher thrombin concentration. PARs are activated when thrombin cleaves the N-terminus at specific site, thereby unmasking new N-terminus that act as tethered ligand to induce transmembrane signaling (Han et al. 2019). PAR1 and PAR4 activate Gq, G12/13 to induce downstream signaling for platelet activation. Gq initiates signaling through activation of PLCβ which hydrolysis phosphatidylinositol 4,5-bisphosphate (PIP2) into IP3 and DAG, which results in Ca^{2+} elevation and activation of PKC respectively. However, G12/13 triggers activation of Rho kinase that induces platelet shape change mediated by phosphorylation of myosin light chain (MLC) (Stegner and Nieswandt 2011).

Apart from PARs, GPIb-IX-V complex also possesses high affinity for thrombin (Stegner and Nieswandt 2011). Fundamentally, GPIb-IX-V complex is formed of 130KDa leucine rich repeats of GPIbα and GP1bβ, which are linked through disulfide bond and then covalently attached to GPIX and GPV. GPIb is profoundly involved in normal hemostasis and arterial thrombosis, however, in signaling it shows resemblance with GP-VI pathways leading to activation of kinases such as PI3K and Btk/Tec. The strongest ligand for GPIb is vWF, but it also binds to other coagulation factors and proteins including FIX and FX, collagen, α-thrombin and thrombospondin (Fig 1.6) (Rivera et al. 2009).
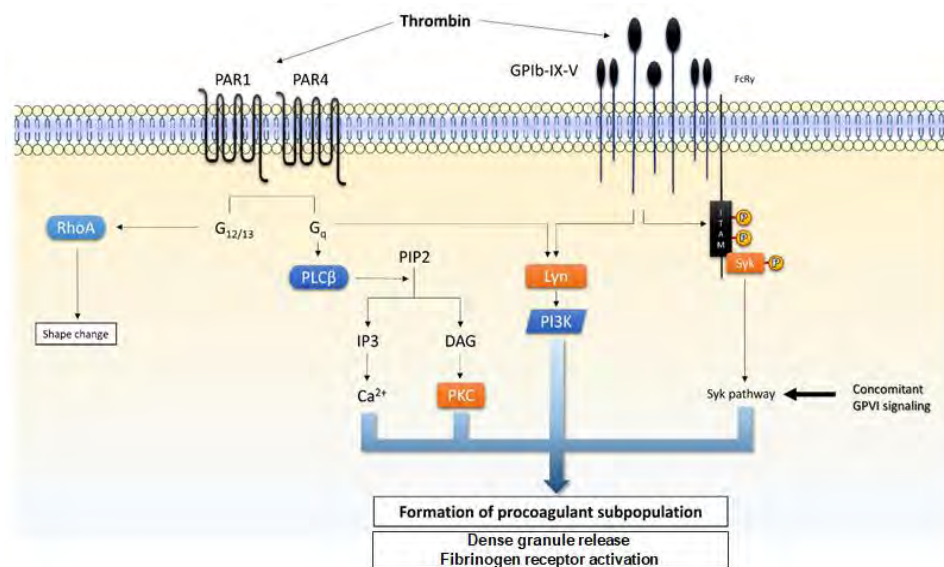
Figure 1.6 Thrombin receptor signaling*: Thrombin induces platelet activation through PAR1, PAR4 and GPIb-IX-V. PAR1 and PAR4 follow the conventional GPCR signaling resulting in shape change by the activation of RhoA and elevation of cytosolic Ca^{2+} subsequently resulting in dense granule release and fibrinogen activation. Thrombin also results in the formation of procoagulant platelet by the activation of GPIb-IX-V receptor accompanied by GPVI signaling following Syk and PI3K pathway (Veuthey et al. 2022)*

Purinergic receptors

ADP is one of the major factors released from the dense granules of activated platelets. It acts as an agonist for the purinergic receptors P2Y1 and P2Y12 that are expressed on the surface of platelets. P2Y receptors are seven transmembrane

proteins with amino terminal being exposed on extracellular side while carboxyl terminal on cytoplasmic side. P2Y1 and P2Y12 bind to heterodimeric GTP binding Gq and Gi proteins respectively (Cattaneo 2019). Gq initiates platelet shape change through Ca^{2+} mobilization following the PLCβ pathway (Oury et al. 2006). Nevertheless, it is also reported that ADP induces cytoskeleton rearrangement and transient aggregation by the stimulation of Rho kinase and phosphorylation of MLC. P2Y12 inhibits adenylate cyclase (AC), which decreases the production of cyclic AMP (cAMP) through Giα followed by impaired activation of protein kinase A (PKA). This will lead to inhibition of vasodilator stimulator protein (VASP), which confines the secretory or adhesive events of platelets, thereby reducing the activation of integrin αIIbβ3 and

subsequently platelet aggregation (Ballerini et al. 2018). P2Y12 receptors also recruit Giβ subunit causing Akt phosphorylation and Rap1b activation through activation of PI3K, which is a key pathway for the integrin activation. It has been reported that ADP also induce TXA2 generation and platelet aggregation through PI3Kβ (Fig 1.7) (Garcia et al. 2010)
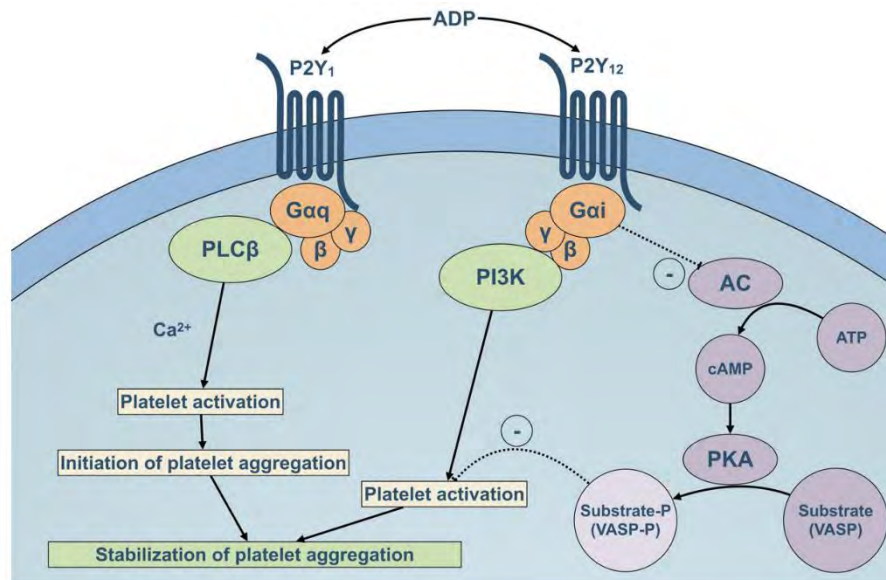
Figure 1.7 Platelet purinergic signaling: *The two purinergic receptors P2Y1 and P2Y12 are activated by ADP. P2Y1 mobilizes Ca²⁺ by activation of PLCβ resulting in stable platelet aggregation. On the other hand P2Y12 induces activation of PI3K and inhibits adenylate cyclase (AC) causing impaired activation of PKA, which consequently leads to platelet activation (Mansour et al. 2020).*

Adrenergic receptors

Unlike ADP, thrombin and collagen, adrenaline/epinephrine is unable to initiate platelet aggregation alone (Offermanns 2006). However, it potentiates the effect of other stimuli by acting on α2A adrenergic receptors present on platelet surface. α2A adrenergic receptors are coupled with Gi protein known as Gz. Gzα inhibits AC and activates PKA leading to platelet activation, whereas Gzβ/γ subunit potentiates PI3K pathway resulting in Akt and Rap1 activation subsequently leading towards granule secretion and integrin activation (Martin et al. 2020).

1.2.2. Inside-out signaling

Platelets express several integrins on its surface like fibrinogen receptor (αIIbβ3), vitronectin receptor (αvβ3), collagen receptor (α2β1), fibronectin receptor (α5β1) and

laminin receptor (α6β1) (Varga-Szabo, Pleines, and Nieswandt 2008). The most abundant integrin, fibrinogen receptor αIIbβ3, exists in an inactive or low affinity state in resting platelets. However, upon activation it is shifted to activated or high affinity state. Integrins are activated by binding to several ligands (vWF, fibrinogen and matrix proteins) that accelerate platelet adhesion, aggregation and thrombus formation (Coller and Shattil 2008). Inside-out signaling can be defined as the intracellular signaling that induce changes in extracellular binding domain of integrin from low affinity or resting state to high affinity or activated state (Li et al. 2010). The intracellular activators including talin and kindlin participate in inside-out signaling and interact with cytoplasmic tail of integrin αIIbβ3 (Huang et al. 2019). For the activation of integrin IP3 releases Ca^{2+} from the intracellular stores leading to increase in concentration of Ca^{2+} into cytosol. DAG and Ca^{2+} activate the PKC and CalDAG-GEF1 which is essential for conversion Rap1 GDP to Rap1 GTP. Rap1 recruits another protein called Rap1-GTP-interating adaptor molecule (RIAM). RIAM as a linker between talin and Rap1 GTP forming an integrin activation complex of Rap1-RIAM-talin (Lee et al. 2009). Furthermore, talin and kindlin interact with the NPLY and NITY motif of β3 tail of integrin. This interaction breaks the salt bridge between α and β3 subunit of integrin which results in a conformational change from bent to extended form and subsequently leading to integrin activation (Ye et al. 2010). Besides this, a hematopoietic adaptor protein (ADAP) acts as a bridge between talin and kindlin to further promote the integrin activation (Fig 1.8) (Kasirer-Friede, Ruggeri, and Shattil 2010)
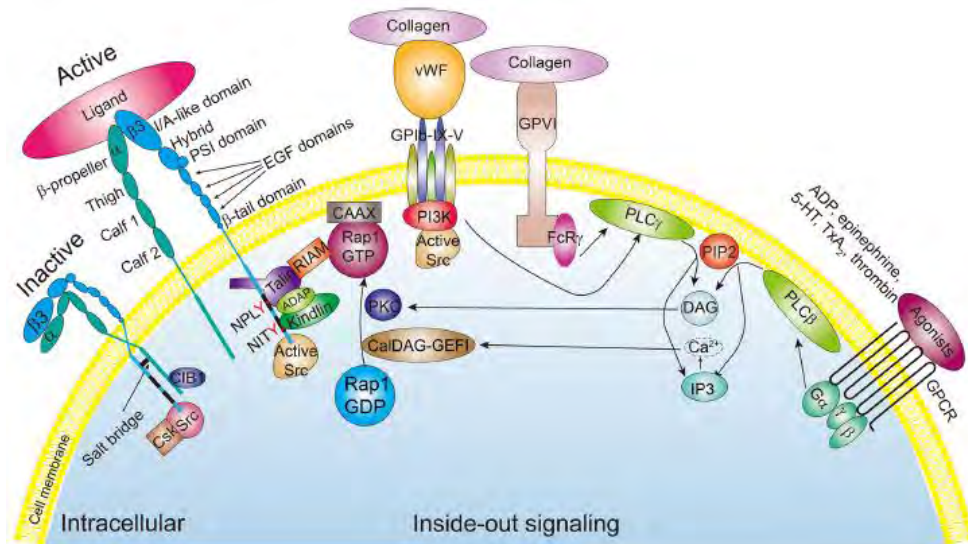
Figure 1.8 Inside-out signaling in platelets: *Platelet agonists like collagen, ADP, thrombin, epinephrine, and TXA2 induce the activation of PLC which leads to mobilization of Ca^{2+}. DAG and Ca^{2+} together activate CalDAG-GEFI, which along with PKC convert Rap1GDP to Rap1GTP. Rap1GTP interacts with talin through linker RIAM forming a complex. Talin binding to the NPLY motif of β3 subunit of integrin disrupting the salt bridge between the two subunits of integrin ultimately shifting the bent (inactive) form of integrin to extended (active) form of integrin (Huang et al. 2019)*

1.2.3. Outside-in signaling

The outside-in signaling of integrin is initiated by bonding of fibrinogen to activated integrin αIIbβ3. The interaction of ligand with α2β1 and αIIbβ3 involves the activation of Src that is associated with the β subunit of integrin (Janus-Bell and Mangin 2023). Subsequent activation of Src recruits Syk, which results in phosphorylation of SLP76 and PLCγ2. Consequently, a signaling cascade is followed for Ca^{2+} mobilization and PKC activation, which induce platelet shape change, filopodia formation, and further integrin activation. Besides this, more downstream signaling from αIIbβ3 has been studied, which involves auto-phosphorylation of Fyn that leads to the phosphorylation of pyk2 followed by activation of PI3Kβ and Akt. Moreover, Fyn also promotes phosphorylation of adaptor proteins such as Dok2, Grb and Shc, which results in activation of mitogen-activated protein kinases MAPK. Likewise, Fyn facilitates interaction of myosin that is linked to β3 cytoplasmic tail of integrin with the actin cytoskeleton. Moreover, Gα13 is also considered as the major player in the outside-in signaling of αIIbβ3 which recruits Rho GTPase

The Contribution of Mitochondrial Calcium Homeostasis in Agonist-Induced Platelet Response

resulting in the activation of Rho A (Durrant, van den Bosch, and Hers 2017). Furthermore, a cleavage induced by calpain on β3 cytoplasmic tail of integrin dissociates partially active Src (c-Src), which leads to phosphorylation and activation of many signaling protein including FAK, RhoGAP, RhoGEF, Syk kinase and PI3K (Huang et al. 2019). Altogether, these events in outside-in signaling of platelets promotes stable integrin activation, platelet shape change, granule release TXA2 formation and clot retraction (Fig 1.9).
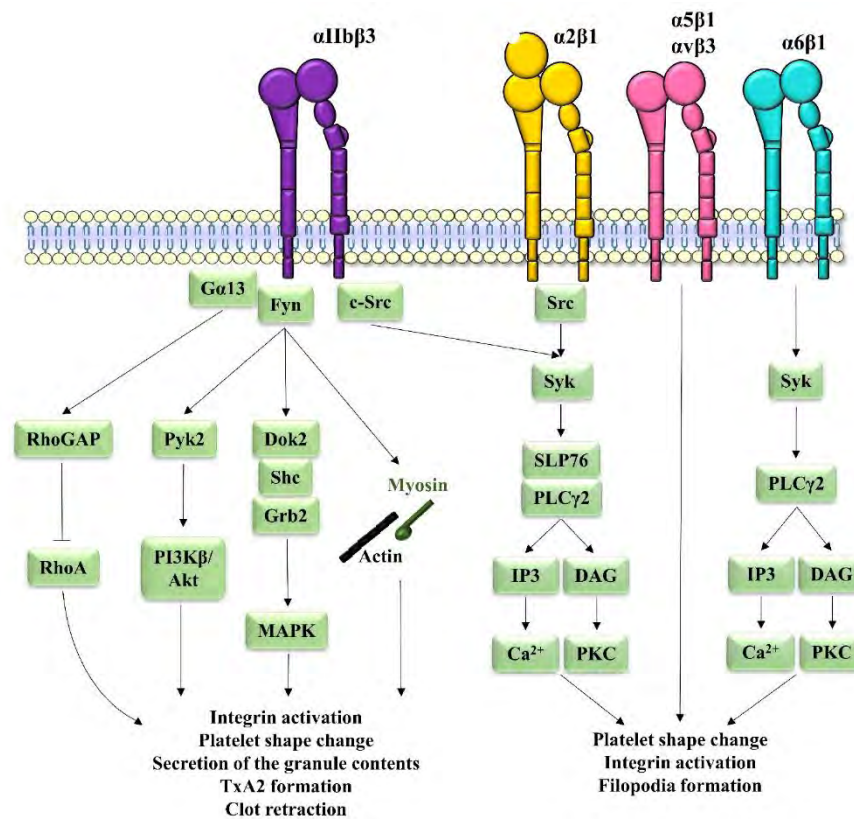
Figure 1.9 Outside-in signaling of platelets: Fibrinogen binding to integrin induces outside-in signaling by the activation of Src which facilitates the activation of Syk resulting in phosphorylation of SLP76 and activation of PLCγ2. On the other hand, autophosphorylation of Fyn activates MAPK and recruits PI3Kβ/Akt and Gα13, which inhibit RhoA. All these events collectively result in integrin activation, platelet shape change, granule release, TXA2 formation and clot retraction (Janus-Bell and Mangin 2023)

1.3. Ca^{2+} signaling in platelets

An elevated level of cytosolic Ca^{2+} is the vital player to promote platelet activation. Agonist-stimulated Ca^{2+} rise in cytosol is facilitated by Ca^{2+} stores in platelets and

extracellular Ca^{2+} entry through plasma membrane exchangers and channels. Moreover, there are also processes, which remove the cytosolic Ca^{2+} by its sequestration via activation of sarco-endoplasmic reticulum calcium ATPase (SERCA) for refilling of intracellular Ca^{2+} stores and by transport out of cell via plasma membrane ATPase (PMCA) and exchanger (NCX).

1.3.1. Mechanisms to increase cytosolic Ca^{2+}

Several mechanisms of platelets have been identified to regulate cytosolic Ca^{2+} influx and efflux pathways (Fig 1.11)

1.3.1.1. Major Ca^{2+} stores in platelets

There are two major calcium stores present in platelets, which are differentiated by the presence of two different isoforms of SERCA and their sensitivity towards inhibitor of SERCA i.e. thapsigargin. SERCA2b is expressed on dense tubular system (DTS) and is more sensitive towards thapsigargin. While another isoform SERCA3 is present on acidic store. which is less sensitive towards thapsigargin but it shows its sensitivity towards 2,5-di-(t-butyl)-1,4-hydroquinone (TBHQ) (Jardín et al. 2008) (Fig 1.10)

> *DTS*
>
> The main source of Ca^{2+} in platelets is dense tubular system (DTS), which release Ca^{2+} upon stimulation with different IP3-generating agonists (Yadav et al. 2023). There are three types of IP3Rs isoforms which exist in platelets with different roles in Ca^{2+} release and Ca^{2+} entry. IP3R-I is expressed on intracellular stores, which helps in release of Ca^{2+} from DTS. IP3R-II is located on plasma membrane which plays a part in influx of Ca^{2+} from extracellular space. IP3R-III is present both on plasma membrane and DTS and it is involved in Ca^{2+} release from DTS and Ca^{2+} entry from extracellular space (Jardín et al. 2008).

> *Acidic Ca^{2+} store*
>
> The second Ca^{2+} store in platelets is smaller than DTS. The Ca^{2+} release from acidic store is mediated by nicotinic acid adenine dinucleotide phosphate (NAADP). The agonists or receptors that contribute to release Ca^{2+} from acidic stores include PARs and GPIb-IX-V.
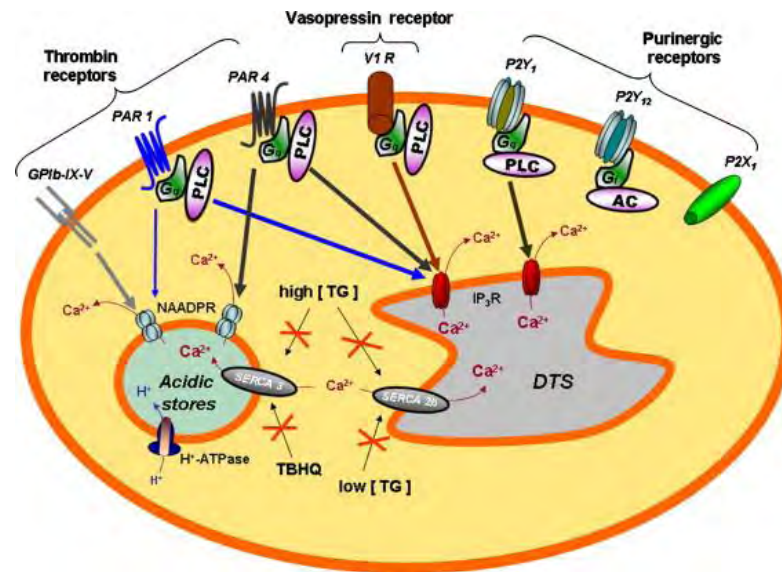
Figure 1.10 Ca²⁺ stores in platelets: *Two Ca²⁺ releasing stores are present in platelets that are differentiated on the basis of SERCA isoforms. Acidic store expresses SERCA3 which is sensitive to TBHQ and has low affinity for thapsigargin (TG), whereas dense tubular system (DTS) expresses SERCA 2b, which is highly sensitive to thapsigargin. Moreover, DTS has IP3-R and acidic store has NAADPR receptors for Ca²⁺ mobilization upon activation. Acidic store is activated by thrombin upon interaction with PAR1, PAR4 and GPIb-IX-V while DTS releases Ca²⁺ upon activation by purinergic receptors, PAR4 and V1R (Jardín et al. 2008)*

1.3.1.2. Store operated Ca²⁺entry (SOCE)

When the intracellular Ca^{2+} stores are depleted, the channels on plasma membrane, which are permeable to Ca^{2+} are activated. This phenomenon of Ca^{2+} entry upon store depletion is called store operated Ca^{2+} entry (SOCE). The major proteins contributing to SOCE are stromal interaction molecule 1 (STIM1) and Ca^{2+} release activated Ca^{2+} channel (CRAC or Orai I). Besides, transient receptor potential channel (TRPC) has also been described to play a role in SOCE (Harper and Sage 2017).

STIM1

STIM 1 is a single transmembrane protein located on the DTS of platelets. It contains two EF-hand domains at N-terminal continued with sterile alpha motif (SAM), transmembrane domain and two coiled-coil regions at the C-terminal. The EF-hand domains of STIM1 are present inside the lumen of DTS on which Ca^{2+} is bound. When store is depleted, the bound Ca^{2+} on EF hands is impaired, which is sensed by STIM1, leading to STIM1 oligomerization that activates SOCE Ca^{2+} channel in plasma membrane (Stathopulos et al. 2008).

Orai1

Orai1 or CRAC is the plasma membrane protein that consists of four transmembrane domains with intracellular C and N terminals. It has been suggested that upon activation of STIM1 on DTS Orai1 oligomerizes itself on plasma membrane to form a pore forming unit for the influx of Ca^{2+} from extracellular space into DTS through plasma membrane (Yeromin et al. 2006) (Vig et al. 2006).

TRPC

Contrary to STIM1 and Orai1, TRPC is further subdivided into seven families. Among them TRPC1 is considered as the major contributor of SOCE in platelets. Mechanistically, it has been described that TRPC1 is activated as a SOCE channel by integrating with IP3R-II on DTS, thereby allowing Ca^{2+} entry (Varga-Szabo, Braun, and Nieswandt 2009).

1.3.1.3. Receptor operated Ca^{2+} entry (ROCE)

Besides SOCE, the phenomenon that allows Ca^{2+} entry from extracellular space by the direct activation of receptors is called non-SOCE or receptor operated Ca^{2+} entry (ROCE). The major receptors, which are involved in ROCE, are P2X1 and TRPC6 (Harper and Sage 2017).

P2X1

P2X1 is a type of purinergic receptor in platelets, which is activated by binding with ATP. P2X1 can be activated by PKC/Erk2 pathway to secrete dense granules and induce reversible shape change. P2X1 acts as an amplification signal for other GPCRs or collagen at lower concentration as it is quickly desensitized at higher concentration. However, stimulation of P2X1 increases cytosolic Ca^{2+} signal by the release of ATP from dense granules evoked by stimulation of other agonists. Ca^{2+} influx via P2X1 can

cause substantial depolarization of membrane, which allows the activation of P2Y1 receptors and further enhances the signals following the activation of PLCβ and GPVI/PLCγ2. It is also likely that Ca^{2+} signals evoked by P2X1 take part in platelet responses including shape change, unstable integrin activation and reversible aggregation (Mahaut-Smith, Jones, and Evans 2011) (Oury et al. 2002).

TPRC6

TRPC6 has been described to from non SOCE or ROCE channel for Ca^{2+} influx in platelets. In contrast to TRPC1, TRPC6 is functionally expressed on platelets and megakaryocytes. TPRC6 is activated by the second messenger DAG which is hydrolyzed by PLC upon activation of platelets with different agonists (Varga-Szabo, Braun, and Nieswandt 2009).

1.3.2. Mechanisms to remove cytosolic Ca^{2+}

In order to keep the platelets in resting state in circulation and to prevent undesired thrombus formation, there are mechanisms that maintain the stable cytosolic Ca^{2+} level in platelets (Harper and Sage 2017).

Ca^{2+} removal by PMCA

Plasma membrane calcium ATPase (PMCA) is described as the major channel to maintain cytosolic Ca^{2+} in resting platelets by extruding Ca^{2+} through plasma membrane. PMCA is a p-type ATPase pump that is comprised of ten transmembrane domains with N and C-terminals residing in cytoplasm. Platelet express two PMCA isoforms PMCA1b and PMCA4b, however, PMCA4b is known as an active form for Ca^{2+} extrusion (Dean 2010). For the Ca^{2+} extrusion, structurally the most important part of PMCA is autoinhibitory calmodulin binding motif. At low level resting state autoinhibitory calmodulin binding motif remains attached to catalytic site keeping the pump inactive. However, when Ca^{2+} level is elevated by agonist stimulation Ca^{2+} or calmodulin binds to the autoinhibitory calmodulin binding motif, causes the conformational change and it is detached from catalytic site thereby allowing access to Ca^{2+} and subsequently the Ca^{2+} transport (Brown and Dean 2007). PMCA is also activated by the caplain cleavage in platelets as caplains also cleave the autoinhibitory calmodulin binding motif to extrude the Ca^{2+} through plasma membrane (Bruce 2018).

Ca^{2+} extrusion through NCX

In addition to PMCA Ca^{2+} efflux across plasma membrane also takes place through sodium calcium exchanger (NCX). Among all the NCX isoforms NCX3 is expressed more abundantly in platelets. It has been reported that NCX3 exchange three sodium ions (Na^+) for one calcium ion (Ca^{2+}) and worked in the forward mode for Ca^{2+} extrusion (Lytton 2007). It has been suggested that NCX works transiently in reverse mode in collagen stimulated platelets while in thrombin evoked platelets it works in forward mode. But it also creates a pericellular source of Ca^{2+}, in which Ca^{2+} is allowed to accumulate in OCS. Pericellualr Ca^{2+} can create a concentration gradient and Ca^{2+} is recycled back into the cytosol through Ca^{2+} permeable ion channel possibly by adopting reverse mode of NCX (Sage et al. 2013).

Ca^{2+} sequestration by SERCA

An additional way to remove cytosolic Ca^{2+} is its sequestration by the activation of sarco/endoplasmic reticulum Ca^{2+} ATPase (SERCA) pump. Two isoforms of SERCA are present in platelets, SERCA2b on DTS and SERCA3 on acidic stores. Topologically SERCA2b resides centrally and SERCA3 is present more towards periphery. SERCA pump is activated during high level of cytosolic Ca^{2+} and it refills the intracellular stores to maintain the Ca^{2+} level in cytosol (Harper and Sage 2017).
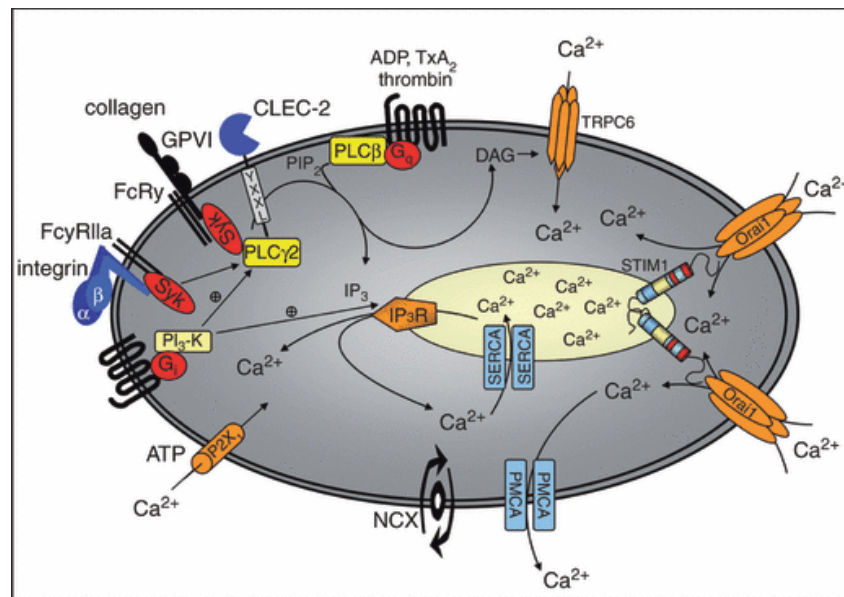
Figure 1.11 Ca^{2+}signaling in platelets: *Ca^{2+} in platelets is released from DTS by the activation of receptors through their respective agonists including collagen, thrombin, ADP, TXA2, and fibrinogen. Cytosolic Ca^{2+} concentration is also increased by direct entry of Ca^{2+} from extracellular milieu through TRPC6, P2X1 and by the activation of SOCE via interaction of STIM1 and Orai1. The counteracting mechanism is also activated to pump cytosolic Ca^{2+} out of the platelet through plasma membrane by PMCA and NCX or by the activation of SERCA to refill the Ca^{2+} stores (Varga-Szabo, Braun, and Nieswandt 2009)*

1.4. Mitochondrial calcium signaling

Besides previously described mechanisms, cytosolic Ca^{2+} level is also regulated by mitochondria to maintain Ca^{2+} homeostasis. However, entry of Ca^{2+} into mitochondria also plays crucial roles in several other cellular functions including metabolism, signaling and cell death. Little is known about mitochondrial Ca^{2+} homeostasis in platelet activation but mitochondrial matrix Ca^{2+} has been reported as a key regulator of ATP synthesis and oxygen consumption along with its participation in the generation of procoagulant platelets. Mitochondrial Ca^{2+} regulates the enzymes of Kreb's cycle and plays a positive role in oxidative phosphorylation (Wang et al. 2014). However, mitochondrial Ca^{2+} overload acts as a stress stimulus, which may lead to opening of mitochondrial Ca^{2+} permeability transition pore (mPTP). The mPTP opening triggers the release of pro-apoptotic proteins subsequently leading to cell death (Mammucari, Gherardi, and Rizzuto

2017). Although outer mitochondrial membrane (OMM) is relatively freely permeable to Ca^{2+} (Sander, Gudermann, and Schredelseker 2021), Ca^{2+} transport through inner membrane (IMM) is tightly regulated by a specialized channel, known as mitochondrial calcium uniporter complex (MCUC) (Patron et al. 2013). The efflux of mitochondrial Ca^{2+} through IMM is mainly controlled by Sodium Ca^{2+} lithium exchanger (NCLX) (Boyman et al. 2013).

1.4.1. Mitochondrial Ca^{2+} influx through outer mitochondrial membrane (OMM)

Ca^{2+} is transported into mitochondria by crossing voltage-dependent anion channel (VDAC) present in the OMM. VDAC is abundantly present on OMM as three isoforms, VDAC1, VDAC2 and VDAC3, and is permeable to Ca^{2+} and other molecules smaller than 5KDa (Romero-Garcia and Prado-Garcia 2019). It is characterized to show a strong cation selection in its closed confirmation, however, in its open form it shows weak anion selectivity (Mertins, Psakis, and Essen 2014). The three isoforms of VDAC can transport Ca^{2+} from cytosol to intermembrane space, but they differ in their specific functions. Principally, IP3R present on ER interacts with VDAC1 and senses low magnitude proapoptotic Ca^{2+} signals. VDACs are also involved in other functions including energy production and regulation of metabolism (Mammucari, Gherardi, and Rizzuto 2017).

1.4.2. Mitochondrial Ca^{2+} influx through inner mitochondrial membrane (IMM)

Mitochondrial Ca^{2+} transport through IMM is tightly regulated by MCUC (Fig 1.12). MCU is a 480KDa complex of multiple proteins, which consists of MCU as a pore forming unit. MCU is a 40KDa protein, comprises of two coil-coiled and two transmembrane domain separated by the small hydrophilic loop containing amino acid residues (Mammucari, Gherardi, and Rizzuto 2017). Both the N and C terminal of MCU face the matrix and each pore forming unit consist of two helical membranes which are connect by a small loop containing DIME motif. DIME motif is negatively charged and it is critically involved in MCU-dependent Ca^{2+} uptake (De Stefani et al. 2011; Martell et al. 2012). The second pore forming protein in the complex is MCUb, which is a 33KDa protein and is encoded by CCDC109b. MCUb showed 50% similarity with MCU with a modified amino acid sequence in DIME motif. It has a dominant negative effect on channel activity (Mammucari, Gherardi, and Rizzuto 2017). MCUb

The uniporter complex comprises of another 10KDa protein known as essential MCU regulator (EMRE), which acts as a structural and regulatory component of MCU.

Structurally EMRE is composed of transmembrane domain, a short N-terminal and a conserved C-terminal domain. As a regulatory protein the function of EMRE is to control the mitochondrial Ca^{2+} overload during Ca^{2+} uptake (Sancak et al. 2013).

Additionally, the three MICU proteins, MICU1, MICU2 and MICU3 are also a part of the MCUC and are localized in IMM containing. MICU1 was the first protein to be identified in MCU complex. It is 54KDa protein with N-terminal containing mitochondrial targeting sequence and two EF hands binding domains. Likewise, MICU2 also contains two EF hands binding domains and it forms a heterodimer with MICU1 by joining through disulfide bond containing conserved residues of cysteine. MICU1 and MICU2 serve as a gatekeeper of MCU channel that sense the rise in cytosolic Ca^{2+} via their EF-hand domains and thus increase the possibility of channel to open (Mammucari, Gherardi, and Rizzuto 2017). MICU1 was identified to prevent small changes in cytosolic Ca^{2+} and, is activated by a strong increase in cytosolic/IMS Ca^{2+}. Recent studies have suggested MICU1 as an inhibitor at low cytosolic Ca^{2+} and a cooperative activator of MCU at high cytosolic Ca^{2+}. However, MICU2 has been proposed to be a negative regulator of MCU. Rise in cytosolic Ca^{2+} is sensed by EF hand domains of MICU1 and MICU2, which undergo a conformational change to promote the Ca^{2+} influx through MCU channel (Wang et al. 2014).

MICU3 is another 55KDa protein of MCUC, structurally it is like MICU1 and MICU2, composed of two EF hand domains and mitochondrial targeting sequence. It shares 34% of sequence similarity with MICU1 and 47% with MICU2. Contrary to MICU1, MICU3 respond more quickly to cytosolic Ca^{2+} changes therefore, deploying a shorter interval between cytosolic Ca^{2+} rise and mitochondrial Ca^{2+} uptake. Therefore, MICU3 exhibits decreased activity of gatekeeping than MICU1. (Patron et al. 2014).

Another regulator of MCU is MCUR1 which is a 40KDa protein residing in IMM. The N and C terminals of MCUR1 are facing towards the inner membrane space (IMS) whereas, the protein sequence is located in matrix of mitochondria. It consists of several domains containing transmembrane domain with two helices, a head domain, β-layer neck, and coiled-coil stalk (Tarasova et al. 2019). In the matrix of the mitochondria, the head domain of MCUR1 is interacted with the N terminal of MCU and is connected through β-layer neck to the stalk which is fastened to the membrane (Adlakha et al. 2019). Studies have suggested that loss of MCUR1 impairs mitochondrial Ca^{2+} uptake and MCUR1 might be

considered as the positive regulator of MCUC. Moreover, MCUR1 is also essential for making a complex of EMRE-MCU and MCUR1 is forms a directly associated with EMRE thus providing a link to complete MCUC assembly (Jin et al. 2019).
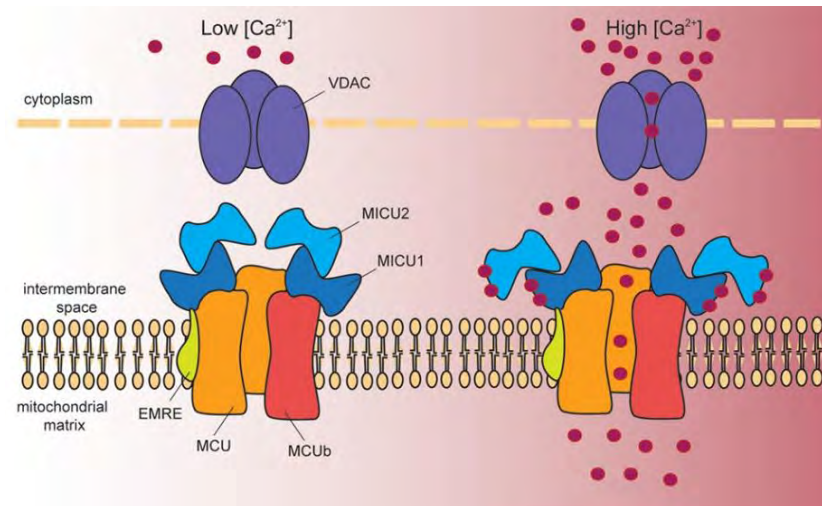
Figure 1.12 Mitochondrial Ca^{2+} influx through MCU: *Cytosolic Ca^{2+} enters the mitochondrial matrix by crossing voltage dependent anionic channel (VDAC) present in the outer mitochondrial membrane (OMM) and through mitochondrial Ca^{2+} uniporter complex (MCUC) in inner mitochondrial membrane (IMM). MCUC consists of a pore forming unit MCU, two gatekeepers MICU1 and MICU2, a negative dominant regulator MCUb and a regulatory protein EMRE. In resting state (left side) when cytosolic Ca^{2+} is low the gatekeepers MICU1 and MICU2 remain closed and do not allow the entry of Ca^{2+} into mitochondrial matrix. However, in an activated state (right side) when there is increased concentration of cytosolic Ca^{2+}, it passes through VDAC and Ca^{2+} ion binds to the EF hand domains of MICU1 and MICU2, which slides away to open the pore of the complex, and allows the influx of Ca^{2+} in mitochondrial matrix(Mammucari, Gherardi, and Rizzuto 2017)*

1.4.3. Mitochondrial Ca^{2+} efflux

Mitochondrial Ca^{2+} efflux is believed to be carried out by hydrogen/calcium exchanger (HCX) and sodium/calcium/lithium exchanger (NCLX) (Carvalho, Stathopulos, and Madesh 2020). It was first reported to be the potassium dependent exchanger and earlier it was named NCKX6. Moreover, it is endogenously expressed in IMM in a monomeric and dimeric form with the size of 50-70KDa monomers and 100KDa dimers. NCLX shares its structural motif similarity with the superfamily of other exchangers like NCLX1-3 and

NCKX1-4 (Boyman et al. 2013). Structurally, NCLX possesses two catalytic domains α1 and α2 attached with the long loop which serves as a regulatory loop. It has PKA-dependent phosphorylation site at serine 258 (S-258). It has been suggested that NCLX is regulated by PTEN-induced putative kinase 1 (PINK1) (Pathak and Trebak 2018). Moreover, it has been suggested that regulatory domain of NCLX contains cluster of positive charges, which form a membrane crossing helix and work as a voltage sensor. Studies showed that this part of channel senses the mitochondrial membrane potential (Ψm) whereas, Ψm provides the driving force for the electrogenic transport of three Na^+ and one Ca^{2+} (Fig 1.13) (Novorolsky et al. 2023). NCLX is the vital and primary route of mitochondrial Ca^{2+} extrusion in excitable cells, which is also essential for maintaining mitochondrial Ca^{2+} homeostasis and inhibiting mitochondrial Ca^{2+} overload in neurons and cardiomyocytes. Thus NCLX is also considered as a promising therapeutic target to protect deleterious effects of mitochondrial Ca^{2+} overload in variety of diseases. In order to understand the regulatory mechanism of NCLX and to modulate the activity of NCLX in therapeutic strategies Garbincius et al has recently identified transmembrane protein 65 (TMEM65) located in the IMM as a potential interactor and regulator of NCLX in cardiomyocytes (Garbincius et al. 2023). In addition to this another channel named sodium/hydrogen exchanger (NHE), is responsible for efflux of Na^+ from mitochondrial matrix to cytosol. It is a major regulator of NCLX activity as it helps to maintain the Na^+ gradient across the IMM (Boyman et al. 2013). Moreover, Hydrogen/Calcium exchanger (CHE) which is identified as a candidate of LETM1 is considered as Ca^+/H^+ antiporter. LETM1 was originally recognized as Potassium/Hydrogen (K^+/H^+) exchanger. In a recent study, it has been reported that LETM1 interacts with transmembrane BAX inhibitor motif containing protein 5 (TMBIM5) to regulate K^+/H^+ exchange in mitochondria, whereas TMBIM5 facilitates the pH dependent mitochondrial Ca^{2+} extrusion (Austin et al. 2022).

Figure 1.13 Ca²⁺efflux through sodium calcium exchanger (NCLX): NCLX consists of two catalytic domains α1 and α1 attached to a regulatory site and docking site. It has a membrane potential (Ψm) sensing site, which senses the Ca²⁺ overload in mitochondrial matrix and exchange three Na⁺ ions with one Ca²⁺ ion. Phosphorylation of NCLX by protein kinase A at Ser258 enhances the exchange of Ca²⁺ (Novorolsky et al. 2023)

1.5. Procoagulant platelets and mitochondrial Ca²⁺

Procoagulant platelets represents a subpopulation of platelets that are phenotypically and functionally different from aggregatory platelets (Kholmukhamedov et al. 2018). Procoagulant platelets are generated upon strong stimulation, which restricts and promotes thrombin generation at the site of vascular injury. They exhibit a negatively charged phosphatidylserine on its surface and sustain the formation of tenase and prothrombinase complex (Veuthey et al. 2022). Several names have been reported for the procoagulant platelets such as superactivated (Mazepa, Hoffman, and Monroe 2013), ballooning (Agbani et al. 2017), capped (Podoplelova et al. 2016), zombie (Storrie 2016), necrotic 4(Hua et al. 2015), SCIP (sustained Ca²⁺-induced platelets) (Kulkarni and Jackson 2004), and COAT platelets. The term COAT explains its activation mode induced by (Collagen And Thrombin) along with their coating with proteins secreted from α-granules (Aliotta et al. 2020). Collagen or convulxin (GPVI agonists) and thrombin are considered to be the most potent agonists of procoagulant platelets (Aliotta, Bertaggia Calderara, and Alberio 2020).Dual stimulation with thrombin and collagen mobilize enough Ca²⁺ signal in

platelets to generate procoagulant platelets, however, single stimulation by either of the agonist can also activate the formation of a low or moderate level of procoagulant platelets (Harper et al. 2013).

One of the key regulator in the intracellular signaling of procoagulant platelets formation is the accumulation of Ca^{2+} in mitochondria through MCU (De Marchi et al. 2014). Studies have suggested that deletion of MCU impairs the formation of procoagulant platelets (Kholmukhamedov et al. 2018). Indeed a high and sustained cytosolic Ca^{2+} induced by dual agonist stimulation is responsible for mPTP opening, thereby resulting in Ca^{2+} leakage from the mitochondria (Abbasian et al. 2020). Inhibition or genetic deletion of cyclophilin D (CyD) (regulator of mPTP) resulted in ablation of mPTP opening and PS exposure (Obydennyy et al. 2016).

1.5.1. Mechanisms of procoagulant platelet formation

Previously, procoagulant platelets were considered to be apoptotic in nature. However, recently a consensus report has been published in which the members of ProCOAGulant and APOptotic platelets (COAGAPO) has suggested that procoagulant platelets undergo necrosis (Josefsson et al. 2023).

Ca^{2+} fluxes, which are triggered by the co-stimulation of collagen and thrombin, generate procoagulant response. However, a great rise in the cytosolic Ca^{2+} concentration is the key element for activated and procoagulant platelets. The sustained cytosolic Ca^{2+} is transported to mitochondrial matrix via MCU that triggers mPTP opening in mitochondria. The opening of mPTP causes a release of Ca^{2+} from mitochondrial leading to a supramaximal Ca^{2+} signal is the cytosol (Veuthey et al. 2022). Moreover, transmembrane 16 (TMEM16) also known as aquaporin 1, present on plasma membrane, allows the entry of Na^+ , Ca^{2+}, Cl^- and water that also promote the higher cytosolic Ca^{2+} concentration,membrane blebbing and balloon formation (Agbani et al. 2018). The other enzymes, which are activated by higher cytosolic Ca^{2+} concentrations, are calpains and scramblases, thus facilitating the membrane remodeling and cytoskeleton rearrangement thereby disrupting membrane integrity (Chu et al. 2021). Scramblases are helpful in flipping of PS from inner leaflet of plasma membrane to outer leaflet, hence facilitating blood coagulation (Abbasian et al. 2020) (Fig 1.14).
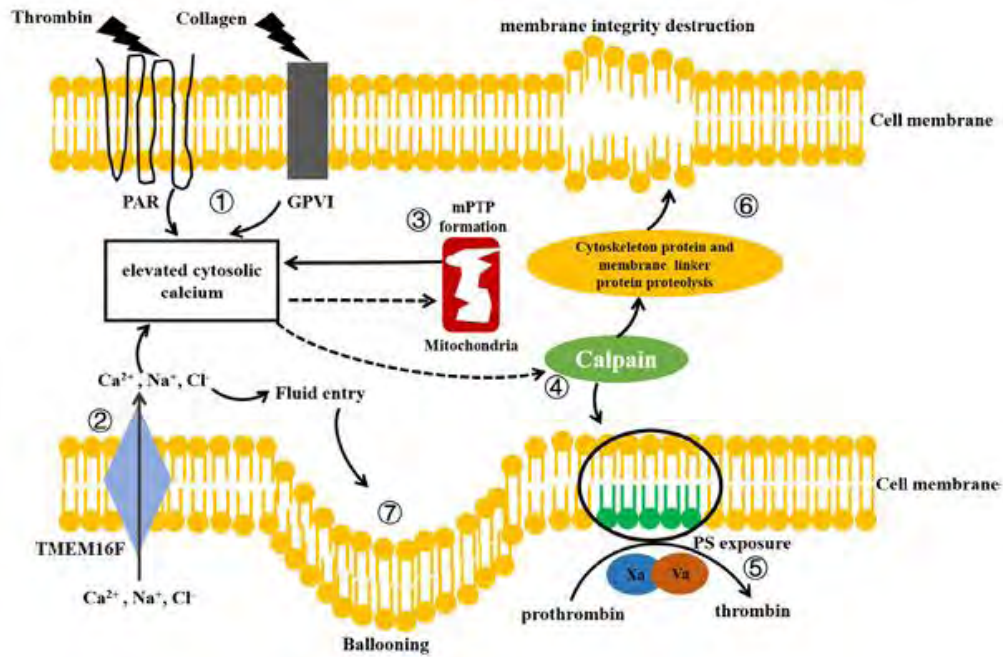
Figure 1.14 Mechanism of procoagulant platelet formation: *Several events take place for the generation of procoagulant platelets (1) dual stimulation of thrombin plus collagen elevates the cytosolic Ca^{2+} (2) TMEM16F present on plasma membrane promotes the entry of Na^+, Ca^{2+}, and Cl^- contributing in elevation of cytosolic Ca^{2+} (3) Ca^{2+} elevation trigger the opening of mitochondrial permeability transition pore (mPTP) in mitochondria, which results in release of Ca^{2+} from mitochondria (4) Increased cytosolic Ca^{2+} activates calpains and scramblases, which flip the phosphotidylserine (PS) from the inner leaflet of plasma membrane to the outer leaflet (5) PS is the prerequisite for the procoagulant activity of platelets as the coagulation proteins bind on the surface of PS converting prothrombin into thrombin (6) Activated calpain destroys the membrane integrity by hydrolyzing the cytoskeleton and membrane linker proteins (7) Fluid entry through TMEM16F causes membrane blebbing, thereby, giving a balloon-like appearance to procoagulant platelets (Chu et al. 2021)*

1.5.2. Characteristics of procoagulant platelets

Procoagulant platelets exhibit special features which differentiate them from aggregating platelets. One of the main feature of procoagulant platelets is externalization of negatively charged phospholipids that is PS. PS exposure provides the site for tenase complex (FVIIIa-FIXa) and prothrombinase complex (FVa-FXa) collectively known as coagulation cascade (Harris and Marles-Wright 2021). Procoagulant platelets are coated with

procoagulant and adhesive protein released from α-granules (Dale 2005). They are retained and irreversibly bound to the surface of coated platelets by serotonin (Dale et al. 2002) and transglutaminase-dependent mechanism (Mattheij et al. 2016). The second important feature of procoagulant platelets is that they lose their aggregatory properties. After strong stimulation all the platelets become pro-aggregatory by activating fibrinogen receptors, though, after 1-2 minutes of activation a population of activated platelets starts distinguishing between aggregation and procoagulant platelet following the phenotypic switch. One of the characteristic of these platelets is downregulation of αIIbβ3 integrin activation (Alberio et al. 2017). After activation, resting platelets change their flattened discoid shape and spread their filopodia, however, when they are adherent on collagen, procoagulant platelets will result in the formation of lamellopodia and consequently undergo membrane blebbing and ballooning (Agbani et al. 2015). Mitochondrial membrane depolarization and opening of mPTP also contributes to procoagulant platelet formation by triggering the sustained signal of supramaximal cytosolic Ca^{2+} (van der Meijden and Heemskerk 2019).

1.6. Aim and Objectives

The main aim of this study is to explore the contribution of mitochondrial Ca^{2+} in agonist-induced platelet responses with following objectives:

1. Contribution of mitochondrial Ca^{2+} influx in agonist-evoked platelet responses.
2. Contribution of mitochondrial Ca^{2+} efflux in agonist-evoked platelet responses.
3. Role of mitochondrial Ca^{2+} in procoagulant platelets.

2. MATERIALS AND METHODS

2.1. Ethical Approval

Ethical approval of the present study was provided by the Institutional Bioethical Committee (IBC) of Quaid-i-Azam University, Islamabad, Pakistan. Healthy individuals were recruited from the Faculty of Biological Sciences of Quaid-i-Azam University, Islamabad, Pakistan, and Transfusion Interregionale CRS, Lausanne, Switzerland. Informed written consent form was signed by the donors who have not ingested any drug, which can affect platelet function including non-steroidal anti-inflammatory drugs (NSAIDs) and aspirin.

2.2. Blood collection

Venous blood was drawn by using 10 ml syringes with 21 ¼ gauge needles in 15 ml, sterile polypropylene, non-pyrogenic conical tubes (SPL Sciences, Germany) containing tri-sodium citrate (Sigma Aldrich, Cat. No. 25116, Germany) as an anticoagulant with 1:9 (1ml sodium citrate + 9ml blood). Moreover, blood was also collected in S-Monovette tube (SARSTEDT, Germany) containing 0.129 mol/L buffered trisodium citrate (pH 5.5). Collected blood was mixed thoroughly with the anticoagulant and was allowed to rest for 15 minutes at room temperature before centrifugation.

2.3. Enrichment of platelets

Platelets were enriched form the collected blood following a differential centrifugation approach. Isolated blood was centrifuged in swing bucket centrifuge machine (Kokusan Model H-103RS, Japan) at 200g for 20 minutes at room temperature. Plasma (2/3) was carefully transferred to a new polypropylene tube without disturbing the layers of buffy coat and red blood cells (RBCs). In order to avoid the contamination of WBCs second centrifugation was performed at 100g for 10 minutes at room temperature (Fig 2.1). Platelet rich plasma (PRP) was separated in a new tube and was used in further experiments.
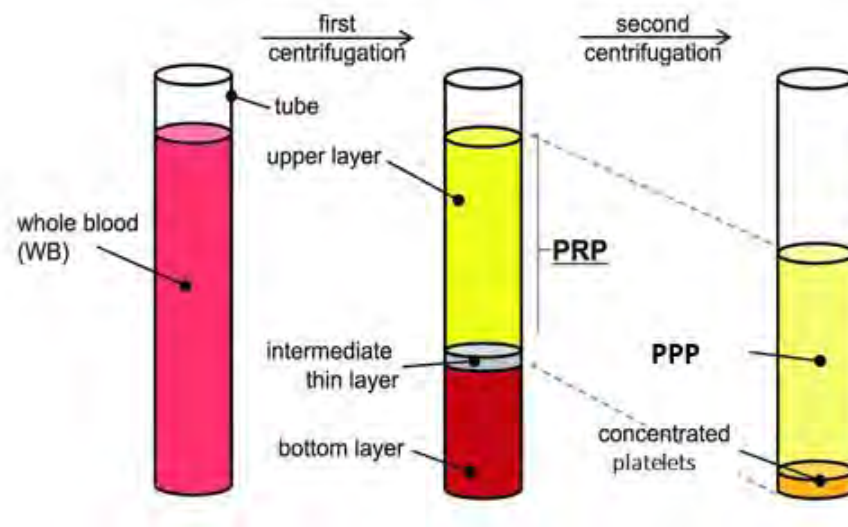
Figure 2.1 Differential centrifugation for the separation of Platelet Rich Plasma (PRP): Whole blood was centrifuged to get three layers: upper layer of PRP, intermediate buffy coat or WBCs and bottom layer of red blood cells (RBCs). Second centrifugation was done to get the enriched platelets [adopted and modified from (Piao, Park, and Jo 2017)]

2.4. Preparation of washed Platelets

In order to remove the plasma of platelets, platelet washing was done by employing a third centrifugation step in fixed angled rotor. PRP was centrifuged at 2000g for 5 minutes at room temperature in the presence of 0.5 µM PGI_2 (Santa Cruz, Cat. No. Sc-201231, USA) by using microcentrifuge machine (Heraeus Fresco 17 Centrifuge, ThermoFisher Scientific USA). Platelet pellet was settled down and platelet poor plasma (PPP) was removed from the top. Platelet pellet was resuspended in modified Tyrod's Buffer (containing NaCl 140mM, Glucose 5mM, KCl 5mM, HEPES 10mM, $MgCl_2$ 1mM) and kept on a home-built rotary mixer at 37^0C till further experiments.

2.5. Platelet Counting

Platelets were counted manually on a Neubauer's counting chambre (Superior Marienfeld, Germany). PRP or washed platelets were diluted 20 times (1/20) in Tyrod's Buffer. About 20µl of PRP or washed platelets were loaded on the counting chambre, covered with the coverslip, and were allowed to rest at room temperature for 12 minutes. Neubauer's counting chambre was placed under a microscope (IRMECO GmbH Model –IM-850,

Germany). Platelets were counted in four corners and one middle square of central big square marked as red in Fig 2.2 using 40X objective. Platelet number was determined by given formula and volume of counted platelets was further adjusted with Tyrod's buffer for further experiments.

$$Platelets/\mu l = \frac{No\ of\ platelets\ counted \times Dilution\ factor}{No\ of\ squares\ counted \times area\ of\ chamber \times depth\ of\ chamber}$$
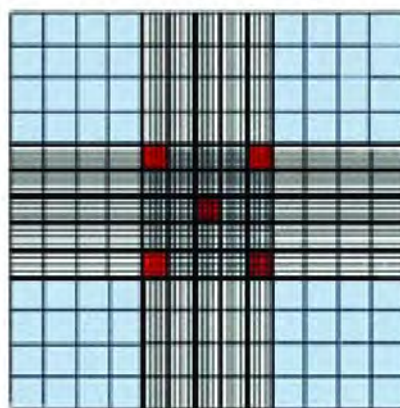
Figure 2.2 Neubauer's Counting Chamber: *Platelets are counted in the red marked boxes of central big square.*

2.6. Platelet aggregation on microplate-based spectrophotometer

Platelet aggregation was optimized on a microplate-based spectrophotometer (Multiskan Go, ThermoFisher, USA) using a time-lapsed assay under the principle of light transmission aggregometry. Platelet count was adjusted to 150,000/μl with modified Tyrod's Buffer and 200 μl of PRP was added in each well of the polystyrene 96-well microplate (SPL, South Korea). PRP was pre-incubated either with 20 μM mitoxantrone (MTX, Santa Cruz Cat no. sc-203136, USA), 200mU Apyrase for 5 minutes or CGP37157 (CGP, Santa Cruz Cat no. sc-203136, USA) or its vehicle dimethyl dulphoxide (DMSO, 20385.01, Serva GmbH, Germany). Protocol for platelet aggregation was designed on Skanit software (Thermo Fisher Scientific, USA) containing two kinetic loops with constant shaking after every 5 seconds. In the first kinetic loop initial absorbance was measured at 595nm without the addition of agonist. In the second kinetic loop 10 μM Adrenaline (AD) and 20μM of ADP was added to PRP in their respective wells and absorbance was measured at 595nm every 5 second for a period of 15 minutes with constant shaking of microplate at room temperature.

2.7. Platelet aggregation measurement on aggregometer

Platelet aggregation was also measured on light transmission aggregometer with strong agonist like thrombin and convulxin (APACT 4004VR; LABiTec GmbH Ahrensburg, Germany). Instrument was first calibrated with cuvette containing 200µl platelet poor plasma (PPP). Platelet count was adjusted to 200,000/µl and 2mM of GPRP (Gly-Pro-Arg-Pro) (Bachem Cat no H-2935.0100 Bubendorf, Switzerland) was added to inhibit fibrin polymerization. PRP was loaded in the cuvette and pre-incubated with 20 µM MTX orDMSO. Aggregation was measuredfor 10 minutes after addition of 0.5U/ml and 5U/ml of thrombin (THR) or 0.06ng/ml, 2ng/ml and 500ng/ml of convulxin (CVX).

2.8. MTT Assay for measuring mitochondrial dehydrogenase activity

MTT (3-(4,5-dimethylthiazol-2-yl)-2,5-diphenyltetrazolium bromide (Serva, Cat no. 20395-03, Germany) assay was performed to measure the mitochondrial dehydrogenase activity in platelets. Yellow colour water-soluble salt of MTT is reduced to purple insoluble formazan crystals by NADPH-dependent oxidoreductase enzymes (Fig 2.3). The assay was performed using 200µl of washed platelets by count adjusting the platelet count to 100,000-150,000/µl. Washed platelets were pretreated with either 20µM MTX or DMSO , followed by stimulation with 10µM AD in the presence of 2mM $CaCl_2$ and kept on rotation at 37°C for 5 minutes. The salt solution of 1mg/ml of MTT was added to washed platelets and incubated for 1 hour at 37°C in dark with constant rotation. After incubation platelets were settled down by centrifuging at 2000g for 5 minutes at room temperature. The purple formazan crystals were lysed by adding 250 µl 100% DMSO, incubated for 10 minutes at 37°C and absorbance was measured on MultiSkan Go at 570nm.
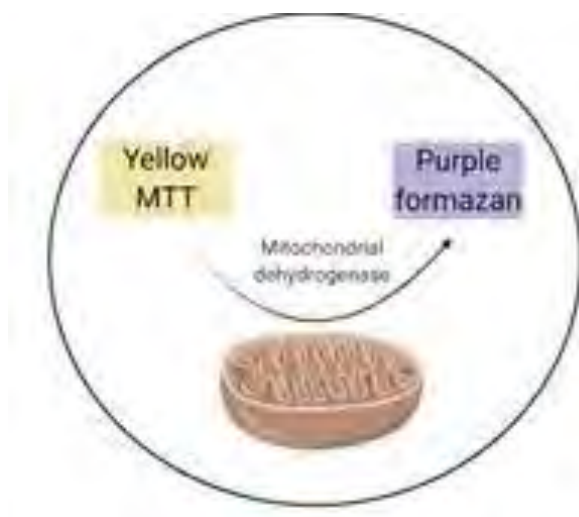
Figure 2.3 MTT assay: *The yellow MTT salt is converted into the purple formazan crystals by the mitochondrial dehydrogenase activity.*

2.9. Trypan blue dye exclusion assay

Trypan blue dye exclusion assay was done to determine the cytotoxic effect of drugs on platelet. Cells with intact plasma membrane exclude the trypan blue dye whereas in the dead cells trypan blue dye penetrate the porous membrane and enter the cell. Platelets were treated either with DMSO or MTX for 20 and 60 minutes and with CGP for 5, 60 and 120 minutes at 37°C. Treated platelet suspension was mixed with trypan blue dye (1:1) (Cat No. 15250061, Thermo Fisher Scientific, USA), 10µl of the suspension was loaded on Neubauer's counting chamber and was allowed to rest for 12 minutes at room temperature. Platelets were counted on microscope under 40X lens and percentage of viable cells were calculated.

2.10. LDH assay

Platelet viability was also assessed by lactate dehydrogenase (LDH) release using LDH assay kit (AMP Diagnostics, Austria). Platelet count was adjusted to 150,000/µl and 200µl of platelets were treated either with DMSO (vehicle) or 20 µM MTX at 5 and 60 minutes and 0.1 µM CGP at 5, 60 and 120 minutes. Additionally, platelets were lysed by adding radioimmunoprecipitation (RIPA) assay buffer to use as positive control for the assay. Treated platelets were pelleted down at 2000g for 5 minutes at room temperature and 10µl of suspension was mixed with 500µl working reagent (4ml Reagent A + 1ml Reagent B). Spectrophotometer was set at 37°C and absorbance was recorded at 340nm for 3 minutes

at 1 minute interval. LDH concentration was calculated by multiplying the mean absorbance difference with a factor provided in kit literature.

2.11. RNA extraction

Total RNA from platelets was extracted using TRIzol reagent (Thermo Fisher, USA) using manufacturer's protocol. Briefly, platelets were lysed using 1ml of TRIzol reagent with incubation of about 20 minutes at room temperature. Chilled chloroform (200µl) was added and mixed well followed by centrifugation at 12000 RPM for 15 minutes at 4°C in order to separate the solution into aqueous and organic phase. Aqueous phase was carefully separated and chilled isopropanol was added (1:1) and incubated on ice for 10 minutes in order to precipitate the RNA. Solution was centrifuged at 12000 RPM for 10 minutes at 4°C. Supernatant was discarded and RNA pellet was washed with 70% ethanol followed by centrifugation at 7500 RPM for 5 minutes at 4°C. Ethanol was removed and RNA pellet was allowed to air dry. RNA was resuspended in 20µl nuclease free water and kept in dry bath at 50°C for 5 minutes to complete the reconstitution.

2.11.1. cDNA synthesis

The concentration of RNA was quantified on Nanodrop (Titertek Berthold, Germany) and 500ng of isolated RNA was reverse transcribed to cDNA with RevertAid First Strand cDNA synthesis kit (Thermo Fisher Scientific, USA) using a Thermocycler (Biometra, Germany). The reverse transcription master mix and thermal cycler protocol are given in table 2.1 and table 2.2.

Table 2.1: Recipe of Reverse Transcription Reaction Mixture

Reverse Transcription Master Mix	
Reagents	**Volume/20µl**
Total RNA	500ng
Random Hexamers	1 µl
5X Reaction buffer	4 µl
RiboLock RNAase inhibitor (20U/µl)	1 µl
10mM dNTP Mix	2 µl
RevertAid M-MuLVRT (200U/µl)	1 µl
Nuclease free water	11 µl

Table 2.2 protocol of Thermocycler for cDNA synthesis

Thermocycler protocol		
Steps	**Temperature**	**Time**
Step 1	25ºC	5 minutes
Step 2	42ºC	60 minutes
Step 3	70ºC	5 minutes
Step 4	4 ºC	∞

2.11.2. Primer Designing

Primers for qPCR were designed at exon-exon junction of the candidate genes. NM number or gene sequence of genes was taken from Genebank data base tool National Center of Biotechnology Information (NCBI). Primers were designed using an online

Integrated DNA Technology (IDT, USA) under its application of qPCR assay design using RealTime PCR tool. In order to access the specificity and single hit of primers, they were analysed in UCSC browser In-Silico PCR. Furthermore, in order to compare nucleotide sequence similarity between different organisms Basic Local Alignment Search Tool (nBLAST) was used. The sequence of primers are given in table 2.3.

Table 2.3 Primers Sequence

Primers sequence			
Name	**Sequence**	**Temperature**	**Product**
GAPDH RTF	TCAACGACCACTTTGTCAAGC	60 °C	110bp
GAPDH RTR	CCAGGGGTCTTACTCCTTGG	60 °C	
MCU RTF	TTCCTGGCAGAATTTGGGAG	60 °C	148bp
MCU RTR	AGAGATAGGCTTGAGTGTGAAC	60 °C	
NCLX1 RTF	ACCATCCTACACCCCTTCA	60 °C	148bp
NCLX1 RTR	ACACATACAAGCCCAGGTAAC	60 °C	

2.11.3. Polymerase chain reaction (PCR) Amplification

The expression of GAPDH, MCU and NCLX was assessed by amplification of polymerase chain reaction using conventional PCR and agarose gel electrophoresis. The reaction mixture for PCR and protocol for PCR amplification reaction given in table 2.4 and table 2.5. The amplified PCR products were visualized by ethidium bromide on agarose gel electrophoresis and documented with a Gel Documentation System using GeneSnap software (Syngene, UK).

Table 2.4 PCR Reaction Mixture

PCR Reaction Mixture	
Reagents	**Volume/25 μl**
10X Taq Buffer	2.5 μl
MgCl2 25mM	1.5 μl
dNTPs (10mM)	0.5 μl
Taq DNA polymerase (5U/ul)	0.2 μl
Forward Primer (0.4uM)	1 μl
Reverse Primer (0.4uM)	1 μl
cDNA Sample	1 μl
Nuclease free water	17.3 μl

Table 2.5 PCR Amplification steps

PCR Amplification Steps		
Steps	**Temperature**	**Time**
Initial Denaturation	95 ^{o}C	10 minutes
Denaturation	95 ^{o}C	1 minute
Annealing	60 ^{o}C	1 minute
Extension	72 ^{o}C	1 minute
Final Extension	72 ^{o}C	10 minutes
Hold	4°C	∞

(40 cycles — Annealing, Extension, Final Extension)

2.11.4. Real Time PCR

In our study we determined the relative expression of MCU and NCLX in platelets cDNA using SybrGreen master mix (Thermo Fisher,USA) on MyGo Pro Real-Time PCR System (IT-IS Life Science Ltd.). The reaction mixture recipe for SybrGreen and the protocol of real time PCR is given in table 2.6 and table 2.7.

Table 2.6 SybrGreen Reaction mixture for real time PCR

SybrGreen Reaction mixture	
Reagents	**Volume/10 µl**
SybrGreen master mix	5 µl
Forward Primer	1 µl
Reverse Primer	1 µl
cDNA	3 µl

Table 2.7 Protocol for real Time PCR

Real time PCR protocol		
Steps	**Temperature**	**Time**
Hold	95 ºC	60 seconds
3 step Amplification 45 cycles	95 ºC	15 seconds
	60 ºC	30 seconds
	72 ºC	30 seconds
Pre-melt hold	95 ºC	10 seconds

2.12. Assessment of platelet activation endpoints by flow cytometry

PRP was separated from the whole blood by already explained method in section 2.3. Platelets were counted on XP-300 automated haematology analyzer (Sysmex Corporation, Kobe, Japan) and was allowed to rest at room temperature for at least 30 minutes before proceeding to flow cytometry measurement.

Platelet count was adjusted to $5 \times 10^3/\mu l$ with 100 µl HEPES buffer (140 mM NaCl, 2.5 mM CaCl2, 10 mM HEPES, pH 7.4) Becton Dickinson (Allschwil, Switzerland) and was supplemented with 2mM GPRP (Bachem Cat no H-2935.0100 Bubendorf, Switzerland) to inhibit clotting. Platelets were preincubated with 20µM MTX or DMSO for 5 minutes or 0.1µM CGP-37157 or DMSO for 60 minutes at room temperature in dark followed by stimulation with either 20µM ADP for 15 minutes at 37°C, 0.5U/ml thrombin or 500ng/ml convulxin for 8 minutes at 37°C. Platelet activation marker for granule release and integrin activation was determined by adding 5µl p-selectin using anti-CD62P-PE antibody (Cat no. 555523 BD Pharmingen, USA) and 5µl PAC-1-FITC (Cat no. 1P-145-T100 Exbio, Czech Republic) respectively. Volume was adjusted to 1000 µl with calcium-containing HEPES buffer and 10,000 events were counted on flow cytometer (BD accuri C6) for the assessment of platelet activation endpoints (Fig 2.4).
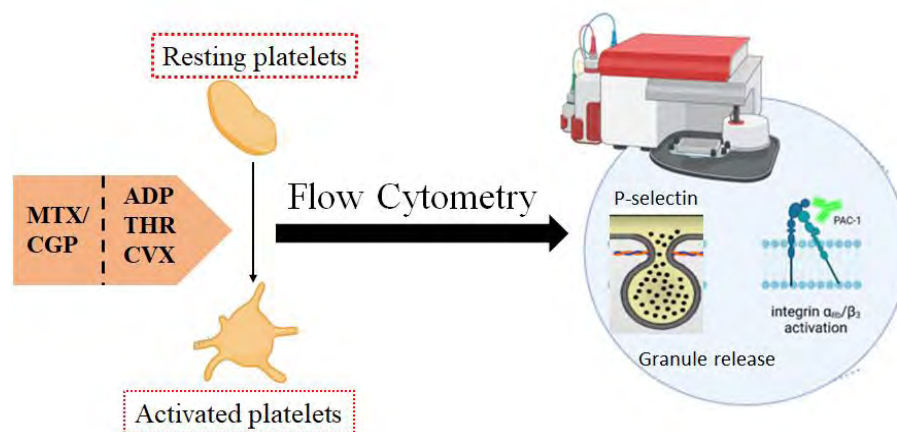
Figure 2.4 Assessment of platelet activation endpoints by flow cytometry: *Platelets were preincubated with MTX CGP or DMSO and then stimulated with ADP, thrombin (THR), or convulxin (CVX). Flow cytometry was employed to determine the granule release by p-selectin expression and integrin activation by PAC-1 binding*

2.13. Assessment of procoagulant platelets

PRP (5×10^3 platelets/µl) was diluted with calcium-containing HEPES buffer with the addition of 2mM GPRP. Platelets were pretreated with two different inhibitors of MCU i.e. 20µM MTX for 5 minutes and 10µM at room temperature and Ru265 for 15 minutes at 37°C. Preincubated platelets were activated with different concentrations (0.5U/ml, 5U/ml and 10U/ml) of thrombin and convulxin (2ng/ml, 500ng/ml) or with dual stimulation of 0.5U/ml thrombin plus 500ng/ml convulxin. Procoagulant activity of platelets were determined by measuring the binding of PS with Annexin V-FITC (Cat no. 640905, Biolegend USA) and integrin αIIbβ3 with PAC-1-FITC (Cat no. 1P-145-T100 Exbio, Czech Republic) by counting 10,000 events on flow cytometer.

2.14. Determination of mitochondrial membrane potential

Platelets (30×10^3 platelets/µl) were loaded with 5µM TMRM (Cat no. 22221 AAT Bioquest, USA) for 15 mins in dark in home-made Tyrode's buffer (containing 137 mM NaCl, 2.8 mM KCl, 12 mM NaHCO3, 1 mM MgCl2, 0.4 mM NaH2PO4, 10 mM HEPES, 3.5 mg/ml bovine serum albumin, 5.5 mM glucose, adjusted to pH 7.4 with NaOH). Loaded platelets were diluted to 10×10^3 platelets/ µl with Tyrode's buffer containing 2.5mM calcium. Platelets were pretreated with 20µM MTX for 5 minutes or 0.1µM CGP-37157 for 30 minutes and 60 minutes at room temperature in dark and then activated by the addition of 20µM ADP for 15 mins at 37°C. Platelets were finally diluted to 5×10^3 platelets/ µl with calcium-containing HEPES buffer and 10,000 events were acquired on flow cytometer.

2.15. Measurement of cytosolic Ca^{2+}

Cytosolic Ca^{2+} was measured by incubating 30×10^3/µl platelets with 2µM Fluo-3 AM (Cat no. F1242 Thermo Fisher, USA) for 60 minutes in the dark. Loaded platelets were incubated with 20µM MTX for 5 mins or 0.1µM CGP-37157 for 60 minutes at room temperature in dark. Platelets were further diluted to 2.5×10^3/µl with 2.5mM calcium-containing Tyrode's buffer. Kinetics of cytosolic Ca^{2+} were measured on flow cytometer by acquiring the baseline reading for 1 minute followed by immediate activation with 20µM ADP and reading was further recorded for another 15 minutes.

2.16. Statistical analysis

For the kinetic experiments, data was normalized with the basal reading and plotted against time on x-axis. The curves were statistically analysed by calculating amplitude using MS

excel (Microsoft, USA). Data was presented as mean ± SEM in GraphPad Prism (version 5, GraphPad Software, Inc. USA). Statistical differences between groups were calculated using student's T-test or one-way ANOVA with Tuckey's multigroup comparison post-hoc test respectively. A p-value less than 0.05 ($P<0.05$) was considered statistically significant.

3.   RESULTS

3.1. Confirmation of MCU and NCLX genes in human platelets

Mitochondrial Ca^{2+} influx and efflux pathways are tightly regulated by mitochondrial calcium uniporter (MCU) and Sodium-Calcium-Lithium Exchanger (NCLX) respectively. However, in order to identify the role of mitochondrial Ca^{2+} homeostasis in platelet physiology, we first confirmed the presence of MCU and NCLX in human platelets. Our results showed the presence of both MCU and NCLX in human platelets with relatively low abundance of NCLX in comparison to MCU (Fig 3.1a & 3.1b).

3.2. MTX did not alter platelet viability and pre-activation

Mitoxantrone (MTX) has been conventionally used as an anti-neoplastic drug that has been used in different cell types where it inhibited the activity of topoisomerase-II (Mikusová et al. 2011). In order to rule out the cytotoxic effect of MTX on platelets we determined platelets viability by trypan blue dye exclusion assay, Lactate dehydrogenase (LDH) release and Annexin-V binding assay. Our results revealed that MTX treatment for 20 and 60 minutes did not alter number of viable cells as determined by trypan blue exclusion assay (Fig 3.2 a). Similarly, it was noticed that platelets remained intact and there was no release of lactate dehydrogenase (LDH) after incubation of MTX for 5 and 60 minutes, while a remarkable release of LDH was observed in lysed platelets (Fig 3.2 b). Moreover, probability of cell death associated with phosphatidylserine (PS) externalization was also excluded as MTX treatment did not affect Annexin-V binding (Fig 3.2 e). Furthermore, we also investigated the effect of MTX on platelets pre-activation in unstimulated platelets by assessing the markers of platelet activation measured by p-selectin and PAC-1 binding. In line with our expectations, we did not observe any significant change in platelet degranulation and integrin activation in the presence of MTX (Fig 3.2 c & 3.2 d).

3.3. CGP37157 (NCLX inhibitor) did not impact platelets integrity and preactivation

CGP37157 (CGP) is a benzodiazepine compound that is is commonly employed as a pharmacological inhibitor of NCLX (Ruiz, Alberdi, and Matute 2014). Before performing the platelet functional measurement, we investigated its impact on platelet integrity by using trypan blue dye exclusion assay, LDH release assay and Annexin V assay. In line with our hypothesis, platelet treatment with CGP for 5, 60 and 120 minutes didn't trigger

any cytotoxicity as indicated by no change in percentage of trypan blue positive cells and LDH release (Fig 3.3a & 3.3b). Similarly, the Annexin V binding representing the externalization of PS (an indicator of apoptosis) was also not observed after CGP treatment for 60 minutes (Fig 3.3e). To further explore the platelet preactivation by CGP, we assessed alpha granule secretion and conformation-dependent αIIbβ3 activation using anti-p-selectin and PAC-1 antibodies respectively. Our data revealed that resting platelets remained unchanged upon treatment with CGP as indicated by no change in p-selectin exposure and PAC-1 binding. (Fig 3.3c & 3.3d).

.
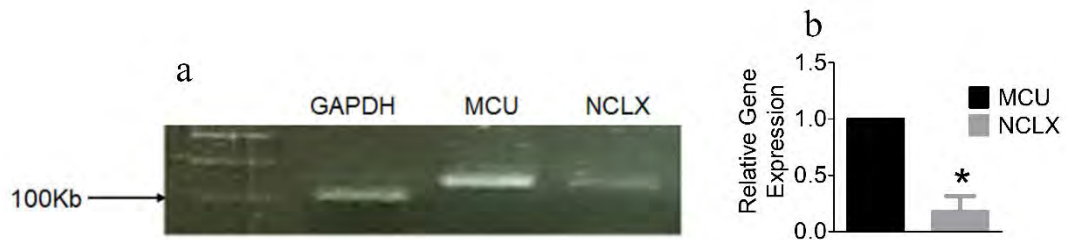
Figure 3.1. MCU and NCLX are expressed in human platelets: (a) PCR products showing the presence of MCU, NCLX and GAPDH (Control) mRNAs in agarose gel images stained with ethidium bromide. (b) Relative mRNA abundance was assessed by Real-Time qPCR. Data represents mean ± SEM and analysed using one-tailed paired T test, n=3 *p<0.05.
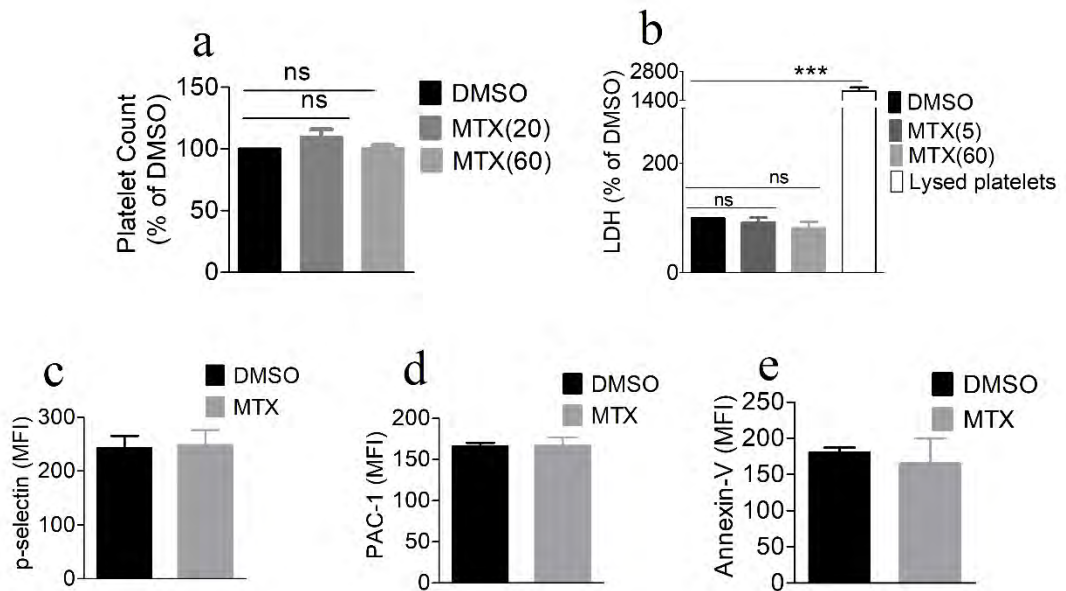
Figure 3.2. Platelets viability and pre-activation remained unaffected by MTX treatment: *Platelets viability was determined by (a) trypan blue exclusion assay after treatment with 20μM MTX for 20 and 60 minutes (b) Lactate dehydrogenase (LDH) release after treatment with 20μM MTX for 5 and 60 minutes. DMSO is used as vehicle and lysed platelets were used as positive control for the assay. Platelets pre-activation was determined by mean florescence (c) P-selectin-FITC (d) PAC-1-FITC after treatment with 20μM MTX for 5 minutes. Platelets cytotoxicity was corroborated by determining the of (e) Annexin-V in the presence of 20μM MTX for 5 minutes. Data represents mean ± SEM and analysed with one-way ANOVA using Tuckey's post-hoc test and one-tailed T-test, n=3, ***p<0.001, ns=non-significant. MTX(5)= platelets + 20 μM MTX for 5 minutes MTX (20) = platelets + 20 μM MTX for 20 minutes, MTX (60) = platelets + 20 μM MTX for 60 minutes.*
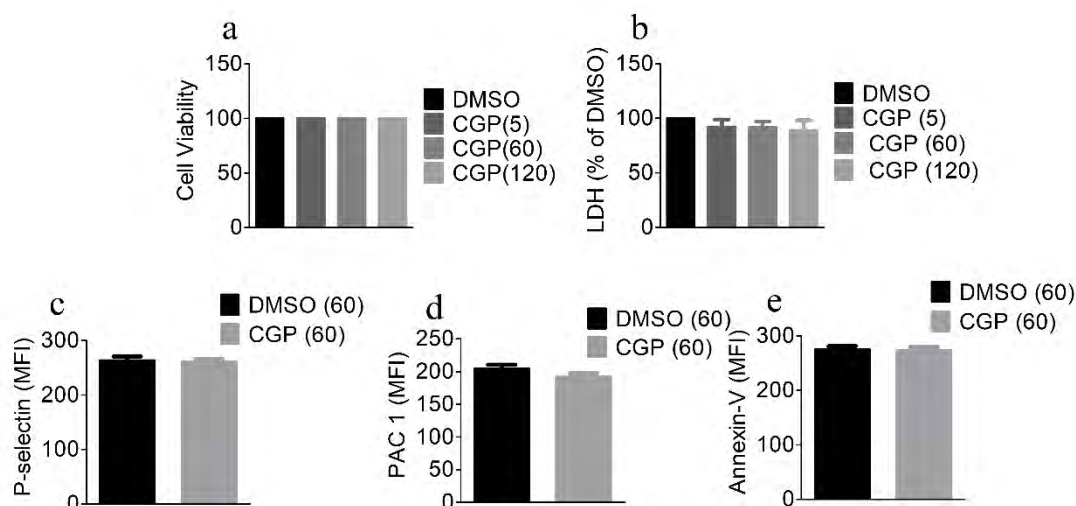
Figure 3.3. CGP treatment yielded no effect on platelet viability and pre-activation: Platelets viability was determined by (a) trypan blue dye exclusion assay after treatment with 0.1μM CGP for 5, 60 and 120 minutes (b) Lactate dehydrogenase (LDH) release after treatment with 0.1μM CGP for 5, 60 and 120 minutes. DMSO was used as vehicle. Platelets pre-activation was determined by the MFI of (c) P-selectin-FITC (d) PAC-1-FITC after treatment with 0.1μM CGP for 60 minutes. Platelets cytotoxicity was measured by the MFI of (e) Annexin-V after treatment with 0.1 μM CGP for 60 minutes. Data is represented by mean ± SEM and analysed statistically with one-way ANOVA using Tuckey's post-hoc test and one-tailed T-test, ns=non-significant. CGP(5)= platelets+0.1 CGP for 5 minutes, CGP(60) = platelets+0.1 μM CGP for 60 minutes, CGP(120) = platelets+0.1 μM CGP for 120 minutes.

3.4. Inhibition of mitochondrial Ca^{2+} influx by MTX inhibited ADP-induced platelet aggregation

Platelet aggregation is generally measured using commercially available aggregometers, but here we optimized the aggregation profiling using a time-lapsed assay on a microplate-based spectrophotometer. Our results demonstrated that upon stimulation with ADP a strong drop in aggregation curve was observed indicating a significant rise in platelet aggregation (Fig 3.4). We investigated the function of mitochondrial Ca^{2+} influx by using a pharmacological inhibitor of mitochondrial Ca^{2+} influx protein MCU i.e. mitoxantone (MTX). Our data revealed the fact that by blocking the platelets with 20µM MTX for 5 minutes platelet aggregation was remarkably reduced in the presence of ADP, whereas a longer incubation of MTX for 60 minutes did not further enhance its effect on platelet aggregation (Fig 3.4a & 3.4b). Our data highlights the fact that MTX inhibited the platelet aggregation in time-independent manner. Moreover, to further explain the role of MTX on platelet aggregation we incubated the platelets with 5µM and 10µM MTX. Our data demonstrated that with a higher dose (10µM) MTX significantly reduced platelet aggregation (Fig 3.4c & 3.4d), whereas, by reducing the dose of MTX (5µM) platelet aggregation remained unaffected (Fig 3.4e & 3.4f). Furthermore, the analysis of inhibitory responses of MTX at different concentrations delineated the fact that MTX attenuated the ADP-induced platelet aggregation in a dose-dependent manner (Fig 3.4g).

3.4.1. ADP-stimulated granule secretion and conformational activation of αIIbβ3 were diminished by MTX

The secretion of platelet alpha-granules and conformation-dependent activation of αIIbβ3 are necessary for platelet activation that leads to their aggregation and clot formation. We assessed the ADP-evoked platelet activation by examining the 1) surface expression of p-selectin that is a marker for exocytosis of alpha granules and 2) conformation-dependent activation of αIIbβ3 using a combination of fluorescently-labelled antibodies and flow cytometery. ADP stimulation triggered a notable increase in the surface exposure of p-selectin as represented by a significant increase in the mean fluorescence intensity (MFI) as compared to unstimulated platelets. (Fig 3.5a & 3.5b). Similarly, there was remarkable increase in the straightening αIIbβ3 as indicates by a significant increase in PAC-1 binding in response to ADP stimulation (Fig. 3.5c & 3.5d). Interestingly and in line with platelet aggregation, platelet treatment with MTX (20 µM) for a short time (5 minutes) caused a

remarkable reduction of both p-selectin externalization (Fig. 3.5e & 3.5f) and integrin $\alpha IIb\beta 3$ activation (Fig. 3.5g & 3.5h) as confirmed by a marked decline in the platelet MFI. It was noted that the platelet pre-treatment with MTX resulted in a more pronounced reduction of $\alpha IIb\beta 3$ activation as compared to the p-selectin surface exposure (84.6% vs 40.9%) (Fig 3.5f & h).

In order to further validate these findings, we assessed the concentration-dependent influence of MTX on ADP-evoked p-selectin surface expression and $\alpha IIb\beta 3$ activation. For this purpose, seven different doses of MTX (0.1 μM - 30 μM) were used to pre-treat platelets for 5 minutes. In line with the previous data, we observed a concentration-dependent effect of MTX on ADP-stimulated platelet activation as measured by by p-selectin surface exposure (Fig 3.5i), and integrin $\alpha IIb\beta 3$ activation (Fig 3.5j). Similar to aforementioned results, MTX treatment yielded a greater inhibitory effect on integrin $\alpha IIb\beta 3$ activation as compared to inhibition of p-selectin surface exposure (Fig 8i & 8j). The half-maximal inhibitory dose (IC50) of MTX was found to be 3.259 μM for p-selectin while it was 2.828μM PAC-1..
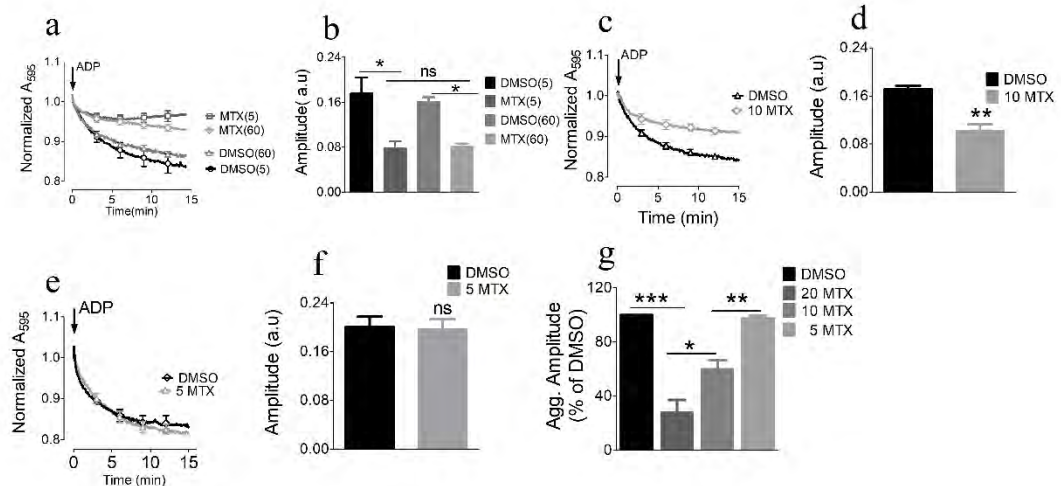
Figure 3.4. ADP-evoked platelet aggregation was attenuated by MTX: *(a) Platelet aggregation profile is represented as average curve of several sample that shows a clear drop in absorbance upon stimulation with 20μM ADP. Platelet werepre-incubated with DMSO or 20μM MTX for 5 and 60 minutes (b) Amplitudes of all curves were calculated and represented as mean ± SEM. (c-f) Platelet aggregation after pre-treatment with 10 μM and 10 μM MTX for 5 minutes. (g) Relative comparison of different concentrations of MTX on ADP-stimulated platelet aggregation. Data represents mean ± SEM and statistically analysed using one-tailed unpaired T-test and One-way ANOVA with Tuckey's post-hoc test. n=3, ***p<0.001, **p<0.01, and *p<0.05. DMSO= Platelets + DMSO + ADP, MTX (5) = platelets + 20 μM MTX for 5 minutes+20 μM ADP, MTX (60) = platelets+20 μM.MTX for 60 minutes+20 μM ADP, 10MTX = platelets + 10 μM MTX for 5 minutes+20 μM ADP and 5 MTX = platelets + 5 μM MTX + ADP, ns = non-significant.*
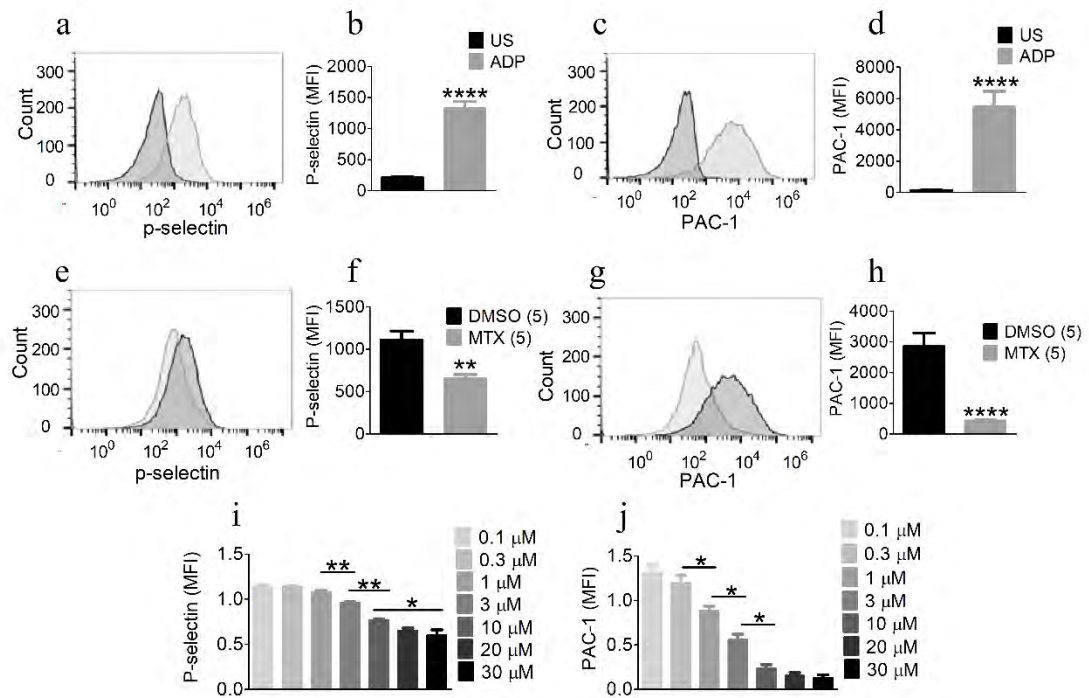
Figure 3.5. MTX inhibited ADP-stimulated platelet activation endpoints: *(a& c) Representative histograms showing changes in the florescence intensity of p-selectin and PAC-1 in ADP-stimulated platelets (Dark grey) vs unstimulated platelets (Light grey) . (b & d) MFI of p-selectin and PAC-1 from all samples shown as mean ± SEM,. Histograms with bar chart showing significant decrease in MFI of ADP-induced (e & f) p-selectin expression and (g & h) PAC-1 after MTX pre-treatment (light grey) vs DMSO (dark grey). (I & J) Dose-dependent effect of MTX at 7 different concentrations on ADP-induced p-selectin expression and PAC-1 binding. Data represents mean ± SEM and analysed by one-tailed unpaired T-test and One-way ANOVA with Tuckey's post-hoc test, n=4-7, *p<0.05, **p<0.01, ***p<0.001, ****p<0.0001. DMSO (5) = platelets + DMSO incubated for 5 mins, MTX (5) = platelets + MTX incubated for 5 mins.*

3.4.2. ADP-stimulated platelet aggregation was enhanced upon NCLX inhibition with CGP37157

Previously, we determined the contribution of mitochondrial Ca^{2+} influx pathway in platelet responses. Here, we investigated the mitochondrial Ca^{2+} efflux pathway by exploring the role of NCLX in platelet aggregation. We elucidated the involvement of NCLX in ADP-evoked platelet responses by employing a pharmacological blocker of NCLX i.e. CGP37157 (CGP). We first measured the time-dependent effect of CGP pre-treatment on ADP-induced platelet aggregation profile at a concentration of 0.1 µM for 5, 60 and 120 minutes). Although we did not observe any considerable effect of CGP at 5 minutes (Fig 3.6 a & 3.6b), there was a substantial rise in the platelet aggregation at 60 and 120 minutes. Interestingly, there was no notable difference in platelet aggregation when compared between 60 and 120 minutes highlighting a maximal impact of CGP after 60 minutes (Fig 3.6c-3.6f). Contrary to the time-dependent effect, CGP did not alter the response of platelet aggregation when its concentration was by increased to 1µM and 10µM (Fig 3.7a-f).

3.4.3. Platelet surface expression of p-selectin and activation of integrin αIIbβ3 upon ADP stimulation was substantially enhanced by NCLX inhibition

To further complement our data, we assessed ADP-induced p-selectin expression and αIIbβ3 activation in CGP-pretreated platelets. Intriguingly, the surface exposure of p-selectin upon stimulation with ADP was significantly increased after platelet pretreatment with 0.1µM CGP (Fig 3.8a & 3.8b). Similarly, CGP pre-incubation resulted in a remarkably increased binding of PAC-1 indicating an enhanced ADP-triggered integrin αIIbβ3 activation (Fig 3.8c & 3.8d). We further explored the effect of different concentrations of CGP on ADP-induced platelet activation by measuring p-selectin expression and αIIbβ3 activation. However, our data revealed no notable dose-dependent effect of CGP on ADP-evoked platelet activation (Fig 3.8e & 3.8f).

3.4.4. Mitochondrial function did and cytosolic Ca^{2+} did not alter in the presence MTX and CGP

The effect of mitochondrial Ca^{2+} transporters in platelets was further investigated by measuring the mitochondrial membrane potential using a combination of flow cytometry and TMRM fluorescence sensor. Our results demonstrated a hyperpolarization of mitochondrial membrane potential after treatment with ADP as shown by a notable rise in

the MFI (Fig 3.9a), which reflects an accelerated bioenergetic activity of mitochondria. Interestingly, mitochondrial membrane potential in ADP-stimulated platelets was significantly diminished in the presence of MTX as (Fig 3.9b). However, there was only a slight increasing tendency in the mitochondrial membrane potential after pre-treatment of platelets with CGP at 30 and 60 minutes (Fig 3.9c & 3.9d).

Furthermore, ADP-stimulated platelet cytosolic Ca^{2+} dynamics were also measured to determine the impact of MCU and NCLX inhibition on cytosolic Ca^{2+} that is a key contributor to platelet activation. However, although we observed a rapid rise of cytosolic Ca^{2+} upon ADP stimulation (Fig 3.9e & 3.9g), there was no notable change in in the cytosolic Ca^{2+} kinetics in the presence of MTX and CGP (Fig 3.9f & 3.9h).
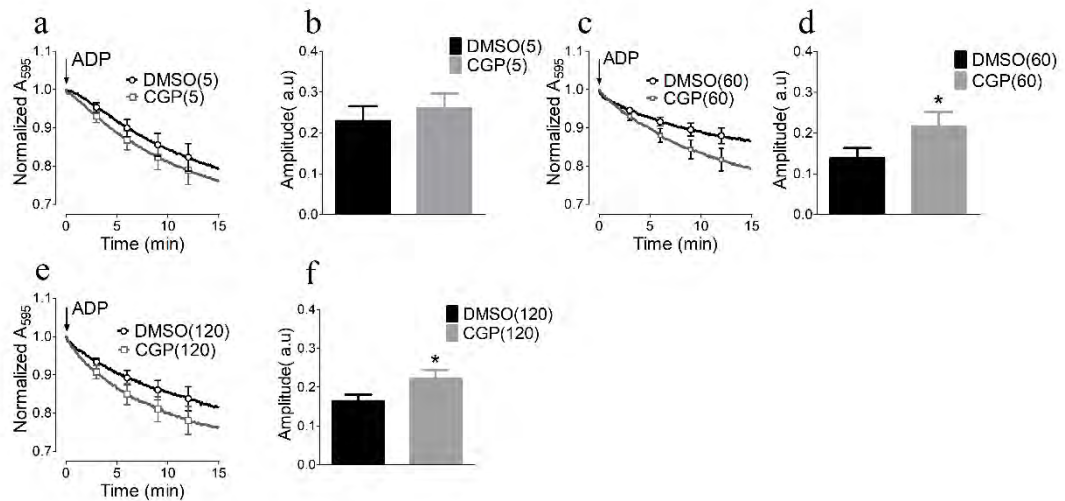
Figure 3.6. CGP enhanced the ADP-induced plateletaggregation: *(a) Platelet aggregation curve and (b) amplitude after pre-incubation with 0.1 0.1µM CGP for 5 minutes. (c-d) Platelet aggregation curve and amplitude in the presence of 0.1µM CGP for 60 minutes. (e-f) Platelet aggregation curve and amplitude in the presence of 0.1µM CGP for 120 minutes after stimulation with 20 µM ADP. Data are presented as mean ± SEM and statistically analysed using one-tailed unpaired T-test, n=7, *p<0.05. DMSO is used as a vehicle. CGP (5) = platelets+0.1 µM CGP for 5 minutes+20 µM ADP, CGP(60)= platelets+0.1 µM CGP for 60 minutes+20 µM ADP, CGP(120)= platelets+0.1 µM CGP for 120 minutes+20 µM ADP.*
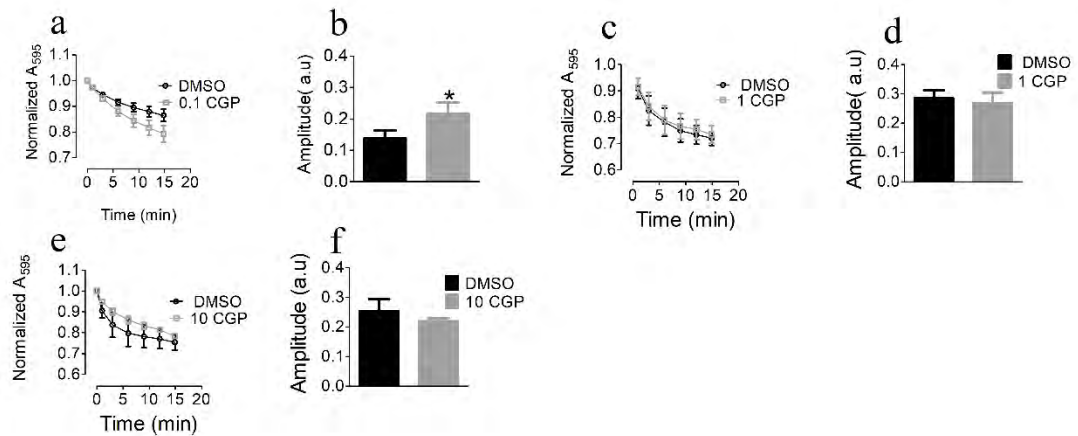
Figure 3.7. Dose independent impact of CGP on platelet aggregation profile: *Platelets aggregation curve and amplitude after pre-incubation either with DMSO or (a & b) 0.1μM CGP, (c & d) 1μM CGP,and (e & f) 1μM CGP upon stimulation with 20 μM ADP. Data is shown as mean ± SEM and statistically analysed by one-tailed unpaired T-test, n=7.*
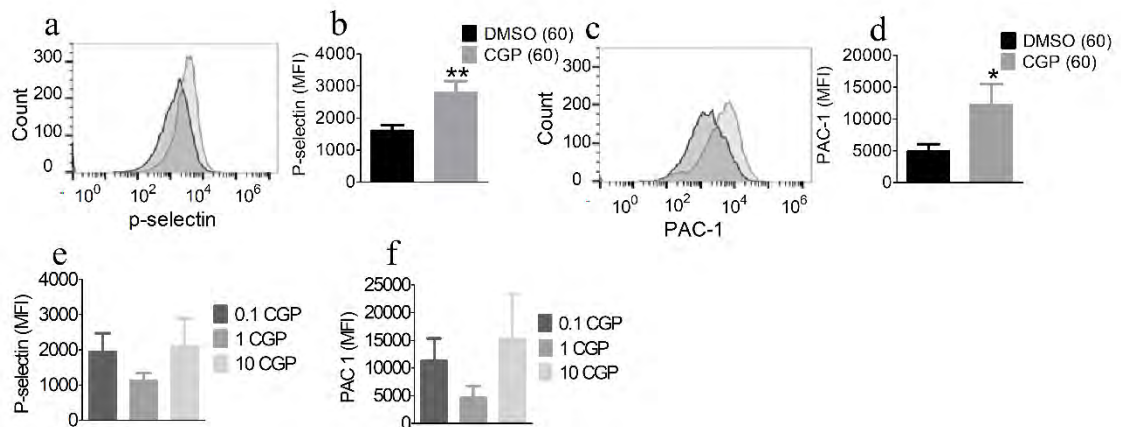
Figure 3.8. CGP enhanced ADP-evoked p-selectin externalization and PAC-1 binding: Histograms showing significant increase in MFI of (a&b) p-selectin and (c & d) PAC-1 after pre-treatment with CGP (0.1 µM , light grey) for 60 minutes vs DMSO (dark grey) on induction with 20 µM ADP. MFI of (i) p-selectin and (j) PAC-1 after pre-incubation of platelets with three different concentrations (0.1 µM, 1 µM and 10 µM) of CGP for 60 minutes followed by ADP stimulation. Data shows mean ± SEM and analysed by one-tailed T-test. n=4-7, *p<0.05, **p<0.01. CGP (60) = platelets+0.1 µM CGP for 60 minutes+20 µM ADP, 0.1 CGP= platelets+0.1 µM CGP for 60 minutes+20 µM ADP, 1 CGP= platelets+1 µM CGP for 60 minutes+20 µM ADP, 10 CGP=platelets+10 µM CGP for 60 minutes+20 µM ADP.
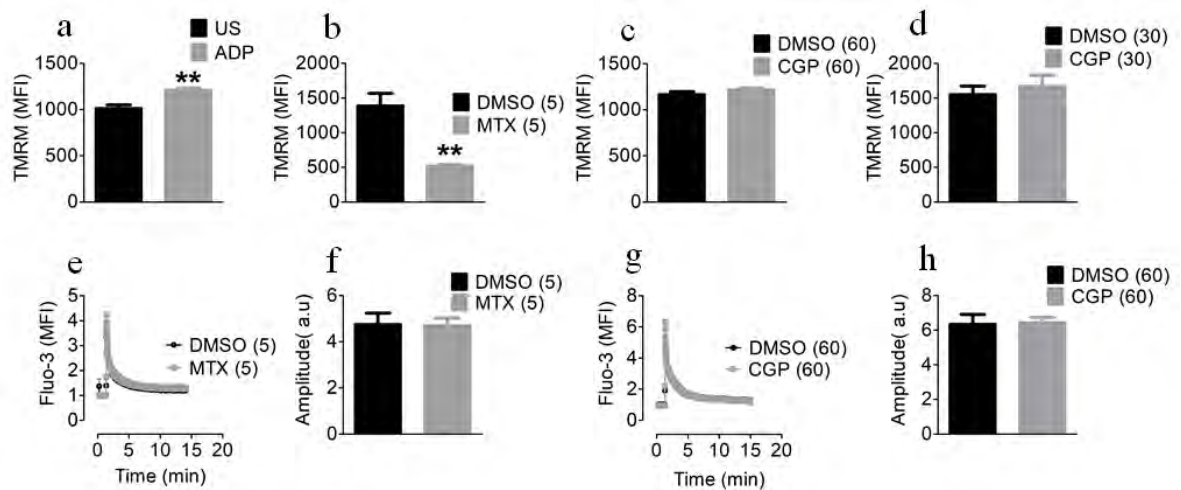
Figure 3.9. Impact of MTX and CGP on ΔΨₘ and cytosolic Ca²⁺: *Platelets loaded with TMRM and Fluo-3. (a) Representative curves demonstrate the MFI of TMRM-loaded unstimulated (US) and ADP-stimulated platelets (ADP). (b) MFI of TMRM after pre-treatment of platelets with 20 μM MTX for 5 minutes vs DMSO (vehicle) followed by addition of 20 μM ADP (c & d) MFI of TMRM after pre-incubation of platelets with 0.1 μM CGP for 60 and 30 minutes vs DMSO followed by stimulation with 20μM ADP.(e &f) ADP-induced Fluo-3 signal after pre-treatment with MTX (grey) vs DMSO (vehicle) (black). (g &h) ADP-stimulated mean MFI of Fluo-3 in the presence of CGP (grey) vs DMSO (black). Data indicates mean ± SEM and analysed by using one-tailed T-test., **p<0.01, MTX(5) platelets+20 μM MTX for 5 minutes+20 μM ADP, CGP (60) and CGP (30) = platelets+0.1 μM CGP for 60 and 30 minutes+20 μM AD*

3.5. MTX-mediated inhibition of thrombin-induced platelet aggregation

Thrombin is generated as a result of coagulation cascade of platelets and being a potent activator, it induces platelet aggregation by PAR-1 and PAR-4 resulting in Ca^{2+} elevation (Scridon 2022). Thrombin at higher dose induced a rapid drop in absorbance that reached the maximum percentage of platelet aggregation (Fig 3.10a & 3.10b). However, upon stimulation with lower dose of thrombin, platelet aggregation proceeded with relatively slower kinetics (Fig 3.10e &3.10f). Interestingly, MTX pre-treatment remarkably reduced the platelet aggregation with higher dose of thrombin (Fig 3.10c &3.10d). However, at lower dose of thrombin, platelet aggregation remained unaffected in the presence of MTX (Fig 3.10g &3.10h).

3.5.1. MTX reduced the thrombin-mediated p-selectin expression and integrin activation

In order to ascertain the impact of mitochondrial Ca^{2+} on thrombin-induced platelet activation we determined the PAC-1 binding and p-selectin exposure in the presence MTX. Our results revealed increased level of platelet activation markers; PAC-1 binding and p-selectin expression on platelets surface upon stimulation with thrombin represented in the form MFI (Fig 3.11a & 3.11c). Conversely, a significant decrease was observed in the MFI of p-selectin and PAC-1 when platelets were inhibited with MTX (Fig 3.11b & 3.11d).

Furthermore, we assessed the dose-dependent effect of MTX on platelet activation markers and it was noted that with increasing concentration of MTX there was significant reduction in p-selectin expression and PAC-1 binding (Fig 3.11e & 3.11f). The IC50 of MTX for p-selectin exposure was 10.17μM and for PAC-1 binding it was 3.168 μM.

3.5.2. Effect of CGP on thrombin-induced degranulation and integrin αIIbβ3 activation

Previously our data revealed a significant role of mitochondrial Ca^{2+} influx on platelet activation markers. Therefore, in order to further explore the role of mitochondrial Ca^{2+} efflux pathway in platelet activation we inhibited mitochondrial Ca^{2+} efflux protein NCLX with CGP. We started measuring platelet activation using lower concentration 0.1μM CGP that did not affect p-selectin exposure (Fig 3.12a). However, a slight decreasing trend was observed in the MFI of PAC-1 with 0.1μM CGP (Fig 3.12b). Furthermore, p-slectin and

PAC-1 remained unaltered even when the concentration of CGP was increased to 1µM (Fig 3.12c & 3.12d).
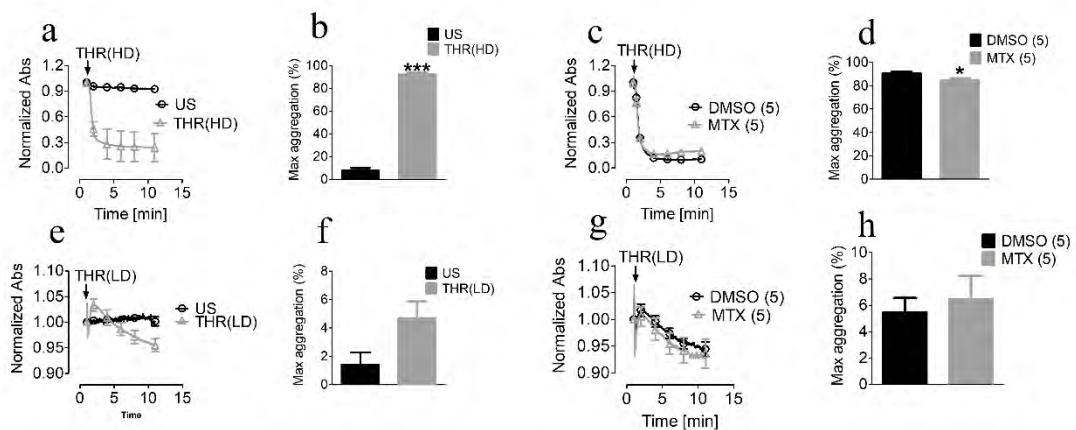
***Figure 3.10 MTX inhibited thrombin-induced platelet aggregation: (**a &b) Platelet aggregation was induced by 5U/ml thrombin higher dose [THR(HD)] and monitored with aggregometer. (c & d) Platelets were either treated with DMSO (vehicle) or 20µM MTX for 5 minutes followed by stimulation with 5U/ml THR(HD). (e & f) Platelet aggregation was induced by 0.005U/ml thrombin lower dose [THR(LD)]. (g & h) Platelets were either treated with DMSO (vehicle) or 20µM MTX for 5 minutes followed by stimulation with 0.005U/ml lower dose of thrombin THR(HD). Data is presented as mean ± SEM and analysed using one-tailed unpaired T-test n=3-5,*p<0.05. US= unstimulated, DMSO (5)= Platelets + DMSO +THR, MTX (5) = platelets + 20 µM MTX for 5 minutes+THR.*
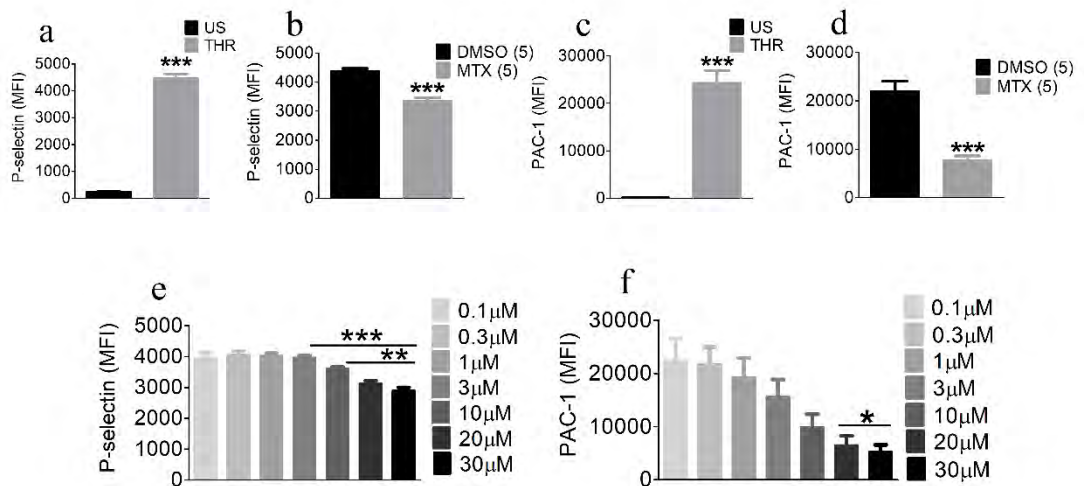
Figure 3.11. MTX inhibited the thrombin-mediated platelet activation: *Platelet activation is represented by MFI of (a) p-selectin after stimulation with 5U/ml thrombin. (b) MFI of p-selectin after preincubation of platelets with DMSO (vehicle) or 20μM MTX MTX for 5 minutes followed by stimulation with 5U/ml THR. (c) MFI of PAC-1 after stimulation of platelets with 5U/ml thrombin. (d) MFI of PAC-1 after preincubation of platelets with DMSO (vehicle) or 20μM MTX MTX for 5 minutes followed by stimulation with 5U/ml THR. Platelets were preincubated with 7 different concentrations (0.1μM to 30μM) of MTX and MFI of (e) p-selectin and (f) PAC-1 was determined followed by stimulation with 5U/ml of thrombin. Data is presented as mean ± SEM and analysed using one-tailed unpaired T-test and One-way ANOVA with Tuckey's post-hoc test n=3-8,*p<0.05, **p<0.001, ***p<0.0001. US= unstimulated, THR=thrombin, DMSO (5)= Platelets + DMSO +THR, MTX (5) = platelets + 20 μM MTX for 5 minutes+THR.*
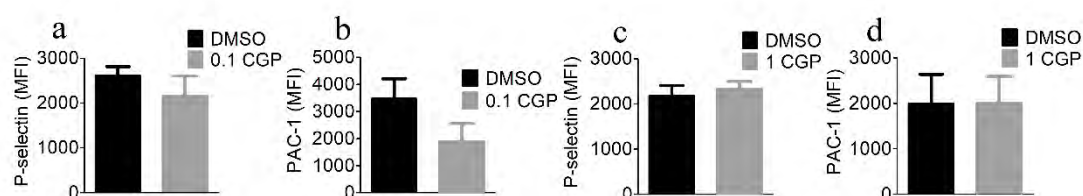
Figure 3.12. Effect of CGP-35157 on thrombin-mediated platelet degranulation and integrin activation: *MFI of (a) p-selectin and (b) PAC-1 is shown in the presence of 0.1μM CGP-37157 (0.1 CGP) incubated for 60 minutes followed by stimulation with 5U/ml. MFI(MFI) of (c) p-selectin and (d) PAC-1 is shown in the presence of 1μM CGP-37157 (1 CGP) incubated for 60 minutes followed by stimulation with 5U/ml THR. Data represents mean ± SEM and analysed by one-tailed unpaired T-test n=3-4. DMSO = Platelets + DMSO +THR, 0.1 CGP = platelets + 0.1μM CGP for 60 minutes+THR, 1 CGP = platelets + 1μM CGP for 60 minutes+THR.*

3.6. Effect of MTX on platelet aggregation induced by CVX

Convulxin (CVX) is a 72KDa glycoprotein, which is isolated from the snake venom and is considered as the extremely potent activator of platelets (Jandrot-Perrus et al. 1997). CVX interacts with platelets through GPVI receptors present on platelet surface. The aggregation and activation induced by CVX is Ca^{2+} dependent that is usually involves the activation of phospholipase C (PLC) pathway and results in increased intracellular Ca^{2+} and granule release (Ragab et al. 2007).

Platelet aggregation induced by higher dose of CVX (500ng/ml) significantly increased platelet aggregation (Fig 3.13a&3.13b). However, MTX did not alter the response of platelet aggregation induced by higher dose of CVX (Fig 3.13c & 3.13d). Furthermore, median effective concentration (EC50) of CVX was used, which induced a remarkable change in platelet aggregation. However, aggregation rate was 20% slower with EC50 in comparison to higher dose of CVX (3.13e &3.13f). Besides, when we determined the effect of MTX on aggregation with EC50 of CVX, there was no difference between DMSO (vehicle) and MTX until 3 minutes but later aggregation started decreasing in MTX-treated platelets (Fig 3.13g & 3.13h). The dose of CVX was further reduced to 0.6ng/ml, which only induced a small response of platelet aggregation (Fig 3.13i &3.13j). Likewise, no effect of MTX was observed with 0.6ng/ml CVX concentration (Fig 3.13k &3.13l).

3.6.1. MTX inhibited CVX mediated platelet activation

Platelet activation induced by CVX was measured by degranulation marker p-selectin expression and integrin activation through PAC-1 binding. Both platelet activation markers were significantly increased upon stimulation of platelets with higher dose of CVX (500ng/ml) (Fig 3.14a &3.14c). Conversely, p-selectin expression and PAC-1 binding was significantly reduced in the presence of MTX when platelets were treated with higher dose of CVX (Fig 3.14b &3.14d). In addition to this, when concentration of CVX was reduced to 2ng/ml (CVX EC50) p-selectin expression was increased with the same tendency as with the higher dose of CVX (Fig 3.14a & 3.14e). On the contrary, PAC-1 binding was significantly increased with 2ng/ml CVX but it showed a slight reduction in the MFI of PAC-1 when compared with high dose of CVX (3.14c &3.14g). Moreover, MTX remarkably reduced the p-selectin expression (3.14f) binding of PAC-1 with 2ng/ml

The Contribution of Mitochondrial Calcium Homeostasis in Agonist-Induced Platelet Response

CVX (Fig 3.14h). Interestingly MTX reduced PAC-1 binding more effectively than p-selectin expression.

3.6.2. Dose dependent impact of MTX on CVX-induced platelet activation

Our previous results have demonstrated that MTX significantly affected the platelet activation markers. However, in order to further validate our results, we have determined the concentration-dependent effect of MTX on CVX-mediated platelet activation. For this prupose, platelets were treated with seven different doses of MTX ranging from 0.1µM to 30µM. It was noted that with increasing concentration of MTX, p-selectin expression and PAC-1 binding is significantly reduced (Fig 3.15a &3.15b). However, the remarkable effect of MTX on p-selectin expression was observed after 20µM MTX (Fig 3.15a). Conversely, MTX started reducing PAC-1 binding after 3µM (Fig 3,15b). The IC50 value of MTX calculated for p-selectin is 19.69 µM, PAC-1 binding is 2.89 µM and (Fig 3.15)

3.6.3. Effect of CGP on CVX-induced platelet activation

The role of mitochondrial Ca^{2+} in CVX-mediated platelet activation was further assessed by exploring the mitochondrial Ca^{2+} efflux pathway. Platelet were treated with lower (0.1µM) and higher (1µM) concentrations of CGP for 60 minutes. Surprisingly, p-selectin exposure and PAC-1 binding remain unaltered with either of the CGP concentrations (Fig 3.16a-d).

3.6.4. Impact of MTX on Thrombin and CVX-induced cytosolic Ca^{2+} kinetics

Ca^{2+} mobilization from cellular stores and subsequent Ca^{2+} elevation due to activation of store-operated Ca^{2+} entry (SOCE) is essential for triggering and sustaining agonist-induced platelet activation (Dolan and Diamond 2014). A part of this elevated Ca^{2+} is taken-up by mitochondria through MCU that contributes to regulation of cytosolic Ca^{2+} (Pathak and Trebak 2018). Therefore, in order to explore the impact of MTX on cellular Ca^{2+} transients, platelets were stimulated with strong agonists like thrombin or CVX and cytosolic Ca^{2+} kinetics were determined in the presence of MTX. Our results revealed the fact that upon stimulation with both thrombin and CVX, a rapid and transient rise in cytosolic Ca^{2+} was observed with relatively larger amplitude in case of CVX. This was followed by a slow Ca^{2+} decline in case of thrombin stimulation. However, CVX stimulation was associated with a sustained cytosolic Ca^{2+} for several minutes, after which it started the decline. MTX-treated platelets did not reveal any change in thrombin and CVX-evoked cytosolic Ca^{2+} increase indicating no effect on Ca^{2+} release from IP3-

dependent stores. Interestingly, the decline of cytosolic Ca^{2+} appeared to be faster with MTX treatment in case of both agonists, with a remarkably bigger increase in cytosolic Ca^{2+} decline upon CVX stimulation. (Fig 3.17a-3.17d).
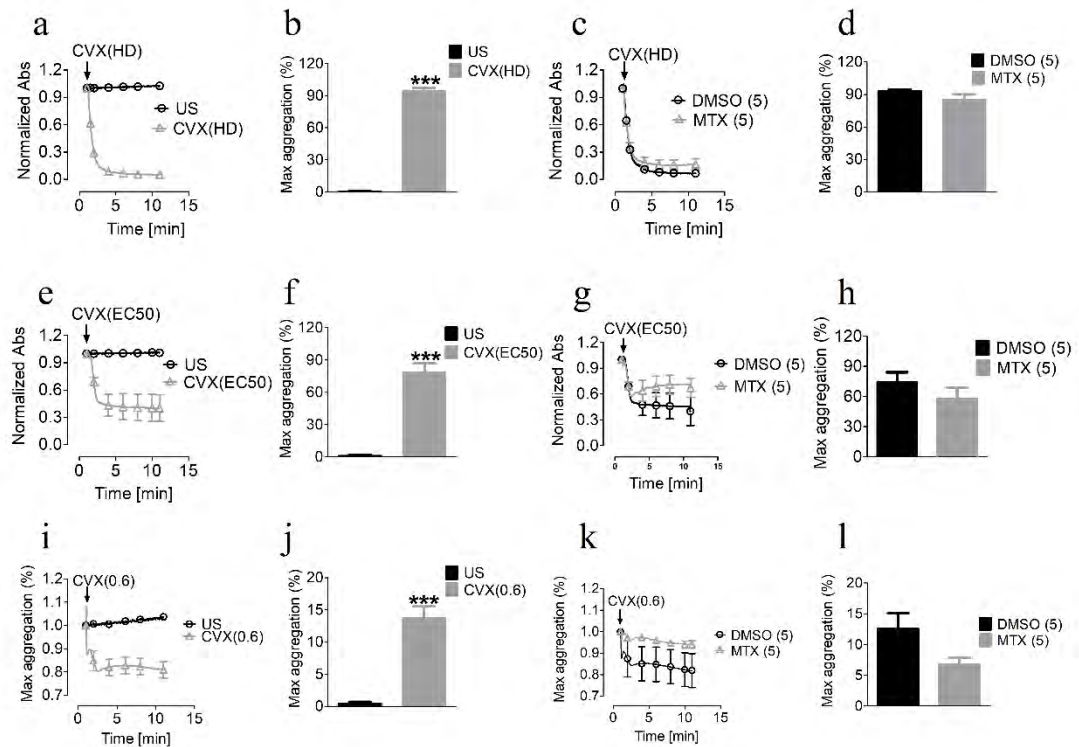
Figure 3.13. Effect of MTX on CVX-mediated platelet aggregation: (*a &b) Platelet aggregation was induced by 500ng/ml CVX higher dose [CVX(HD)] and monitored with aggregometer. (c & d) Platelets were either treated with DMSO or 20µM MTX for 5 minutes followed by stimulation with 500ng/ml higher dose of CVX [CVX(HD)]. (e & f) Platelet aggregation was induced by 2ng/ml CVX median effective concentration (EC50) [CVX(EC50)]. (g &h) Platelets were either treated with DMSO or 20µM MTX for 5 minutes followed by stimulation with 2ng/ml CVX median effective concentration (EC50) [CVX(EC50)] . (i-k) Platelet aggregation was induced by 0.6ng/ml convulxin [CVX(0.6)].Platelets were either treated with DMSO or 20µM MTX for 5 minutes followed by stimulation with 0.6ng/ml CVX. Data represents mean ± SEM and analysed by one-tailed unpaired T-test, n=4-5, ***p<0.0001. US=unstimulated, DMSO(5)= Platelets + DMSO +CVX, MTX (5) = platelets + 20 µM MTX for 5 minutes+CVX.*
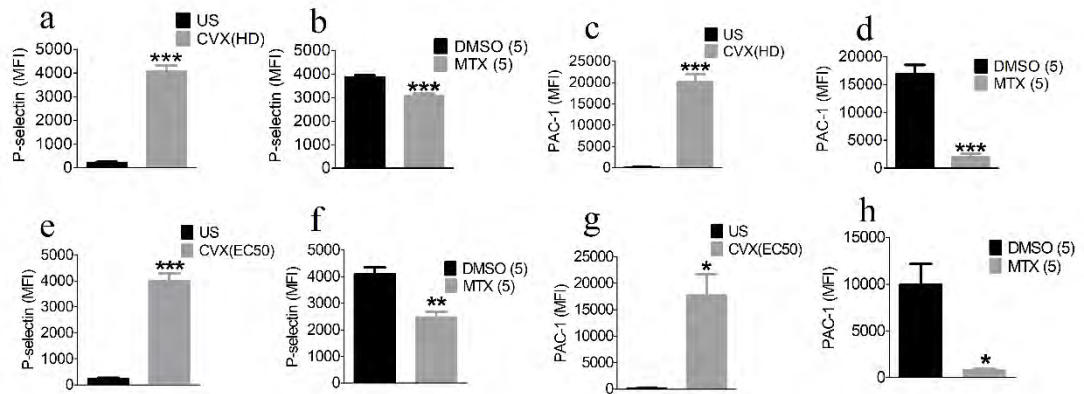
Figure 3.14. MTX inhibited the CVX-mediated platelet activation: *Platelet activation is represented by MFI of (a) p-selectin after stimulation with 500ng/ml higher dose of CVX [CVX(HD)] . (b) MFI of p-selectin after preincubation of platelets with DMSO or 20µM MTX for 5 minutes followed by stimulation with 500ng/ml higher dose of CVX [CVX(HD)] (c) MFI of PAC-1 after stimulation of platelets with 500ng/ml higher dose of CVX [CVX(HD)]. (d) MFI of PAC-1 after preincubation of platelets with DMSO or 20µM MTX for 5 minutes followed by stimulation 500ng/ml higher dose of CVX [CVX(HD)]. (e) MFI of p-selectin after stimulation of platelets with 2ng/ml median effective concentration (EC50) of CVX [CVX(EC50)]. (f) MFI of p-selectin after preincubation of platelets with DMSO or 20µM MTX for 5 minutes followed by stimulation with 2ng/ml median effective concentration (EC50) of CVX [CVX(EC50)]. (g) MFI of PAC-1 after stimulation of platelets with 2ng/ml median effective concentration (EC50) of CVX [CVX(EC50)]. (h) MFI of PAC-1 after preincubation of platelets with DMSO or 20µM MTX for 5 minutes followed by stimulation with 2ng/ml median effective concentration (EC50) of CVX [CVX(EC50)]. Data is presented as mean ± SEM and analysed by one-tailed unpaired T-test n=3-7, **p<0.001, ***p<0.0001. US= unstimuled, DMSO (5)= Platelets + DMSO +CVX, MTX (5) = platelets + 20 µM MTX for 5 minutes+CVX.*
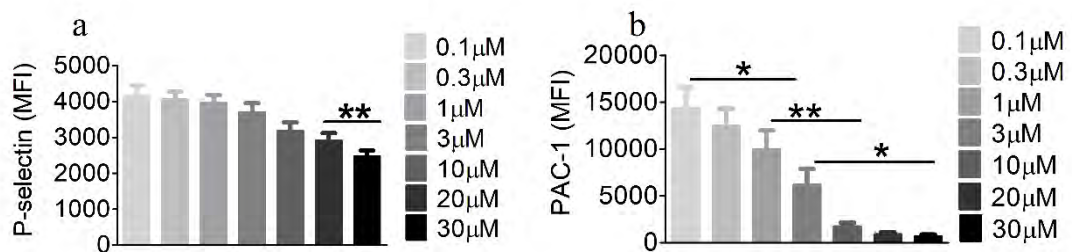
Figure 3.15. Dose-dependent effect of MTX on CVX-dependent platelet activation:
Platelets were preincubated with seven different concentrations (0.1μM to 30μM) of
MTX and MFI of (a) p-selectin (b) PAC-1. Data is presented as mean ± SEM and
analysed by One-way ANOVA with Tuckey's post-hoc test n=3,*p<0.05, **p<0.001,
***p<0.0001.
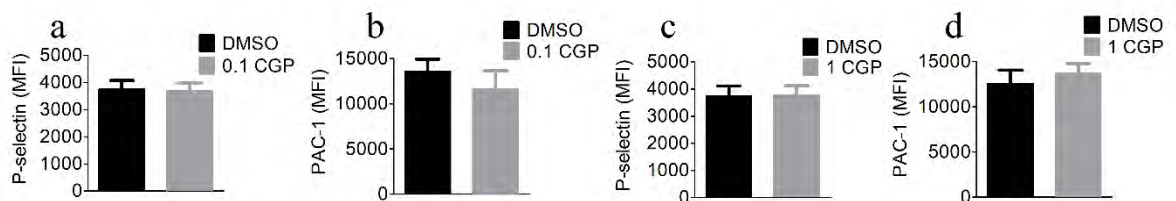
Figure 3.16. Impact of CGPon CVX-stimulated platelet degranulation and
integrin activation marker: *MFIof (a) p-selectin and (b) PAC-1 is shown in the*
presence of 0.1μM CGP (0.1 CGP) incubated for 60 minutes followed by stimulation
with 500ng/ml CVX. MFI of (c) p-selectin and (d) PAC-1 is shown in the presence
of 1μM CGP incubated for 60 minutes followed by stimulation with 500ng/ml CVX.
Data represent mean ± SEM and analysed by one-tailed unpaired T-test n=4-5.
DMSO (vehicle) = Platelets + DMSO for 60 minutes +CVX, 0.1 CGP = platelets +
0.1μM CGP for 60 minutes+THR, 1 CGP = platelets + 1μM CGP for 60
minutes+CVX.
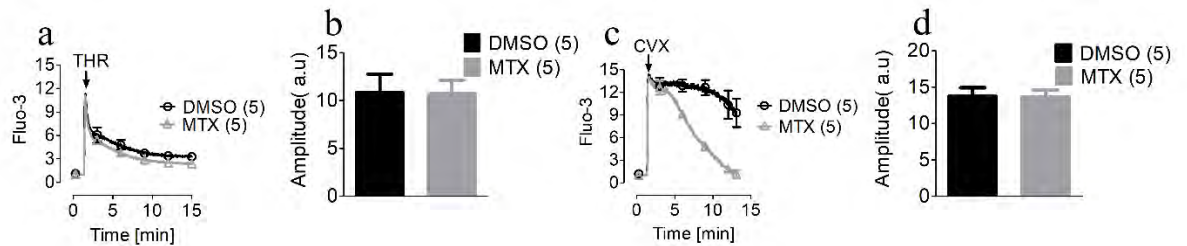
Figure 3.17. Cytosolic* Ca²⁺ *is decreased in the presence of MTX: *Platelets were loaded with fluorescent dye Fluo-3 and incubated with either DMSO or MTX for 5 minutes. Fluorescence was first acquired for 1 minute (baseline) and platelets were then stimulated with (a & b) 5U/ml thrombin (THR) and (c & d) 500ng/ml convulxin (CVX) and then fluorescence was acquired up to 15 minutes. Data is represented as mean ± SEM and statistically analysed using one-tailed unpaired T-test n=3 DMSO(5)=platelets loaded with fluo-3±DMSO for 5 minutes + THR/CVX, MTX(5)= platelets loaded with fluo-3+ 20µM MTX for 5 minutes + THR/CVX.*

3.7. Impact of mitochondrial Ca^{2+} on adrenaline-mediated platelet aggregation

Adrenaline or epinephrine is released into the blood circulation by the activation of sympathetic nervous system in response to stress (Oury et al. 2002; Bruce 2018). These hormones along with other neurotransmitters are essential for controlling the function of several cells in the body (Paravati, Rosani, and Warrington 2018). Platelets also express α2A adrenergic receptors of epinephrine and nor-epinephrine on their surface which is known to induce platelet aggregation (Stalker et al. 2012).

3.7.1. Determination of platelet aggregation through adrenergic receptors by time-lapsed spectrophotometric assay

Platelets get activated through α2A adrenergic signaling by binding to their respective receptors via PI3K pathway followed by secretion and integrin activation (Martin et al. 2020). Our data demonstrated a drop in absorbance in adrenaline-treated platelets indicating adrenaline-induced platelet aggregation (Fig 3.18a & 3.18b). Moreover, it is already known that adrenaline alone is not able to induce strong aggregation rather it share some part of platelet aggregation with other stimuli or it only potentiates the effect of aggregation of other platelets agonists. To further determine this pathway, platelets were pre-incubated with Apyrase which is known to degrade ADP. A slight decreasing trend in of aggregation was noted in the presence of apyrase (Fig 3.18c & 3.18d). This data indicates the probability that adrenaline causes a synergistic effect on platelet aggregation.

3.7.2. MTX reduced adrenaline-mediated platelet aggregation

Previously, it has been known that adrenaline potentiate the effect of ADP by its upon platelet activation. ADP stimulates P2Y1 and P2Y12 receptors following the pathway of PI3K and PLC to release Ca^{2+} into cytosol from DTS. The rise in cytosolic Ca^{2+} is essential for integrin activation and eventually for platelet aggregation. We hypothesized that the released Ca^{2+} may also accumulate into the mitochondria through MCU and may contribute to platelet aggregation. Therefore, in order to investigate the role of mitochondrial Ca^{2+} in platelet aggregation, MCU was blocked with MTX and aggregation response was measured. Interestingly, MTX markedly reduced the platelet aggregation, which may signify the role of mitochondrial Ca^{2+} in platelet aggregation (Fig 3.19a & 3.19b).

3.7.3. MTX decreased the mitochondrial dehydrogenase activity triggered by adrenergic signaling

It is generally believed that the Ca^{2+}, which enters the mitochondria, activates mitochondrial dehydrogenases for its proper functioning. However, in order to identify the role of mitochondrial Ca^{2+} homeostasis, mitochondrial bioenergetics were measured by determining mitochondrial dehydrogenases activity through MTT assay. Surprisingly, there was a significant increase in the absorbance of MTT when platelets were stimulated with adrenaline (Fig 3.20a). Moreover, when mitochondrial Ca^{2+} was blocked with MTX, our data intriguingly showed a significant decrease in the absorbance of MTT (Fig 3.20b).
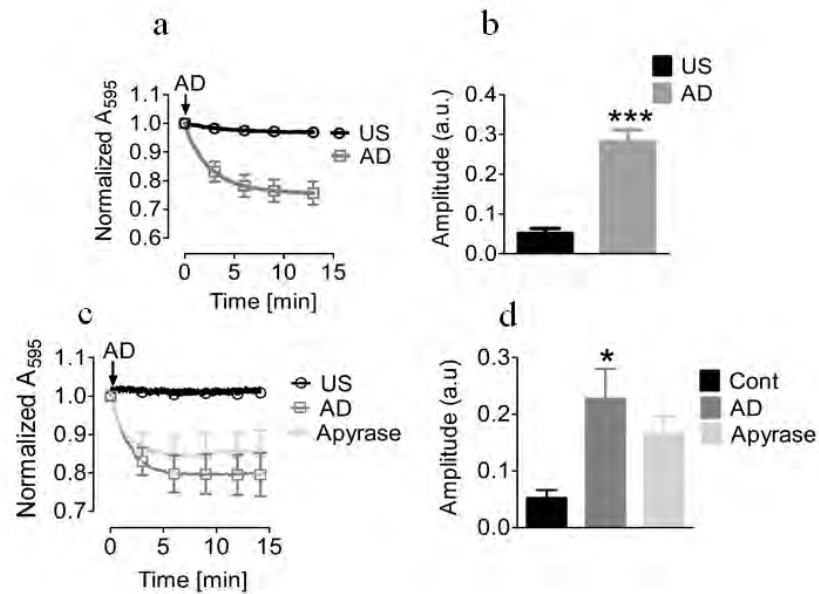
Figure 3.18. Role of MTX in platelet aggregation with adrenergic stimulation: *(a) Platelet aggregation is represented in the form of curve as decrease in absorbance upon addition of 10µM AD (Adrenaline) (b) Amplitude of the curve is calculated showing significant difference between Unstimulated (US) and Adrenaline-treated platelets (AD) (c) Curve represented the platelet aggregation in response to pre incubation of 200mU Apyrase for 5 mins and further stimulation with 10µM adrenaline (AD) (d) Bar graph showing amplitude calculated form aggregation curve. Data is statistically represented by mean ± SEM, n=5-6 ***p<0.0001, *p<0.05*
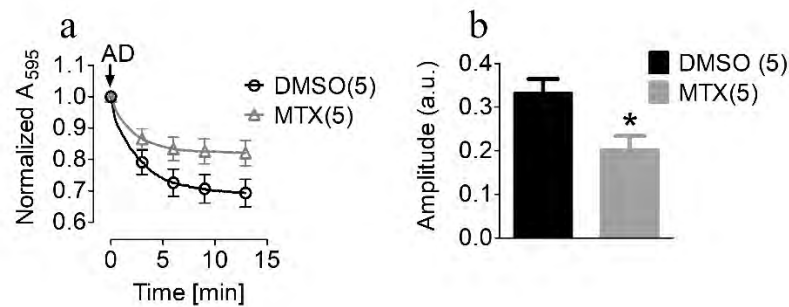
Figure 3.19. Effect of MTX on adrenaline-mediated platelet aggregation: (a) Aggregation curve showed decrease in absorbance in platelets preincubated with 20μM MTX for 5 mins followed by the stimulation of 10μM AD in comparison to DMSO (b) Bar graph represents curve amplitude showing significant difference between DMSO and MTX treated platelets. Data represents mean ± SEM and analysed using one tailed unpaired T test n=5 DMSO (vehicle) = Platelets + DMSO for 5minutes+10μM AD, MTX= platelets + MTX for 5minutes+10μM AD
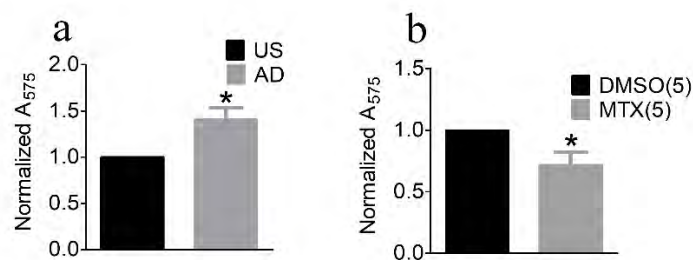
Figure 3.20. MTX decreased the mitochondrial dehydrogenase activity: (a) Bar graph showed significant increase in the activity of mitochondrial dehydrogenases upon treatment with 10μM adrenaline (AD) compared to control confirmed by MTT assay. (b) Bar graph showed the significant decrease in the activity of mitochondrial dehydrogenases in platelets preincubated with 20μM Mitoxantrone (MTX) for 5 minutes followed by treatment of 10μM Adrenaline (AD) in comparison its DMSO (vehicle) confirmed by MTT assay. Data represented the normalized absorbance of mean ± SEM, n=6 *p<0.05. DMSO(5)=platelets incubated with DMSO for 5 minutes + AD, MTX(5)=platelets incubated with MTX for 5 minutes + AD

3.8. Effect of MTX on thrombin-generated Annexin-V positive platelets

Besides, p-selectin and PAC-1 binding Annexin-V is also considered as a marker of platelet activation. Flow cytometry Annexin-V is a feasible and rapid method to measure procoagulant activity of platelets. It has been reported previously that procoagulant platelets are only generated with dual stimulation of thrombin and convulxin. We were interested to investigate single agonist-stimulated procoagulant platelets and whether mitochondrial Ca^{2+} has any role in it. Therefore, we started by using lower to higher concentration of thrombin and measured the percentage of Annexin-V positive platelets. Our data revealed that at lower concentration (0.5U/ml THR) thrombin only generated 3% of Annexin V positive platelets. Thereby MTX dides not alter the percentage of Annexin-V positive platelets after 0.5U/ml thrombin stimulation (Fig 3.21a). Furthermore, by increasing the concentration of thrombin to 5U/ml the percentage of Annexin-V positive platelets were increased up to 15%, but MTX was yet not able to induce a significant change in Annexin-V positive platelets in comparison to vehicle (Fig 3.21b). We further increased the concentration of thrombin to 10U/ml and our data revealed that even at higher concentration of thrombin MTX has no impact on the percentage of Annexin-V (Fig 3.21c).

3.8.1. MTX markedly decreased Annexin-V positive platelets with higher concentration of CVX

Besides, thrombin the second agonist responsible for generation of procoagulant platelets is CVX and is considered as more potent agonist of platelets as compared to thrombin. Consequently, we measured the impact of MTX on CVX generated procoagulant platelets. It was observed that lower concentration or EC50 (2ng/ml) of CVX triggered poor procoagulant platelet formation. Hence, MTX did not show any effect on percentage of Annexin-V positive platelets in comparison to vehicle (DMSO) (Fig 3.22a). Moreover, by increasing the concentration of CVX up to 500ng/ml, it generated moderate procoagulant platelets. Interestingly, MTX yielded a significant drop in the generation of Annexin-V positive platelets at higher CVX dose (Fig 3.22b).

3.8.2. MTX played significant role in procoagulant platelet formation with dual agonists (THR/CVX)

Our previous results exhibited the fact that MTX did not show any effect on single thrombin stimulated platelets as it triggered poor procoagulant platelet formation. In

contrast, CVX generated moderate procoagulant platelets and MTX showed a significant change in the generation of Annexin V positive platelets. Furthermore, we co-stimulated the platelets with thrombin-plus-CVX and interestingly MTX exhibited a significant decrease ($23\% \pm 1.26$) in procoagulant platelets. On the contrary there was a remarkable increase ($36\% \pm 4.6$) in PAC-1 positive platelets (Fig 3.23a & 3.23b). Similarly, we corroborated our data by using an alternate inhibitor of MCU i.e. Ru265, which is another blocker of MCU. Remarkably, our data was replicated with a significant decrease in procoagulant platelets in response to dual agonists (Fig 3.23c)

Sustained cytosolic Ca^{2+} concentrations and mitochondrial Ca^{2+} signaling play an integral part in the generation of procoagulant platelets. Our results revealed the fact that inhibition of mitochondrial Ca^{2+} decreased the formation of procogulant platelets. Thus, we further investigated the cytosolic Ca^{2+} kinetics in the presence of MTX. Our data revealed that upon dual stimulation with thrombin and convulxin, there was a rapid and transient increase in cytosolic Ca^{2+}, which decreased overtime. Interestingly in the presence of MTX cytosolic Ca^{2+} declined much faster as compared to vehicle (DMSO) (Fig 3.23d).
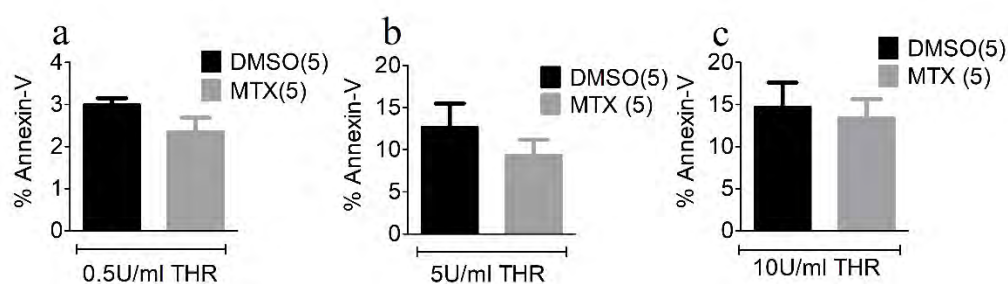
Figure 3.21. Effect of MTX on thrombin-stimulated Annexin-V positive platelets: *Cells were preincubated either with DMSO (vehicle) or 20μM MTX for 5 minutes and percentage of Annexin-V positive platelets were measured after stimulation with (a) 0.5U/ml thrombin (0.5U/ml THR) (b) 5U/ml thrombin (5U/ml THR) and (c) 10U/ml thrombin (10U/ml THR). Data represents mean ± SEM and analysed by one-tailed unpaired T-test n=3. DMSO(5) = Platelets + DMSO for 5 minutes + THR, MTX(5)= Platelets + 20μM MTX for 5 minutes + THR.*
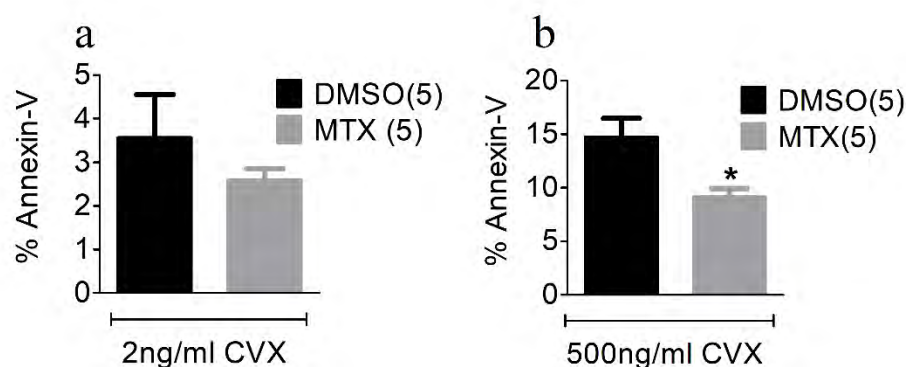
Figure 3.22. Effect of MTX on CVX-generated Annexin-V positive platelets. *Cells were preincubated either with DMSO (vehicle) or 20μM MTX for 5 minutes and percentage of Annexin-V positive platelets were measured after stimulation with (a) 2ng/ml convulxin (2ng/ml CVX) (b) 500ng/ml convulxin (500ng/ml CVX). Data represents mean ± SEM and analysed by one-tailed unpaired T-test n=3-5. DMSO(5) = Platelets + DMSO for 5 minutes + CVX, MTX(5)= Platelets + 20μM MTX for 5 minutes + CVX.*
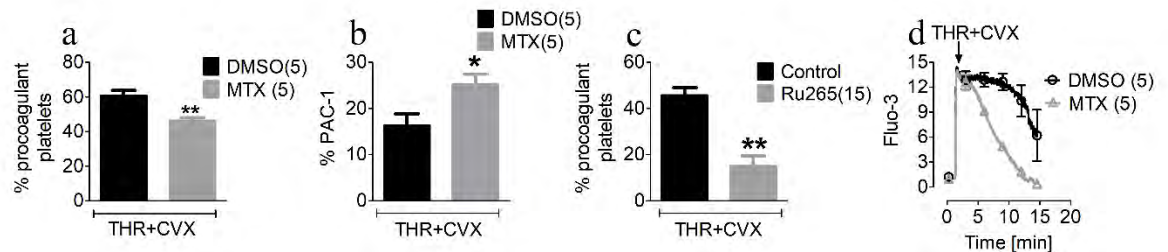
Figure 3.23. MTX decreased the formation of procoagulant platelets: *Platelets were preincubated either with DMSO (vehicle) or 20μM MTX for 5 minutes followed by stimulation of 5U/ml thrombin plus 500ng/ml convulxin (THR+CVX) and percentage of (a) procoagulant platelets was determined with Annexin-V. (b) percentage of PAC-1 positive platelets was determined. (c) Platelets were preincubated with 10μM Ru265 for 15 minutes followed by stimulation of 5U/ml thrombin plus 500ng/ml convulxin (THR+CVX). (d) Platelets were loaded with fluorescent dye Fluo-3 and incubated with either DMSO or MTX for 5 minutes. Fluorescence was first acquired for 1 minute baseline and platelets were stimulated with 5U/ml thrombin plus 500ng/ml convulxin (THR+CVX) with and then fluorescence was acquired up to 15 minutes. Data is represented as mean ± SEM and analysed by one-tailed unpaired T-test n=3-4. DMSO(5) = Platelets + DMSO for 5 minutes + 5U/ml thrombin plus 500ng/ml convulxin, MTX(5)= Platelets + 20μM MTX for 5 minutes + 5U/ml thrombin plus 500ng/ml convulxin, Control=platelets+5U/ml thrombin plus 500ng/ml convulxin, Ru265(15)=Platelets+Ru265 for 15 minutes+5U/ml thrombin plus 500ng/ml convulxin.*

4. DISCUSSION

Cytosolic Ca^{2+} mobilization in response to agonist stimulation remains one of the main events to trigger all the functions of platelets essential for platelet activation and thrombus formation (Anand and Harper 2020). Besides, the activation of platelets cytosolic Ca^{2+} is also taken up by mitochondria, which is particularly known in the formation of procoagulant platelets after dual stimulation with thrombin and collagen (Millington-Burgess and Harper 2021). However, the contribution of mitochondrial Ca^{2+} transport in platelet function in case of single stimulation with strong agonists like thrombin and collagen or with weak agonists like adrenaline and ADP remain poorly identified. In this work we reported hitherto vague contribution of mitochondrial Ca^{2+} uptake and extrusion by pharmacologically blocking MCU and NCLX, which are key players in mitochondrial Ca^{2+} transport. Our study uncovers a distinct roles of MCU and NCLX in platelet activation and aggregation. We uncovered that mitoxantrone (MTX), a pharmacological inhibitor of MCU (Arduino et al. 2017), reduced agonist-induced platelet aggregation and activation. These results are supported by another interesting fact that CGP-dependent inhibition of NCLX enhanced the platelet responses.

MTX has been demonstrated as an anti-neoplastic drug that acts as a poison for topoisomerase II in mammalian cells (Park et al. 2018), and therefore halts its activity by intercalating into the nuclear DNA. However, for the platelets we may speculate that the cytotoxic effect of MTX may be negligible owing to the lack of nucleus in addition to absence of Topoisomerase-2A in platelets as indicated by our unpublished data. Nonetheless, to eliminate the likelihood of MTX-mediated platelet cytotoxicity, we employed several cell death assays including trypan-blue dye exclusion, LDH release and apoptosis-associated Annexin V-binding. Our findings highlight that MTX does not cause a loss of platelet viability at least for shorter incubation times used in this study. Likewise, MTX was not associated with any pre-activation as determined by markers of platelet degranulation and conformation-dependent αIIbβ3 activation under resting conditions. Thus, based on recently reported inhibitory effect of MTX on MCU (Arduino et al. 2017; Bermont et al. 2020), along with absence of Topoisomerase-2A in platelets (Kosovsky and Soslau 1991), we speculate that MTX attenuated agonist-induced platelet activation by reducing MCU-dependent Ca^{2+} trasnport into mitochondria. Additionally, it is unlikely that a short platelet treatment with MTX would cause cytoxocity as compared to a longer

time required for cytotoxicity for *in vivo* chemotherapy (Arduino et al. 2017; Yang et al. 2014).

Together with MCU-dependent uptake, the matrix Ca^{2+} homeostasis is maintained by NCLX that is considered the major pathway for Ca^{2+} efflux (Blomeyer et al. 2013). But, there is no published evidence about the presence and functioning of NCLX in platelets. We, for the very first time, demonstrate the expression and working of NCLX in human platelets. We blocked NCLX-mediated Ca^{2+} efflux by using well established pharmacological inhibitor, CGP37157 (CGP), to support our data generated with MTX in agonist-induced platelet responses. CGP is a benzothiazepine that has a neuroprotective role in several excitotoxic models including disruption of intracellular Ca^{2+} homeostasis (Ruiz, Alberdi, and Matute 2014). It has been reported that CGP has shown interactions with several Ca^{2+} channels including Ryanodine Receptors and L-type Ca^{2+} channel (Palty and Sekler 2012), which are not present in platelets (Boyanova et al. 2012). However, the nanomolar dose of CGP employed in this work undermines the odds of any drug interaction with plasma membrane NCX or other off target effects reported earlier (Palty and Sekler 2012). Moreover, our data indicates that treatment of resting platelet with NCLX does not induce any preactivation in platelets or cause a loss of platelet integrity going in line with the fact that no cytotoxic effects of CGP have been reported in literature yet.

Genetic manipulation of MCU has been reported to effect the production of procoagulant platelets triggered by thrombin-collagen dual treatment without impacting ADP-induced platelet activation (Kholmukhamedov et al. 2018). Likewise, Ru-360, a well-known pharmacological blocker of MCU, has also been reported to influence procoagulant platelet formation without any data on ADP-induced platelet activation (Choo et al. 2012). However, it is important to highlight the fact that Ru-360 has notoriously poor membrane permeability and Choo et al. only managed to observe a minute drop in mitochondrial Ca^{2+} despite applying a very high dose of Ru-360 for very long time (Choo et al. 2012). On the other hand, we have seen a rapid effect of MTX on ADP-stimulated platelet aggregation at low micromolar dose confirming the previous studies about MTX concentration known for inhibiting mitochondrial Ca^{2+} uptake in other cell types. (Bermont et al. 2020; Arduino et al. 2017).

To the best of our knowledge, there are no reports both on the presence of NCLX or its functional participation in platelets. Therefore, we report the expression of NCLX in human platelets with a relatively low abundance of NCLX mRNA as compared to MCU mRNA. In addition to the inhibition of platelet aggregation, MTX remarkably reduced ADP-induced platelet activation endpoints (alpha granule release and integrin $\alpha IIb\beta 3$ activatio) at the same concentration ($20\mu M$) which was reported by Arduino et al in yeast mitochondria (Arduino et al. 2017). Mitochondrial Ca^{2+} entry in the activated platelets regulates the synthesis of ATP which is essential for granule secretion (Millington-Burgess and Harper 2021). Agonist-induced platelet responses including platelet aggregation, granule release and integrin activation are energy demanding processes. Therefore, it may be speculated that inhibition of mitochondrial Ca^{2+} may result in reduction of ATP synthesis in mitochondria that may affect the cytosolic ATP pool. This could greatly influence alpha granule release which is a high energy intensive processes in platelets. On the contrary, ATP synthesis is reported to have no effect on integrin $\alpha IIb\beta 3$ activation in stimulated platelets with a probable involvement of mitochondrial ROS (Kulkarni et al. 2022). Ca^{2+} accumulation in mitochondria induces hyperpolarization and mitochondrial respiration which could increase reactive oxygen species (ROS) in mitochondria (Baev et al. 2022). In line with this explanation ROS has been shown to actively contribute to platelet activation and aggregation (Masselli et al. 2020). Strikingly, selective inhibition of mitochondrial ROS with mitoTEMPO markedly decreased platelet aggregation along with a reduction of integrin $\alpha IIb\beta 3$ activation (Sonkar et al. 2019). In contrast, genetic ablation of of MCUb (a negative regulator of MCU) in mice platelets has been shown to reduce ADP-triggered platelet aggregation. However, surprisingly, deletion of MCUb did not modify the mitochondrial Ca^{2+}, besides it also influenced the glucose uptake and aerobic glycolysis in activated platelets (Ghatge et al. 2023) which could be explained as a result of compensatory changes in MCUb knockout (KO) mouse platelets. Remarkably, this study has also demonstrated no impact of increased mitochondrial Ca^{2+} on Ψm in MCUb-KO platelets (Ghatge et al. 2023).

Besides the regulation of mitochondrial Ca^{2+} influx pathway, the mitochondrial Ca^{2+} efflux pathway is regulated by the presence of NCLX in other cell types (Blomeyer et al. 2013). However, uptil now there is no data presenting the presence and function of NCLX in human platelets. In order to support our data generated with MTX in ADP-elicited platelet

responses, we explored the mitochondrial Ca^{2+} extrusion pathway in human platelets by blocking NCLX-mediated Ca^{2+} efflux by using well known pharmacological inhibitor, CGP. Interestingly, in contrast to MTX, CGP markedly increased platelet aggregation after treating the platelets for 60-120 minutes, possibly by accumulation of Ca^{2+} in mitochondrial matrix concentration and enhanced ATP production. Likewise, it also exhibited a remarkable increase in ADP-evoked platelet degranulation (p-selectin exposure) and integrin $\alpha IIb\beta3$ activation (PAC-1) binding. The effect of CGP on ADP-induced platelet responses may be speculated due to higher activity of Ca^{2+}-dependent mitochondrial dehydrogenases that are ultimately involved in cellular respiration. In a recent study on mouse astrocytes, inhibition of NCLX by CGP has been shown increased ATP production (Cabral-Costa et al. 2022) which may increase the effect of energy-dependent processes like aggregation and cellular secretion. Furthermore, in some cases accumulation of mitochondrial Ca^{2+} in platelets may elicit mPTP opening that is involved in generation of procoagulant platelets (Veuthey et al. 2022).On the contrary, upon ADP-stimulation, Ca^{2+} which is accumulated in mitochondrial matrix by inhibition of NCLX might not be enough to open mPTP. However, Ca^{2+} level in the matrix may be sufficient to sustain $\alpha IIb\beta3$ integrin activation in a pro-aggregatory response possibly due to modulation of ROS (Kulkarni et al. 2022). Thus, our results explain that CGP enhanced ADP-evoked platelet aggregation by increasing the availability of ATP and ROS for different platelet responses.

Thrombin and convulxin, being the stronger agonists of platelets, induce platelet activation and aggregation following the PLC activation via IP3 generation and release of Ca^{2+} from intracellular stores. Ca^{2+} is one of the fundamental secondary messengers, which regulates various essential processes in many cell types (Zou et al. 2022). However, in platelets during their resting state a low level of Ca^{2+} is maintained by plasma membrane Ca^{2+} ATPase (PMCA) pump (Dean 2010). Upon activation all the cellular events in platelets including shape change, granule release, integrin activation and platelet aggregation begin with the elevation of cytosolic Ca^{2+} (Theofilis et al. 2022). Mitochondria is also able to uptake the elevated Ca^{2+} through MCU and then release it through NCLX. This role of cytosolic Ca^{2+} in platelet responses is well-known.

Our data corroborated the already reported thrombin and convulxin-induced platelet aggregation. Thrombin induce mitochondrial ROS and mitochondrial depolarization (Kim

et al. 2019), which might be the result of overload of mitochondrial Ca^{2+} that is a trigger for mPTP opening (Leytin et al. 2009). However, our data showed that by inhibiting the mitochondrial Ca^{2+} with MTX, thrombin-induced platelet aggregation was significantly reduced. This could be explained by the fact that MTX might have attenuated mitochondrial Ca^{2+} overload responsible for the induction of platelet aggregation. On the contrary, MTX was not able to reduce convulxin-evoked platelet aggregation with a high dose (HD). Nevertheless, in the presence of MTX a small trend of decrease in platelet aggregation was observed upon reducing the concentration of convulxin from HD (500ng/ml) to EC50 (2ng/ml) and low dose 0.6ng/ml. Since convulxin is a potent platelet activating glycoprotein and it activates platelets in a pattern similar to other GPVI activator i.e. collagen. It is known that most of the platelet activators elicit a rapid increase in cytosolic Ca^{2+} starting from resting level of <100nm to the activation level of up to 1-2µM (Millington-Burgess and Harper 2021). Convulxin is reported to cause a gradual and more sustained cytosolic Ca^{2+} rise than thrombin (Choo et al. 2012). However, it might be possible that by inhibiting MCU, mitochondria may not be able to buffer a sustained and elevated level of cytosolic Ca^{2+}. Furthermore, the inhibition of mitochondrial Ca^{2+} uptake may reduce the ATP production that may explain a compromised response of platelets. But aggregation induced by strong agonists like thrombin and convulxin remains unaffected upon inhibition of mitochondrial ATP production. Therefore, from the present data it may be postulated that sustained platelet aggregation induced by strong agonists is compensated by the flow of glycolytic ATP (Kulkarni et al. 2022).

Platelet activation mechanism is well studied and plays a crucial role in hemostasis and thrombosis (Estevez and Du 2017). Platelet activation responses including integrin activation, platelet spreading, release of granules from intracellular stores, and procoagulant activity are dependent upon increase in concentration of cytosolic Ca^{2+} (Bergmeier and Stefanini 2009). In line with the previous literature, we documented a marked increase in platelet activation endpoints after stimulation with thrombin and convulxin (Panzer, Höcker, and Koren 2006; Senchenkova et al. 2019). Besides, cytosolic Ca^{2+}, mitochondrial Ca^{2+} uptake is poorly explored phenomenon in platelet activation. Interestingly, our results showed a significant decrease of p-selectin expression (α-granule secretion) and PAC-1 binding (αIIbβ3 integrin activation) in the presence of MTX with thrombin and convulxin. However, it has been explained earlier that inhibition of

mitochondrial ATP could greatly affect highly energy-intensive process (p-selectin expression) but dispensable for αIIbβ3 integrin activation (Kulkarni et al. 2022). Interestingly, αIIbβ3 integrin activation was greatly reduced by inhibition of ROS produced after stimulation with thrombin or convulxin without affecting any other platelet functions such as platelet shape change and α or dense granule release (Begonja et al. 2005).

Moreover, we also investigated inhibition of NCLX with CGP after strong stimulation of platelets. In contrast to ADP-evoked platelet responses, thrombin/convulxin-mediated platelet activation remain unaffected after treatement with CGP. The change induced by CGP in platelet responses is fairly small, and mitochondrial Ca^{2+} accumulated in response to ADP-stimulation may be blocked by CGP to enhance ATP production and hence increased platelet activation and aggregation. While, the Ca^{2+} sustained by mitochondria after strong stimulation with thrombin/convulxin may crossed the threshold to trigger opening of mPTP (Varjú et al. 2018). Therefore, due to mPTP opening mitochondria was unable to hold Ca^{2+} for ATP production, thus no impact of CGP was observed on thrombin/convulxin-stimulated platelet activation.

Various platelet receptors induce platelet activation by release of Ca^{2+} from intracellular stores and activation of SOCE. Our data complements the already published study that strong agonists caused a sudden and transient rise in cytosolic Ca^{2+} (Choo et al. 2012). Interestingly, with the inhibition of MCU we observed a distinct response of cytosolic Ca^{2+} in thrombin and convulxin stimulated platelets. In line with our data, MCU-KO cells significantly enhances cytosolic Ca^{2+} levels along with the inactivation of SOCE in differen cell types (Yoast et al. 2021; Deak et al. 2014) . However, in order to stabilize the level of cytosolic Ca^{2+}, the counteracting mechanism PMCA and SERCA were activated to remove the cytosolic Ca^{2+} (Harper and Sage 2017). Moreover, we perceived a greater decline in Ca^{2+} peak in the presence of MTX upon stimulation with convulxin as compared to thrombin. One of the main reasons for difference in Ca^{2+} levels of thrombin and convulxin is response to SOCE. It has not been clearly demonstrated that why impaired SOCE has stronger impact on convulxin receptors than thrombin and ADP receptors. However, it can be suspected that the two agonists may be activating different isoforms of PLC (Varga-Szabo, Braun, and Nieswandt 2009). Moreover, a model presented by Dolan and Diamond in 2014, proposed that in thrombin and ADP stimulated platelets, no refilling

of store was observed in the absence of extracellular Ca^{2+} however, when platelets were supplemented with Ca^{2+} after ER depletion, merely an incomplete filling of stores were observed in response to thrombin (Dolan and Diamond 2014).

Adrenaline stimulates α2 adrenergic receptors by the activation of PI3K pathway followed by Akt which eventually promotes persistent activation and granule secretion. Adrenaline is shown to potentiate platelet aggregation with ADP, however when ADP is degraded by an endonuclease enzyme apyrase it causes reversal of platelet aggregation induced by TRAP-6 (Trumel et al. 1999) and ADP (Jones, Evans, and Mahaut-Smith 2011). But in our study apyrase did not significantly cause reversible aggregation induced by adrenaline. This may be due to the fact that adrenaline only shares a part of its signaling with ADP. Moreover, it might trigger PI3K and inhibits adenylate cyclase by stimulation of Gzα receptor for integrin activation (Martin et al. 2020).

Adrenaline being a weak agonist may induce platelet aggregation by increased mitochondrial Ca^{2+} is an unknown phenomenon. Here we report an intriguing fact for the first time that platelet aggregation triggered by α2 adrenergic receptors agonist is reduced via inhibition of mitochondrial Ca^{2+}uptake with MTX. This data is corroborated by our results that adrenaline stimulation increased mitochondrial dehydrogenase activity and MCU inhibition with MTX significantly reduced this effect. In strong-stimulated platelets sustained Ca^{2+} elevation may result in collapse of membrane potential and Cyclophilin-D dependent mPTP opening (Choo et al. 2017). However, mild agonist does not open mPTP and exhibit CypD-independent platelet activation (Varjú et al. 2018). An immunosuppressive drug Cyclosporin A (CsA) has been identified to be the inhibitor of CypD, which is also used as a therapeutic target for cardio protection (Hausenloy, Boston-Griffiths, and Yellon 2012). An earlier study on platelets of CypD knockout (CypD$^{-/-}$) mice reported a lower ADP-induced aggregation in comparison to wild type (WT). However CsA-treated platelets enhanced platelet aggregation stimulated by ADP (Varjú et al. 2018) and adrenaline (Grace et al. 1987). MTX has been identified as inhibitor of MCU in the yeast mitochondria (Arduino et al. 2017). It strongly reduced kampferol induced mitochondrial Ca^{2+}, which is an activator of MCU in pancreatic β-cells (Bermont et al. 2020). Thus, a combination of our data and information from already published literature provide clues about the possible involvement of mitochondrial activities in adrenaline-induced platelet aggregation that requires further exploration.

The Contribution of Mitochondrial Calcium Homeostasis in Agonist-Induced Platelet Response

In this study we also determined an intriguing role of MCU in procoagulant/COAT platelets. Our data is consistent with already published studies that procoagulant COAT platelets are generated mainly by the co-stimulation of convulxin and thrombin. However, in addition to determining the role of mitoxantone we also investigated the formation of procoagulant platelets in response to single stimulation with thrombin or convulxin. Interestingly, thrombin stimulation alone triggered only a small increase in PS exposure, a hallmark of procoagulant platelets, that was not inhibited by MTX. In contrast, convulxin generated moderate procoagulant platelets and MTX showed a significant drop in the generation of Annexin V positive platelets. The key regulator in the generation of procoagulant platelets is related to elevated and more sustained level of intracellular Ca^{2+}. Taking in consideration the sustained level of cytosolic Ca^{2+} our data supports the fact already mentioned that convulxin triggers more sustained level of cytosolic Ca^{2+} than thrombin. Therefore, relatively higher percentage of Annexin-V was obtained with convulxin as compared to thrombin.

Furthermore, inhibition of MCU with MTX has strongly reduced the procoagulant platelet generated by dual stimulation with thrombin-plus-convulxin which goes in line with already published study that MCU is key regulator for generation of procoagulant platelets. It has been reported earlier that MCU KO murine platelets has decreased procoagulant platelet formation in comparison to MCU WT (wild type). Likewise, MCU-KO platelets have been demonstrated to have enhanced integrin activation (Kholmukhamedov et al. 2018) complementing our data of PAC-1 binding with MTX. Similarly, inhibition of cyclophilin D (CypD) with cyclosporine (CsA) and genetic ablation of CypD has also markedly abrogated the formation of procoagulant platelets. It is also noted that sustained cytosolic Ca^{2+} and mPTP opening are essential regulators of procoagulant platelets generation after dual stimulation (Choo et al. 2012). Besides this, we validated our result by inhibiting MCU with a recently developed inhibitor Ru265, which has demonstrated a much higher membrane permeability as compared to Ru360 (Woods et al. 2020), Like MTX, Ru-265 showed a remarkable inhibitory effect on generation of procoagulant platelets upon stimulation with dual agonists. Based on these findings, we speculated that downstream signaling pathway of GPVI is involved in procoagulant platelet formation, which strongly depends on MCU-mediated Ca^{2+} uptake (Choo et al. 2012) (Abbasian et al. 2020).

In a nutshell, our study revealed the unidentified role of mitochondrial Ca^{2+} in agonist-induced platelet responses. Particularly, mitochondrial Ca^{2+} influx pathways remarkably reduced the platelet responses including platelet aggregation and platelet activation stimulated by strong and weak agonists. On the contrary, mitochondrial Ca^{2+} efflux pathway has only enhanced ADP-induced platelet aggregation and activation; while, with strong agonist mitochondrial Ca^{2+} efflux pathways didn't show any involvement. Moreover, mitochondrial Ca^{2+} influx pathway has shown a significant role in procoagulant platelets formation revealing that MCU is a key regulator in collagen/convulxin-dependent procoagulant platelets with a questionable role in thrombin-induced effects.

5.REFRENCES

Abbasian, Nima, Sarah L Millington-Burgess, Shirom Chabra, Jean-Daniel Malcor, and Matthew T Harper. 2020. 'Supramaximal calcium signaling triggers procoagulant platelet formation', *Blood advances*, 4: 154-64.

Adlakha, Jyoti, Ioanna Karamichali, Juthaporn Sangwallek, Silvia Deiss, Kerstin Bär, Murray Coles, Marcus D Hartmann, Andrei N Lupas, and Birte Hernandez Alvarez. 2019. 'Characterization of MCU-binding proteins MCUR1 and CCDC90B—representatives of a protein family conserved in prokaryotes and eukaryotic organelles', *Structure*, 27: 464-75. e6.

Agbani, Ejaife O, Marion TJ van den Bosch, Ed Brown, Christopher M Williams, Nadine JA Mattheij, Judith MEM Cosemans, Peter W Collins, Johan WM Heemskerk, Ingeborg Hers, and Alastair W Poole. 2015. 'Coordinated membrane ballooning and procoagulant spreading in human platelets', *Circulation*, 132: 1414-24.

Agbani, Ejaife O, Christopher M Williams, Ingeborg Hers, and Alastair W Poole. 2017. 'Membrane ballooning in aggregated platelets is synchronised and mediates a surge in microvesiculation', *Scientific Reports*, 7: 2770.

Agbani, Ejaife O, Christopher M Williams, Yong Li, Marion TJ van den Bosch, Samantha F Moore, Adele Mauroux, Lorna Hodgson, Alan S Verkman, Ingeborg Hers, and Alastair W Poole. 2018. 'Aquaporin-1 regulates platelet procoagulant membrane dynamics and in vivo thrombosis', *JCI insight*, 3.

Alberio, Lorenzo, Catherine Ravanat, Béatrice Hechler, Pierre H Mangin, François Lanza, and Christian Gachet. 2017. 'Delayed-onset of procoagulant signalling revealed by kinetic analysis of COAT platelet formation', *Thrombosis and haemostasis*, 117: 1101-14.

Aliotta, Alessandro, Debora Bertaggia Calderara, and Lorenzo Alberio. 2020. 'Flow cytometric monitoring of dynamic cytosolic calcium, sodium, and potassium fluxes following platelet activation', *Cytometry Part A*, 97: 933-44.

Aliotta, Alessandro, Manuel Krüsi, Debora Bertaggia Calderara, Maxime G Zermatten, Francisco J Gomez, Ana P Batista Mesquita Sauvage, and Lorenzo Alberio. 2020.

'Characterization of procoagulant coat platelets in patients with glanzmann thrombasthenia', *International Journal of Molecular Sciences*, 21: 9515.

Anand, Peterson, and Alan GS Harper. 2020. 'Human platelets use a cytosolic Ca^{2+} nanodomain to activate Ca^{2+}-dependent shape change independently of platelet aggregation', *Cell Calcium*, 90: 102248.

Arduino, Daniela M, Jennifer Wettmarshausen, Horia Vais, Paloma Navas-Navarro, Yiming Cheng, Anja Leimpek, Zhongming Ma, Alba Delrio-Lorenzo, Andrea Giordano, and Cecilia Garcia-Perez. 2017. 'Systematic identification of MCU modulators by orthogonal interspecies chemical screening', *Molecular cell*, 67: 711-23. e7.

Austin, Shane, Ronald Mekis, Sami EM Mohammed, Mariafrancesca Scalise, Wen-An Wang, Michele Galluccio, Christina Pfeiffer, Tamara Borovec, Katja Parapatics, and Dijana Vitko. 2022. 'TMBIM5 is the Ca^{2+}/H^+ antiporter of mammalian mitochondria', *EMBO reports*, 23: e54978.

Baev, Artyom Y, Andrey Y Vinokurov, Irina N Novikova, Viktor V Dremin, Elena V Potapova, and Andrey Y Abramov. 2022. 'Interaction of mitochondrial calcium and ROS in neurodegeneration', *Cells*, 11: 706.

Ballerini, Patrizia, Melania Dovizio, Annalisa Bruno, Stefania Tacconelli, and Paola Patrignani. 2018. 'P2Y12 receptors in tumorigenesis and metastasis', *Frontiers in Pharmacology*, 9: 66.

Begonja, Antonija Jurak, Stepan Gambaryan, J.rg Geiger, Barsom Aktas, Miroslava Pozgajova, Bernhard Nieswandt, and Ulrich Walter. 2005. 'Platelet NAD (P) H-oxidase–generated ROS production regulates αIIbβ3-integrin activation independent of the NO/cGMP pathway', *Blood*, 106: 2757-60.

Bergmeier, Wolfgang, and Lucia Stefanini. 2009. 'Novel molecules in calcium signaling in platelets', *Journal of thrombosis and haemostasis*, 7: 187-90.

Bermont, Flavien, Aurelie Hermant, Romy Benninga, Christian Chabert, Guillaume Jacot, Jaime Santo-Domingo, Marine RC Kraus, Jerome N Feige, and Umberto De Marchi. 2020. 'Targeting mitochondrial calcium uptake with the natural flavonol

kaempferol, to promote metabolism/secretion coupling in pancreatic β-cells', *Nutrients*, 12: 538.

Blomeyer, Christoph A, Jason N Bazil, David F Stowe, Ranjan K Pradhan, Ranjan K Dash, and Amadou KS Camara. 2013. 'Dynamic buffering of mitochondrial Ca 2+ during Ca 2+ uptake and Na+-induced Ca 2+ release', *Journal of bioenergetics and biomembranes*, 45: 189-202.

Boyanova, Desislava, Santosh Nilla, Ingvild Birschmann, Thomas Dandekar, and Marcus Dittrich. 2012. 'PlateletWeb: a systems biologic analysis of signaling networks in human platelets', *Blood, The Journal of the American Society of Hematology*, 119: e22-e34.

Boyman, Liron, George SB Williams, Daniel Khananshvili, Israel Sekler, and WJ Lederer. 2013. 'NCLX: the mitochondrial sodium calcium exchanger', *Journal of molecular and cellular cardiology*, 59: 205-13.

Brass, Lawrence F, and SK Joseph. 1985. 'A role for inositol triphosphate in intracellular Ca^{2+} mobilization and granule secretion in platelets', *Journal of Biological Chemistry*, 260: 15172-79.

Brown, Charles S, and William L Dean. 2007. 'Regulation of plasma membrane Ca^{2+}-ATPase in human platelets by calpain', *Platelets*, 18: 207-11.

Bruce, Jason IE. 2018. 'Metabolic regulation of the PMCA: Role in cell death and survival', *Cell Calcium*, 69: 28-36.

Bye, Alex P, Amanda J Unsworth, and Jon M Gibbins. 2016. 'Platelet signaling: a complex interplay between inhibitory and activatory networks', *Journal of thrombosis and haemostasis*, 14: 918-30.

Cabral-Costa, João Victor, Carlos Vicente-Gutiérrez, Jesús Agulla, Rebeca Lapresa, John W Elrod, Ángeles Almeida, Juan P Bolaños, and Alicia J Kowaltowski. 2022. 'Mitochondrial sodium/calcium exchanger NCLX regulates glycolysis in astrocytes, impacting on cognitive performance', *Journal of Neurochemistry*.

Carvalho, Edmund J, Peter B Stathopulos, and Muniswamy Madesh. 2020. 'Regulation of Ca^{2+} exchanges and signaling in mitochondria', *Current opinion in physiology*, 17: 197-206.

Cattaneo, Marco. 2019. 'The platelet P2 receptors.' in, *Platelets* (Elsevier).

Choo, Hyo-Jung, Andaleb Kholmukhamedov, ChengZing Zhou, and Shawn Jobe. 2017. 'Inner mitochondrial membrane disruption links apoptotic and agonist-initiated phosphatidylserine externalization in platelets', *Arteriosclerosis, thrombosis, and vascular biology*, 37: 1503-12.

Choo, Hyo-Jung, Talib B Saafir, Laura Mkumba, Mary B Wagner, and Shawn M Jobe. 2012. 'Mitochondrial calcium and reactive oxygen species regulate agonist-initiated platelet phosphatidylserine exposure', *Arteriosclerosis, thrombosis, and vascular biology*, 32: 2946-55.

Chu, Yaxin, Han Guo, Yuncong Zhang, and Rui Qiao. 2021. 'Procoagulant platelets: Generation, characteristics, and therapeutic target', *Journal of Clinical Laboratory Analysis*, 35: e23750.

Coller, Barry S, and Sanford J Shattil. 2008. 'The GPIIb/IIIa (integrin αIIbβ3) odyssey: a technology-driven saga of a receptor with twists, turns, and even a bend', *Blood, The Journal of the American Society of Hematology*, 112: 3011-25.

Dale, George L, Paul Friese, Peter Batar, Stephen F Hamilton, Guy L Reed, Kenneth W Jackson, Kenneth J Clemetson, and Lorenzo Alberio. 2002. 'Stimulated platelets use serotonin to enhance their retention of procoagulant proteins on the cell surface', *Nature*, 415: 175-79.

Dale, GL. 2005. 'Coated-platelets: an emerging component of the procoagulant response', *Journal of thrombosis and haemostasis*, 3: 2185-92.

De Marchi, Elena, Massimo Bonora, Carlotta Giorgi, and Paolo Pinton. 2014. 'The mitochondrial permeability transition pore is a dispensable element for mitochondrial calcium efflux', *Cell Calcium*, 56: 1-13.

De Stefani, Diego, Anna Raffaello, Enrico Teardo, Ildikò Szabò, and Rosario Rizzuto. 2011. 'A forty-kilodalton protein of the inner membrane is the mitochondrial calcium uniporter', *Nature*, 476: 336-40.

Deak, Andras T, Sandra Blass, Muhammad J Khan, Lukas N Groschner, Markus Waldeck-Weiermair, Seth Hallström, Wolfgang F Graier, and Roland Malli. 2014. 'IP3-

mediated STIM1 oligomerization requires intact mitochondrial Ca^{2+} uptake', *Journal of cell science*, 127: 2944-55.

Dean, William L. 2010. 'Role of platelet plasma membrane Ca^{2+}-ATPase in health and disease', *World journal of biological chemistry*, 1: 265.

Dolan, Andrew T, and Scott L Diamond. 2014. 'Systems modeling of Ca^{2+} homeostasis and mobilization in platelets mediated by IP3 and store-operated Ca^{2+} entry', *Biophysical journal*, 106: 2049-60.

Durrant, Tom N, Marion T van den Bosch, and Ingeborg Hers. 2017. 'Integrin αIIbβ3 outside-in signaling', *Blood, The Journal of the American Society of Hematology*, 130: 1607-19.

Ebbeling, Lori, Catherine Robertson, Archibald McNicol, and Jon M Gerrard. 1992. 'Rapid ultrastructural changes in the dense tubular system following platelet activation'.

Estevez, Brian, and Xiaoping Du. 2017. 'New concepts and mechanisms of platelet activation signaling', *Physiology*, 32: 162-77.

Fitch-Tewfik, Jennifer L, and Robert Flaumenhaft. 2013. 'Platelet granule exocytosis: a comparison with chromaffin cells', *Frontiers in endocrinology*, 4: 77.

Flaumenhaft, Robert, and Anish Sharda. 2019. 'Platelet secretion.' in, *Platelets* (Elsevier).

Fritsma, George A. 2015. 'Platelet structure and function', *Clinical laboratory science*, 28: 125.

Fukami, MH. 1997. 'Dense granule factors.' in, *Platelets and their Factors* (Springer).

Garbincius, Joanne F, Oniel Salik, Henry M Cohen, Carmen Choya-Foces, Adam S Mangold, Angelina D Makhoul, Anna E Schmidt, Dima Y Khalil, Joshua J Doolittle, and Anya S Wilkinson. 2023. 'TMEM65 regulates NCLX-dependent mitochondrial calcium efflux', *bioRxiv*.

Garcia, Analia, Soochong Kim, Kamala Bhavaraju, Simone M Schoenwaelder, and Satya P Kunapuli. 2010. 'Role of phosphoinositide 3-kinase β in platelet aggregation and thromboxane A2 generation mediated by Gi signalling pathways', *Biochemical Journal*, 429: 369-77.

Ghatge, Madankumar, Manasa K Nayak, Gagan D Flora, Mariia Kumskova, Aditi Jain, Rakesh B Patel, Zhihong Lin, Yuriy M Usachev, and Anil K Chauhan. 2023. 'Mitochondrial calcium uniporter b deletion inhibits platelet function and reduces susceptibility to arterial thrombosis', *Journal of thrombosis and haemostasis*.

Ghoshal, Kakali, and Maitree Bhattacharyya. 2014. 'Overview of platelet physiology: its hemostatic and nonhemostatic role in disease pathogenesis', *The Scientific World Journal*, 2014.

Grace, Andrew A, Manuel A Barradas, Dimitri P Mikhailidis, Jamie Y Jeremy, John F Moorhead, Paul Sweny, and Paresh Dandona. 1987. 'Cyclosporine A enhances platelet aggregation', *Kidney international*, 32: 889-95.

Gremmel, Thomas, Andrew L Frelinger III, and Alan D Michelson. 2016. "Platelet physiology." In *Seminars in thrombosis and hemostasis*, 191-204. Thieme Medical Publishers.

Gurbel, Paul A, Athan Kuliopulos, and Udaya S Tantry. 2015. 'G-protein–coupled receptors signaling pathways in new antiplatelet drug development', *Arteriosclerosis, thrombosis, and vascular biology*, 35: 500-12.

Hamad, Muataz Ali, Krystin Krauel, Nancy Schanze, Nadine Gauchel, Peter Stachon, Thomas Nuehrenberg, Mark Zurek, and Daniel Duerschmied. 2022. 'Platelet subtypes in inflammatory settings', *Frontiers in Cardiovascular Medicine*, 9: 823549.

Han, Xu, Emma G Bouck, Elizabeth R Zunica, Amal Arachiche, and Marvin T Nieman. 2019. 'Protease-activated receptors.' in, *Platelets* (Elsevier).

Harper, Alan GS, and Stewart O Sage. 2017. 'Platelet signalling: calcium', *Platelets in Thrombotic and Non-Thrombotic Disorders: Pathophysiology, Pharmacology and Therapeutics: an Update*: 285-96.

Harper, Matthew T, Juan E Camacho Londoño, Kathryn Quick, Julia Camacho Londoño, Veit Flockerzi, Stephan E Philipp, Lutz Birnbaumer, Marc Freichel, and Alastair W Poole. 2013. 'Transient receptor potential channels function as a coincidence signal detector mediating phosphatidylserine exposure', *Science signaling*, 6: ra50-ra50.

Harris, J Robin, and Jon Marles-Wright. 2021. *Macromolecular Protein Complexes III: Structure and Function* (Springer).

Hartwig, John H. 2006. "The platelet: form and function." In *Seminars in hematology*, S94-S100. Elsevier.

Hausenloy, Derek J, EA Boston-Griffiths, and DM Yellon. 2012. 'Cyclosporin A and cardioprotection: from investigative tool to therapeutic agent', *British journal of pharmacology*, 165: 1235-45.

Heemskerk, JWM, NJA Mattheij, and JMEM Cosemans. 2013. 'Platelet-based coagulation: different populations, different functions', *Journal of thrombosis and haemostasis*, 11: 2-16.

Hua, Vu Minh, Latasha Abeynaike, Elias Glaros, Heather Campbell, Leonardo Pasalic, Philip J Hogg, and Vivien MY Chen. 2015. 'Necrotic platelets provide a procoagulant surface during thrombosis', *Blood, The Journal of the American Society of Hematology*, 126: 2852-62.

Huang, Jiansong, Xia Li, Xiaofeng Shi, Mark Zhu, Jinghan Wang, Shujuan Huang, Xin Huang, Huafeng Wang, Ling Li, and Huan Deng. 2019. 'Platelet integrin αIIbβ3: signal transduction, regulation, and its therapeutic targeting', *Journal of hematology & oncology*, 12: 1-22.

Jandrot-Perrus, Martine, Anne-Hél.ne Lagrue, Minoru Okuma, and Cassian Bon. 1997. 'Adhesion and Activation of Human Platelets Induced by Convulxin Involve Glycoprotein VI and Integrin α2˘1', *Journal of Biological Chemistry*, 272: 27035-41.

Janmey, Paul A, Christopher A McCulloch, and Richard Tyler Miller. 2016. 'Extracellular Regulation of Cell-to-Matrix Adhesion.' in, *Functional Cell Biology* (Elsevier Inc.).

Janus-Bell, Emily, and Pierre H Mangin. 2023. 'The relative importance of platelet integrins in hemostasis, thrombosis and beyond', *Haematologica*, 108: 1734.

Jardín, Isaac, José J López, José A Pariente, Ginés M Salido, and Juan A Rosado. 2008. 'Intracellular calcium release from human platelets: different messengers for multiple stores', *Trends in cardiovascular medicine*, 18: 57-61.

Jennings, Lisa K. 2009. 'Mechanisms of platelet activation: need for new strategies to protect against platelet-mediated atherothrombosis', *Thrombosis and haemostasis*, 102: 248-57.

Jin, Mingpeng, Jiaojiao Wang, Xiaoying Ji, Haiyan Cao, Jianjun Zhu, Yibing Chen, Jin Yang, Zheng Zhao, Tingting Ren, and Jinliang Xing. 2019. 'MCUR1 facilitates epithelial-mesenchymal transition and metastasis via the mitochondrial calcium dependent ROS/Nrf2/Notch pathway in hepatocellular carcinoma', *Journal of experimental & clinical cancer research*, 38: 1-13.

Jones, Sarah, Richard J Evans, and Martyn P Mahaut-Smith. 2011. 'Extracellular Ca^{2+} modulates ADP-evoked aggregation through altered agonist degradation: implications for conditions used to study P2Y receptor activation', *British journal of haematology*, 153: 83-91.

Josefsson, Emma C, Sofia Ramström, Johannes Thaler, Marie Lordkipanidzé, Ejaife O Agbani, Lorenzo Alberio, Tamam Bakchoul, Beth A Bouchard, Marina Camera, and Vivien Chen. 2023. 'Consensus report on markers to distinguish procoagulant platelets from apoptotic platelets: communication from the Scientific and Standardization Committee of the ISTH', *Journal of thrombosis and haemostasis*.

Kasirer-Friede, Ana, Zaverio M Ruggeri, and Sanford J Shattil. 2010. 'Role for ADAP in shear flow–induced platelet mechanotransduction', *Blood, The Journal of the American Society of Hematology*, 115: 2274-82.

Kholmukhamedov, A, R Janecke, H-J Choo, and SM Jobe. 2018. 'The mitochondrial calcium uniporter regulates procoagulant platelet formation', *Journal of thrombosis and haemostasis*, 16: 2315-21.

Kim, Oleg V, Tatiana A Nevzorova, Elmira R Mordakhanova, Anastasia A Ponomareva, Izabella A Andrianova, Giang Le Minh, Amina G Daminova, Alina D Peshkova, Mark S Alber, and Olga Vagin. 2019. 'Fatal dysfunction and disintegration of thrombin-stimulated platelets', *Haematologica*, 104: 1866.

Kosovsky, Marshall J, and Gerald Soslau. 1991. 'Mitochondrial DNA topoisomerase I from human platelets', *Biochimica et Biophysica Acta (BBA)-Protein Structure and Molecular Enzymology*, 1078: 56-62.

Kulkarni, Paresh P, Mohammad Ekhlak, Vijay K Sonkar, and Debabrata Dash. 2022. 'Mitochondrial ATP generation in stimulated platelets is essential for granule secretion but dispensable for aggregation and procoagulant activity', *Haematologica*, 107: 1209.

Kulkarni, Suhasini, and Shaun P Jackson. 2004. 'Platelet factor XIII and calpain negatively regulate integrin αIIbβ3 adhesive function and thrombus growth', *Journal of Biological Chemistry*, 279: 30697-706.

Lecut, Christelle, Véronique Arocas, Hans Ulrichts, Anthony Elbaz, Jean-Luc Villeval, Jean-Jacques Lacapere, Hans Deckmyn, and Martine Jandrot-Perrus. 2004. 'Identification of residues within human glycoprotein VI involved in the binding to collagen: evidence for the existence of distinct binding sites', *Journal of Biological Chemistry*, 279: 52293-99.

Lee, Ho-Sup, Chinten James Lim, Wilma Puzon-McLaughlin, Sanford J Shattil, and Mark H Ginsberg. 2009. 'RIAM activates integrins by linking talin to ras GTPase membrane-targeting sequences', *Journal of Biological Chemistry*, 284: 5119-27.

Leytin, Valery, David J Allen, Asuman Mutlu, Armen V Gyulkhandanyan, Sergiy Mykhaylov, and John Freedman. 2009. 'Mitochondrial control of platelet apoptosis: effect of cyclosporin A, an inhibitor of the mitochondrial permeability transition pore', *Laboratory Investigation*, 89: 374-84.

Li, Zhenyu, M Keegan Delaney, Kelly A O'Brien, and Xiaoping Du. 2010. 'Signaling during platelet adhesion and activation', *Arteriosclerosis, thrombosis, and vascular biology*, 30: 2341-49.

Lindemann, S, B Krämer, P Seizer, and M Gawaz. 2007. 'Platelets, inflammation and atherosclerosis', *Journal of thrombosis and haemostasis*, 5: 203-11.

Linden, Matthew D. 2013. 'Platelet physiology', *Haemostasis: Methods and Protocols*: 13-30.

Lytton, Jonathan. 2007. 'Na$^+$/Ca^{2+} exchangers: three mammalian gene families control Ca^{2+} transport', *Biochemical Journal*, 406: 365-82.

Ma, Yan, Qian Jiang, Bingxin Yang, Xiaoyu Hu, Gang Shen, Wei Shen, and Jing Xu. 2023. 'Platelet mitochondria, a potent immune mediator in neurological diseases', *Frontiers in Physiology*, 14.

Mahaut-Smith, Martyn P, Sarah Jones, and Richard J Evans. 2011. 'The P2X1 receptor and platelet function', *Purinergic signalling*, 7: 341-56.

Mammucari, Cristina, Gaia Gherardi, and Rosario Rizzuto. 2017. 'Structure, activity regulation, and role of the mitochondrial calcium uniporter in health and disease', *Frontiers in oncology*, 7: 139.

Mansour, Alexandre, Christilla Bachelot-Loza, Nicolas Nesseler, Pascale Gaussem, and Isabelle Gouin-Thibault. 2020. 'P2Y12 inhibition beyond thrombosis: effects on inflammation', *International Journal of Molecular Sciences*, 21: 1391.

Martell, Jeffrey D, Thomas J Deerinck, Yasemin Sancak, Thomas L Poulos, Vamsi K Mootha, Gina E Sosinsky, Mark H Ellisman, and Alice Y Ting. 2012. 'Engineered ascorbate peroxidase as a genetically encoded reporter for electron microscopy', *Nature biotechnology*, 30: 1143-48.

Martin, Anne-Céline, Diane Zlotnik, Guillaume Porta Bonete, Elodie Baron, Benoît Decouture, Tiphaine Belleville-Rolland, Bernard Le Bonniec, Sonia Poirault-Chassac, Marie-Christine Alessi, and Pascale Gaussem. 2020. 'Epinephrine restores platelet functions inhibited by ticagrelor: A mechanistic approach', *European Journal of Pharmacology*, 866: 172798.

Masselli, Elena, Giulia Pozzi, Mauro Vaccarezza, Prisco Mirandola, Daniela Galli, Marco Vitale, Cecilia Carubbi, and Giuliana Gobbi. 2020. 'ROS in platelet biology: functional aspects and methodological insights', *International Journal of Molecular Sciences*, 21: 4866.

Mattheij, Nadine JA, Frauke Swieringa, Tom G Mastenbroek, Michelle A Berny-Lang, Frauke May, Constance CFMJ Baaten, Paola EJ van der Meijden, Yvonne MC Henskens, Erik AM Beckers, and Dennis PL Suylen. 2016. 'Coated platelets function in platelet-dependent fibrin formation via integrin $\alpha IIb\beta3$ and transglutaminase factor XIII', *Haematologica*, 101: 427.

Mazepa, Marshall, Maureane Hoffman, and Dougald Monroe. 2013. 'Superactivated platelets: thrombus regulators, thrombin generators, and potential clinical targets', *Arteriosclerosis, thrombosis, and vascular biology*, 33: 1747-52.

Mertins, Barbara, Georgios Psakis, and Lars-Oliver Essen. 2014. 'Voltage-dependent anion channels: the wizard of the mitochondrial outer membrane', *Biological chemistry*, 395: 1435-42.

Mikusová, V, A Tichý, M Rezáčová, and J Vávrová. 2011. 'Mitoxantrone in combination with a DNA-PK inhibitor: possible therapy of promyelocytic leukaemia resistant forms', *Folia Biol (Praha)*, 57: 200-5.

Millington-Burgess, Sarah L, and Matthew T Harper. 2021. 'Cytosolic and mitochondrial Ca^{2+} signaling in procoagulant platelets', *Platelets*, 32: 855-62.

Novorolsky, Robyn J, Gracious DS Kasheke, Antoine Hakim, Marianna Foldvari, Gabriel G Dorighello, Israel Sekler, Vidyasagar Vuligonda, Martin E Sanders, Robert B Renden, and Justin J Wilson. 2023. 'Preserving and enhancing mitochondrial function after stroke to protect and repair the neurovascular unit: novel opportunities for nanoparticle-based drug delivery', *Frontiers in Cellular Neuroscience*, 17.

Obydennyy, Sergey I, Anastasia N Sveshnikova, Fazly I Ataullakhanov, and Mikhail A Panteleev. 2016. 'Dynamics of calcium spiking, mitochondrial collapse and phosphatidylserine exposure in platelet subpopulations during activation', *Journal of thrombosis and haemostasis*, 14: 1867-81.

Offermanns, Stefan. 2006. 'Activation of platelet function through G protein–coupled receptors', *Circulation research*, 99: 1293-304.

Ordaz, Elisa Gloria Gorostieta. 2016. 'Blood and Hemopoiesis'. https://elisagorostietaordaz.blogspot.com/2012/12/blood-and-hemopoiesis.html.

Oury, Cécile, Emese Toth-Zsamboki, Jos Vermylen, and Marc F Hoylaerts. 2002. 'P2X1-mediated activation of extracellular signal-regulated kinase 2 contributes to platelet secretion and aggregation induced by collagen', *Blood, The Journal of the American Society of Hematology*, 100: 2499-505.

Oury, Cécile, Emese Toth-Zsamboki, Jozef Vermylen, and Marc F Hoylaerts. 2006. 'The platelet ATP and ADP receptors', *Current pharmaceutical design*, 12: 859-75.

Palacios-Acedo, Ana Luisa, Diane Mège, Lydie Crescence, Françoise Dignat-George, Christophe Dubois, and Laurence Panicot-Dubois. 2019. 'Platelets, thrombo-inflammation, and cancer: collaborating with the enemy', *Frontiers in immunology*, 10: 1805.

Palty, R., and I. Sekler. 2012. 'The mitochondrial Na(+)/Ca(2+) exchanger', *Cell Calcium*, 52: 9-15.

Panzer, Simon, Lisa Höcker, and Daniela Koren. 2006. 'Agonists-induced platelet activation varies considerably in healthy male individuals: studies by flow cytometry', *Annals of hematology*, 85: 121-25.

Paravati, Stephen, Alan Rosani, and Steven J Warrington. 2018. 'Physiology, catecholamines'.

Park, See-Hyoung, Jongsung Lee, Mi Kang, Kyu Yun Jang, and Jung Ryul Kim. 2018. 'Mitoxantrone induces apoptosis in osteosarcoma cells through regulation of the Akt/FOXO3 pathway', *Oncology letters*, 15: 9687-96.

Pathak, Trayambak, and Mohamed Trebak. 2018. 'Mitochondrial Ca^{2+} signaling', *Pharmacology & therapeutics*, 192: 112-23.

Patron, Maria, Vanessa Checchetto, Anna Raffaello, Enrico Teardo, Denis Vecellio Reane, Maura Mantoan, Veronica Granatiero, Ildikò Szabò, Diego De Stefani, and Rosario Rizzuto. 2014. 'MICU1 and MICU2 finely tune the mitochondrial Ca^{2+} uniporter by exerting opposite effects on MCU activity', *Molecular cell*, 53: 726-37.

Patron, Maria, Anna Raffaello, Veronica Granatiero, Anna Tosatto, Giulia Merli, Diego De Stefani, Lauren Wright, Giorgia Pallafacchina, Anna Terrin, and Cristina Mammucari. 2013. 'The mitochondrial calcium uniporter (MCU): molecular identity and physiological roles', *Journal of Biological Chemistry*, 288: 10750-58.

Piao, Linfeng, Hyungmin Park, and Chris Hyunchul Jo. 2017. 'Theoretical prediction and validation of cell recovery rates in preparing platelet-rich plasma through a centrifugation', *PloS one*, 12: e0187509.

Poddar, Mrinal K, and Soumyabrata Banerjee. 2020. 'Molecular Aspects of Pathophysiology of Platelet Receptors', *Platelets*.

Podoplelova, Nadezhda A, Anastasia N Sveshnikova, Yana N Kotova, Anita Eckly, Nicolas Receveur, Dmitry Yu Nechipurenko, Sergey I Obydennyi, Igor I Kireev, Christian Gachet, and Fazly I Ataullakhanov. 2016. 'Coagulation factors bound to procoagulant platelets concentrate in cap structures to promote clotting', *Blood, The Journal of the American Society of Hematology*, 128: 1745-55.

Ragab, Ashraf, Sonia Séverin, Marie-Pierre Gratacap, Enrique Aguado, Marie Malissen, Martine Jandrot-Perrus, Bernard Malissen, Jeannie Ragab-Thomas, and Bernard Payrastre. 2007. 'Roles of the C-terminal tyrosine residues of LAT in GPVI-induced platelet activation: insights into the mechanism of PLCγ2 activation', *Blood, The Journal of the American Society of Hematology*, 110: 2466-74.

Reed, Guy L. 2002. 'Platelet secretion', *Platelets*, 2: 309-18.

Ribatti, Domenico, and Enrico Crivellato. 2007. 'Giulio Bizzozero and the discovery of platelets', *Leukemia research*, 31: 1339-41.

Rivera, José, María Luisa Lozano, Leyre Navarro-Núñez, and Vicente Vicente. 2009. 'Platelet receptors and signaling in the dynamics of thrombus formation', *Haematologica*, 94: 700.

Romero-Garcia, Susana, and Heriberto Prado-Garcia. 2019. 'Mitochondrial calcium: Transport and modulation of cellular processes in homeostasis and cancer', *International journal of oncology*, 54: 1155-67.

Ruiz, A, E Alberdi, and C Matute. 2014. 'CGP37157, an inhibitor of the mitochondrial Na^+/Ca^{2+} exchanger, protects neurons from excitotoxicity by blocking voltage-gated Ca^{2+} channels', *Cell death & disease*, 5: e1156-e56.

Sage, Stewart O, Nicholas Pugh, Richard W Farndale, and Alan GS Harper. 2013. 'Pericellular Ca^{2+} recycling potentiates thrombin-evoked Ca^{2+} signals in human platelets', *Physiological Reports*, 1.

Sancak, Yasemin, Andrew L Markhard, Toshimori Kitami, Erika Kovács-Bogdán, Kimberli J Kamer, Namrata D Udeshi, Steven A Carr, Dipayan Chaudhuri, David

E Clapham, and Andrew A Li. 2013. 'EMRE is an essential component of the mitochondrial calcium uniporter complex', *Science*, 342: 1379-82.

Sander, Paulina, Thomas Gudermann, and Johann Schredelseker. 2021. 'A calcium guard in the outer membrane: Is VDAC a regulated gatekeeper of mitochondrial calcium uptake?', *International Journal of Molecular Sciences*, 22: 946.

Scridon, Alina. 2022. 'Platelets and their role in hemostasis and thrombosis—From physiology to pathophysiology and therapeutic implications', *International Journal of Molecular Sciences*, 23: 12772.

Selvadurai, Maria V, and Justin R Hamilton. 2018. 'Structure and function of the open canalicular system–the platelet's specialized internal membrane network', *Platelets*, 29: 319-25.

Senchenkova, Elena Y, Janice Russell, Alper Yildirim, D Neil Granger, and Felicity NE Gavins. 2019. 'Novel Role of T Cells and IL-6 (Interleukin-6) in angiotensin II–induced microvascular dysfunction', *Hypertension*, 73: 829-38.

Sonkar, Vijay K, Rahul Kumar, Melissa Jensen, Brett A Wagner, Anjali A Sharathkumar, Francis J Miller Jr, MaryBeth Fasano, Steven R Lentz, Garry R Buettner, and Sanjana Dayal. 2019. 'Nox2 NADPH oxidase is dispensable for platelet activation or arterial thrombosis in mice', *Blood advances*, 3: 1272-84.

Stalker, Timothy J, Debra K Newman, Peisong Ma, Kenneth M Wannemacher, and Lawrence F Brass. 2012. 'Platelet signaling', *Antiplatelet agents*: 59-85.

Stathopulos, Peter B, Le Zheng, Guang-Yao Li, Michael J Plevin, and Mitsuhiko Ikura. 2008. 'Structural and mechanistic insights into STIM1-mediated initiation of store-operated calcium entry', *Cell*, 135: 110-22.

Stegner, David, and Bernhard Nieswandt. 2011. 'Platelet receptor signaling in thrombus formation', *Journal of molecular medicine*, 89: 109-21.

Storrie, Brian. 2016. 'A tip of the cap to procoagulant platelets', *Blood, The Journal of the American Society of Hematology*, 128: 1668-69.

Tarasova, Nadezhda V, Polina A Vishnyakova, Yulia A Logashina, and Andrey V Elchaninov. 2019. 'Mitochondrial calcium uniporter structure and function in

different types of muscle tissues in health and disease', *International Journal of Molecular Sciences*, 20: 4823.

Theofilis, Panagiotis, Marios Sagris, Evangelos Oikonomou, Alexios S Antonopoulos, Konstantinos Tsioufis, and Dimitris Tousoulis. 2022. 'Factors associated with platelet activation-recent pharmaceutical approaches', *International Journal of Molecular Sciences*, 23: 3301.

Trumel, Catherine, Bernard Payrastre, Monique Plantavid, Béatrice Hechler, Cécile Viala, Peter Presek, Elizabeth A Martinson, Jean-Pierre Cazenave, Hugues Chap, and Christian Gachet. 1999. 'A key role of adenosine diphosphate in the irreversible platelet aggregation induced by the PAR1-activating peptide through the late activation of phosphoinositide 3-kinase', *Blood, The Journal of the American Society of Hematology*, 94: 4156-65.

van der Meijden, Paola EJ, and Johan WM Heemskerk. 2019. 'Platelet biology and functions: new concepts and clinical perspectives', *Nature Reviews Cardiology*, 16: 166-79.

Van Geet, Christel, Benedetta Izzi, Veerle Labarque, and Kathleen Freson. 2009. 'Human platelet pathology related to defects in the G-protein signaling cascade', *Journal of thrombosis and haemostasis*, 7: 282-86.

Varga-Szabo, David, Irina Pleines, and Bernhard Nieswandt. 2008. 'Cell adhesion mechanisms in platelets', *Arteriosclerosis, thrombosis, and vascular biology*, 28: 403-12.

Varga-Szabo, D, A Braun, and B Nieswandt. 2009. 'Calcium signaling in platelets', *Journal of thrombosis and haemostasis*, 7: 1057-66.

Varjú, Imre, Veronika Judit Farkas, László Kőhidai, László Szabó, Ádám Zoltán Farkas, Lívia Polgár, Christos Chinopoulos, and Krasimir Kolev. 2018. 'Functional cyclophilin D moderates platelet adhesion, but enhances the lytic resistance of fibrin', *Scientific Reports*, 8: 5366.

Veuthey, Lucas, Alessandro Aliotta, Debora Bertaggia Calderara, Cindy Pereira Portela, and Lorenzo Alberio. 2022. 'Mechanisms underlying dichotomous procoagulant

COAT platelet generation—a conceptual review summarizing current knowledge', *International Journal of Molecular Sciences*, 23: 2536.

Vig, Monika, Andreas Beck, James M Billingsley, Annette Lis, Suhel Parvez, Christine Peinelt, Dana L Koomoa, Jonathan Soboloff, Donald L Gill, and Andrea Fleig. 2006. 'CRACM1 multimers form the ion-selective pore of the CRAC channel', *Current Biology*, 16: 2073-79.

Wang, Lele, Xue Yang, Siwei Li, Zheng Wang, Yu Liu, Jianrong Feng, Yushan Zhu, and Yuequan Shen. 2014. 'Structural and mechanistic insights into MICU 1 regulation of mitochondrial calcium uptake', *The EMBO journal*, 33: 594-604.

Watson, SP, JM Auger, OJT McCarty, and AC Pearce. 2005. 'GPVI and integrin αIIbβ3 signaling in platelets', *Journal of thrombosis and haemostasis*, 3: 1752-62.

White, James G. 2002. 'Morphology and ultrastructure of platelets', *Platelets in Thrombotic and Non-Thrombotic Disorders: Pathophysiology, Pharmacology and Therapeutics*: 41-69.

White, James G, and A Michelson. 2007. 'Platelet structure', *Platelets*, 2: 45-71.

White, JG. 1987. 'An overview of platelet structural physiology', *Scanning microscopy*, 1: 19.

Woods, Joshua J, James Lovett, Barry Lai, Hugh H Harris, and Justin J Wilson. 2020. 'Redox Stability Controls the Cellular Uptake and Activity of Ruthenium-Based Inhibitors of the Mitochondrial Calcium Uniporter (MCU)', *Angewandte Chemie*, 132: 6544-53.

Yadav, Pooja, Abhishek R Panigrahi, Samir K Beura, and Sunil K Singh. 2023. 'Platelet-derived microvesicles induce intracellular calcium mobilization in human platelets', *Cell Biology International*, 47: 1964-75.

Yang, Jianliang, Yuankai Shi, Chunlei Li, Lin Gui, Xi Zhao, Peng Liu, Xiaohong Han, Yuanyuan Song, Ning Li, and Ping Du. 2014. 'Phase I clinical trial of pegylated liposomal mitoxantrone plm60-s: pharmacokinetics, toxicity and preliminary efficacy', *Cancer chemotherapy and pharmacology*, 74: 637-46.

Ye, Feng, Guiqing Hu, Dianne Taylor, Boris Ratnikov, Andrey A Bobkov, Mark A McLean, Stephen G Sligar, Kenneth A Taylor, and Mark H Ginsberg. 2010. 'Recreation of the terminal events in physiological integrin activation', *Journal of Cell Biology*, 188: 157-73.

Yeromin, Andriy V, Shenyuan L Zhang, Weihua Jiang, Ying Yu, Olga Safrina, and Michael D Cahalan. 2006. 'Molecular identification of the CRAC channel by altered ion selectivity in a mutant of Orai', *Nature*, 443: 226-29.

Yoast, Ryan E, Scott M Emrich, Xuexin Zhang, Ping Xin, Vikas Arige, Trayambak Pathak, J Cory Benson, Martin T Johnson, Ahmed Emam Abdelnaby, and Natalia Lakomski. 2021. 'The Mitochondrial Ca^{2+} uniporter is a central regulator of interorganellar Ca^{2+} transfer and NFAT activation', *Journal of Biological Chemistry*, 297.

Zou, Jinmi, Frauke Swieringa, Bas de Laat, Philip G de Groot, Mark Roest, and Johan WM Heemskerk. 2022. 'Reversible Platelet Integrin αIIbβ3 Activation and Thrombus Instability', *International Journal of Molecular Sciences*, 23: 12512.

ANNEXURE

Publications

➢ **Shehwar, D**., Barki, S., Aliotta, A., Veuthey, L., Bertaggia Calderara, D., Alberio, L., & Alam, M. R. (2024). Inhibition of mitochondrial calcium transporters alters adp-induced platelet responses. *Molecular Biology Reports*, *51*(1), 177.

➢ Ali, S. G., **Shehwar, D**., & Alam, M. R. (2021). Mitoxantrone Inhibits FMLP-Induced Degenerative Changes in Human Neutrophils. *Molecular Biology*, *55*(5), 752-762.

Turnitin Originality Report

The Contribution of Mitochondrial Calcium Homeostasis in Agonist-Induced Platelet Responses   by Durre Shehwar

From PhD (PhD DRSML)

Dr. M. Rizwan Alam

26-2-24

Associate Professor
Department of Biochemistry
QUAID-I-AZAM UNIVERSITY ISLAMABAD

- Processed on 26-Feb-2024 08:28 PKT
- ID: 2304439177
- Word Count: 20805

Similarity Index
16%
Similarity by Source

Internet Sources:
8%
Publications:
12%
Student Papers:
4%

sources:

1 2% match ("Platelets in Thrombotic and Non-Thrombotic Disorders", Springer Nature, 2017)
"Platelets in Thrombotic and Non-Thrombotic Disorders", Springer Nature, 2017

2 1% match (student papers from 11-Jun-2020)
Submitted to Higher Education Commission Pakistan on 2020-06-11

3 1% match (Internet from 11-Jan-2023)
https://theses.ncl.ac.uk/jspui/bitstream/10443/4848/1/Singh%20E%202019.pdf

4 1% match (Swiss Society of Medical Oncology, Swiss Society of Hematology, Swiss Group for Clinical Cancer Research. "Supplementum 274: Abstracts of the Swiss Oncology & Hematology Congress (SOHC)", Swiss Medical Weekly, 2023)
Swiss Society of Medical Oncology, Swiss Society of Hematology, Swiss Group for Clinical Cancer Research. "Supplementum 274: Abstracts of the Swiss Oncology & Hematology Congress (SOHC)", Swiss Medical Weekly, 2023

5 < 1% match (student papers from 22-Jan-2018)
Submitted to Higher Education Commission Pakistan on 2018-01-22

6 < 1% match (student papers from 11-Jun-2020)
Submitted to Higher Education Commission Pakistan on 2020-06-11

7 < 1% match (student papers from 16-Jun-2023)
Submitted to Higher Education Commission Pakistan on 2023-06-16

8 < 1% match (student papers from 31-Jan-2018)
Submitted to Higher Education Commission Pakistan on 2018-01-31

9 < 1% match (student papers from 27-Aug-2020)
Submitted to Higher Education Commission Pakistan on 2020-08-27

10

ORIGINAL ARTICLE

Inhibition of mitochondrial calcium transporters alters adp-induced platelet responses

Durre Shehwar[1] · Saima Barki[1] · Alessandro Aliotta[2] · Lucas Veuthey[2] · Debora Bertaggia Calderara[2] ·
Lorenzo Alberio[2] · Muhammad Rizwan Alam[1]

Abstract

Introduction ADP-stimulated elevation of cytosolic Ca^{2+} is an important effector mechanism for platelet activation. The rapidly elevating cytosolic Ca^{2+} is also transported to mitochondrial matrix via Mitochondrial Ca^{2+} Uniporter (MCU) and extruded via $Na^+/Ca^{2+}/Li^+$ Exchanger (NCLX). However, the exact contribution of MCU and NCLX in ADP-mediated platelet responses remains incompletely understood.

Methods and results The present study aimed to elucidate the role of mitochondrial Ca^{2+} transport in ADP-stimulated platelet responses by inhibition of MCU and NCLX with mitoxantrone (MTX) and CGP37157 (CGP), respectively. As these inhibitory strategies are reported to cause distinct effects on matrix Ca^{2+} concentration, we hypothesized to observe opposite impact of MTX and CGP on ADP-induced platelet responses. Platelet aggregation profiling was performed by microplate-based spectrophotometery while p-selectin externalization and integrin αIIbβ3 activation were analyzed by fluorescent immunolabeling using flow cytometery. Our results confirmed the expression of both MCU and NCLX mRNAs with relatively low abundance of NCLX in human platelets. In line with our hypothesis, MTX caused a dose-dependent inhibition of ADP-induced platelet aggregation without displaying any cytotoxicity. Likewise, ADP-induced p-selectin externalization and integrin αIIbβ3 activation was also significantly attenuated in MTX-treated platelets. Concordantly, inhibition of NCLX with CGP yielded an accelerated ADP-stimulated platelet aggregation which was associated with an elevation of p-selectin surface expression and αIIbβ3 activation.

Conclusion Together, these findings uncover a vital and hitherto poorly characterized role of mitochondrial Ca^{2+} transporters in ADP-induced platelet activation.

Graphical Abstract
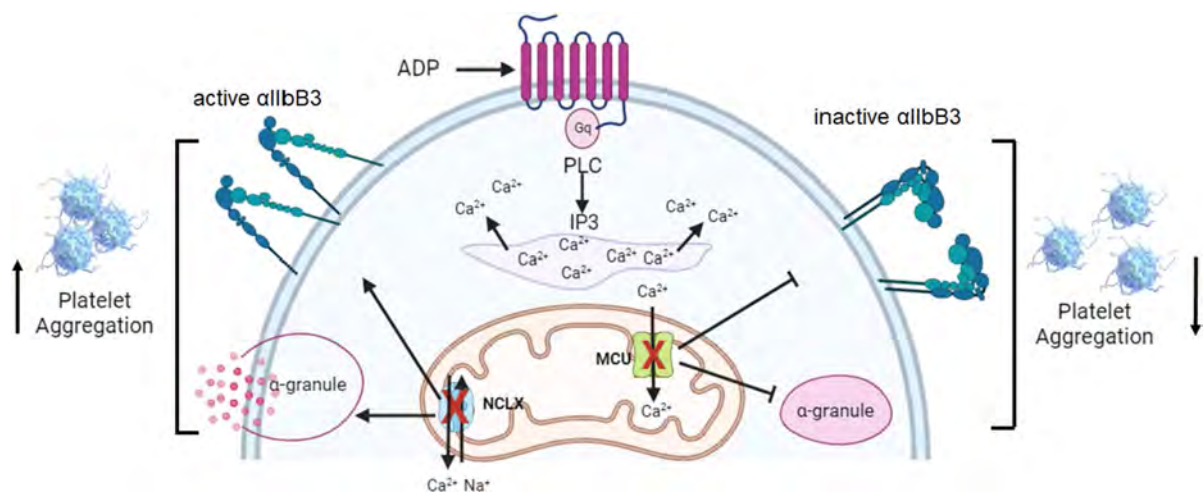
Extended author information available on the last page of the article

Abbreviations

ADP	Adenosine 5'-diphosphate
MCU	Mitochondrial Calcium Uniporter
NCLX	Sodium Calcium Lithium Exchanger
$\Delta\Psi_m$	Mitochondrial membrane potential
ROS	Reactive oxygen species
mPTP	Mitochondrial permeability transition pore
MTX	Mitoxantrone
CGP	CGP37157

Introduction

Platelets are anucleated cells derived from megakaryocytes with an established role in hemostasis, thrombosis and inflammation. Several physiological and pathological stimuli are known to trigger platelet activation, degranulation and aggregation [1]. Adenosine 5'-diphosphate (ADP) is one of the important agonists that contributes to platelet activation in both autocrine and paracrine manners [2, 3]. Platelets express two purinergic receptors for ADP, namely P2Y1 and P2Y12, which contribute to platelet activation through distinct signaling pathways [3]. Agonist-induced platelet activation is associated with a rise in cytosolic Ca^{2+} [4], that is essentially responsible for a plethora of functions. Although, a moderate cytosolic Ca^{2+} level can trigger platelet shape change, thromboxane generation, granule secretion, integrin $\alpha IIb\beta 3$ activation and aggregation of platelets, a persistent Ca^{2+} overload can lead to formation of procoagulant platelets or even cause cell death [5, 6]

In nucleus-free mammalian platelets, mitochondria are considered to be responsible for platelet health and lifespan [7]. Along with energy production, mitochondria are appreciated for their role in cellular signaling, immunoregulation and cell death [8]. Platelet bioenergetic machinery relies both on glycolysis and oxidative phosphorylation to meet cellular energy demands in resting and activated states [9]. Besides, mitochondrial alterations such as changes in membrane potential ($\Delta\Psi_m$), enhanced production of reactive oxygen species (ROS), and opening of permeability transition pore (mPTP) have also been found to modulate agonist-induced platelet responses [7]. Platelets express Mitochondrial Calcium Uniporter (MCU) that contributes to voltage-dependent transport of Ca^{2+} across the inner mitochondrial membrane [10–12]. The pharmacological and genetic inhibition of MCU is known to impair phosphatidylserine (PS) externalization [10], mPTP opening

[13] and ROS production [14]. The increased matrix Ca^{2+} is primarily removed by Sodium/Calcium/Lithium exchanger (NCLX) [15], which remains unexplored in platelets.

The release of ADP from activated platelets further amplifies the platelet hemostatic response by purinergic signaling [16] ADP-induced elevation of cytosolic Ca^{2+} via P2Y1 receptor contributes to platelet activation and aggregation. Although, the role MCU in the generation of procoagulant platelets by strong agonists has been demonstrated [7, 14], the involvement of MCU and NCLX in platelet activation by weak agonists is incompletely explored. Therefore, this study was designed to investigate the contribution of MCU and NCLX in ADP-induced platelet activation by using pharmacological inhibitors, namely mitoxantrone (MTX) [17, 18] and CGP37157 (CGP) [19]. Our results unveil the interesting fact that these mitochondrial Ca^{2+} transporters are also key players for ADP-induced platelet aggregation that is associated with secretion of alpha granules (p-selectin externalization) and conformational activation of integrin $\alpha IIb\beta 3$. Based on this data we propose that MCU and NCLX inhibition modulates ADP-stimulated platelet activation and aggregation most likely by regulating Ca^{2+}-dependent mitochondrial activities.

Materials and methods

Blood collection and platelet enrichment

Ethical approval for the study was obtained from the institutional bioethics committee of Quaid-i-Azam University Islamabad, Pakistan. Fresh venous blood was collected in acid-citrate-dextrose-A (ACD-A) solution (9:1; v/v) from healthy consenting volunteers who had not taken any non-steroidal anti-inflammatory drugs (NSAIDs) for the past two weeks. Platelet rich plasma (PRP) was obtained by two-step differential centrifugation approach; 200xg for 20 min followed by 100xg for 10 min using a swing bucket centrifuge (Kokusan, Model#H-103RS, Japan) without brakes. All steps were carried out at room temperature (RT) if otherwise indicated. Platelets were manually counted using the improved Neubauer's counting chamber (Marienfeld, Germany) with the help of a brightfield microscope (Olympus Japan). Platelet count was adjusted to $150 \times 10^3/\mu L$ for both washed and unwashed platelets with a modified Tyrode's buffer (MTB) containing 140 mM NaCl, 5 mM KCl, 5 mM glucose, 10 mM HEPES and 1 mM $MgCl_2$.

Suspension of washed platelets was prepared by centrifugation of PRP at 2000xg for 15 min in the presence of 0.5 μM prostaglandin I$_2$ (PGI$_2$, Cat no. sc-201231B, Santa Cruz, USA) and the pellet was resuspended in PGI$_2$ free MTB.

Platelet aggregation profiling

Platelet aggregation was measured as a function of change in absorbance over time on a microplate-based spectrophotometer (MultiSkan GO, ThermoFisher Scientific, USA) equipped with the feature of kinetic data acquisition. Platelet aggregation dynamics were measured and recorded as a drop in absorbance at 595 nm for 15 min with 5 s intervals using SkanIt software (ThermoFisher Scientific, USA). Platelets were stimulated by adenosine 5'-diphosphate (ADP, Cat no. sc-291846A, Santa Cruz, USA) in the presence and absence of either Mitoxantrone (MTX, Cat no. sc-203136, Santa Cruz, USA) or CGP37157 (CGP, Cat no. sc-203136, Santa Cruz, USA) and their vehicle Dimethyl Sulphoxide (DMSO, 20,385.01, Serva GmbH, Germany) in a transparent 96-well microplate. A drop in absorbance over time was taken as platelet aggregation whereas unstimulated platelets were used as control (Con). The data were reported to Microsoft Excel for further processing and analysis. All curves were normalized and quantified in the form of amplitude (maximum aggregation) of the curves.

Trypan blue dye exclusion assay

The cytotoxic effect of MTX was studied by mixing equal volume of trypan blue dye (Cat no. 15250061, Thermo Fisher Scientific, USA) with MTX-treated platelet suspension. Percentage viability was determined by platelet counting using Neubauer's chamber.

LDH assay

The effect of MTX on cell viability was also assessed by lactate dehydrogenase (LDH) release assay with slight modification of manufacturer's protocol (AMP Diagnostics, Austria). Briefly, MTX treated platelets were pelleted down and the supernatant was used as the sample whereas the platelets, lysed by radioimmunoprecipitation (RIPA) assay buffer, were used as a positive control.

RNA extraction, polymerase chain reaction (PCR) and gel electrophoresis

Total RNA from platelets was extracted using TRIzol reagent by following the company's protocol (Thermo Fisher, USA). 500 ng of isolated RNA was reverse transcribed to cDNA using a cDNA synthesis kit (Vivantis Technologies,

Malaysia). The expression of *GAPDH*, *MCU* and *NCLX* was assessed by conventional PCR and agarose gel electrophoresis. The primer sequences used in this study were as follows: GAPDH Human F: TCAACGACCACTTTGTCA AGC, GAPDH Human R: CCAGGGGTCTTACTCCTTGG, MCU Human F: TTCCTGGCAGAATTTGGGAG, MCU Human R: AGAGATAGGCTTGAGTGTGAAC, NCLX Human F1: ACCATCCTACACCCCTTCA, NCLX Human R1: ACACATACAAGCCCAGGTAAC, NCLX Human F2: ACTGTGATTCTCTGCACCTG, NCLX Human R2: CAC CGTAGTCATAGCTGTTGG. The amplified PCR products were visualized by ethidium bromide on agarose gel electrophoresis and documented with a Gel Documentation System using GeneSnap software (Syngene, UK). The mRNA expression of MCU and NCLX was quantified through real time polymerase chain reaction using SyberGreen qPCR master mix (Cat no. 4344463, ThermoFisher, USA).

Flow cytometry

Whole blood from healthy donors was obtained in S-Monovette tube (SARSTEDT, Germany) containing 0.129 mol/L buffered trisodium citrate (pH 5.5). Donors had not taken any medication which could affect platelet function for 10 days prior to blood sampling. Blood was allowed to rest for 15 min at RT before centrifugation. Blood was centrifuged at 200xg for 10 min at 22 °C and PRP was recovered. Platelet count was measured on XP-300 automated hematology analyzer (Sysmex Corporation, Kobe, Japan). Before proceeding with experiments PRP was allowed to rest for at least 30 min at RT.

Diluted PRP (5×10^3 platelets/μL) were preincubated with 20 μM MTX for 5 min or 0.1 μM CGP-37157 for 60 min at RT in dark. After incubation platelets were stimulated with 20 μM ADP for 15 min at 37 °C in calcium containing HEPES buffer (140 mM NaCl, 2.5 mM CaCl$_2$, 10 mM HEPES, pH 7.4). Alpha granule release was determined by measuring surface expression of p-selectin using anti-CD62P-PE antibody (Cat no. 555523 BD Pharmingen, USA) and integrin αIIbβ3 activation was determined by binding of PAC-1-FITC (Cat no. 1P-145-T100 Exbio, Czech Republic). Phosphatidylserine exposure were determined by Annexin V-FITC (Cat no. 640905 Biolegend). The fluorescence was acquired using BD Accuri C6 flow cytometer (BD Biosciences, USA).

Measurement of mitochondrial membrane potential

PRP was adjusted to 3×10^4 platelets/μL with Tyrode's buffer and loaded with 5 μM TMRM (Cat no. 22221 AAT Bioquest, USA) for 15 min in dark. Loaded platelets were split and diluted to 10×10^3 platelets/μL with 2.5 mM calcium containing Tyrode's buffer. Diluted platelets were

preincubated with 20 µM MTX for 5 min or 0.1 µM CGP-37157 for 30 min and 60 min at RT in dark followed by the stimulation of 20 µM ADP for 15 min at 37 °C. Platelets were acquired (final concentration: 5×10^3 platelets/µL) on flow cytometer (BD Accuri C6).

Measurement of cytosolic calcium

Platelets were adjusted to 3×10^4 platelets/µL in Tyrode's buffer and incubated with 2 µM Fluo-3 AM (Cat no. F1242 Thermo Fisher, USA) for 60 min in dark. Loaded platelets were incubated with 20 µM MTX for 5 min or 0.1 µM CGP-37157 for 60 min at RT in dark. For each experiment platelets were diluted to 2.5×10^3 platelets/µL with 2.5 mM calcium containing Tyrode's buffer, baseline was recorded for 1 min and immediately stimulated with 20 µM ADP and acquisition was continued for 15 min using BD Accuri C6 flow cytometer.

Statistical analysis

Each experiment was performed on platelets obtained from, at least, three individuals and all the experimental data are presented as mean ± SEM. Statistical differences between groups were determined using student's T-test or one-way ANOVA with Tuckey's multigroup comparison post-hoc test and $P < 0.05$ was considered statistically significant. Data were processed and analyzed on MS Excel (Microsoft, USA) and GraphPad Prism (version 5, GraphPad Software, Inc. USA).

Results

MTX treatment was not associated with the loss of cell viability and platelet pre-activation

MTX has been traditionally used as anti-neoplastic drug for several cancers that induces cytotoxicity via inhibition of Topoisomerase II. [20]. Therefore, we addressed the cytotoxic potential of MTX by assessing platelet integrity with trypan blue dye exclusion assay, Lactate dehydrogenase (LDH) release and Annexin-V binding assay. Notably, a 20- and 60-min incubation of platelets with MTX did not influence platelet integrity as observed by no alteration in the number of trypan blue positive platelets (Fig. 1a). Likewise, there was no noticeable impact of MTX treatment on platelet LDH release after 5 and 60 min of incubation while a greater LDH was present in the platelet lysates (Fig. 1b). Furthermore, Annexin-V FITC binding was unaffected in MTX treated platelets, thus, excluding the probability of apoptosis-associated phosphatidylserine (PS) externalization (Fig. 1e). In summary, this data ruled out the possibility of platelet death by MTX via necrosis or apoptosis. Next, we analyzed the impact of MTX on platelet pre-activation by measuring alpha granule release and integrin αIIbβ3 activation in unstimulated cells. In agreement with the aforementioned data, there was no significant change in the p-selectin surface exposure and PAC-1 binding in MTX-treated platelets excluding the likelihood of pre-activation (Fig. 1c & 1d).
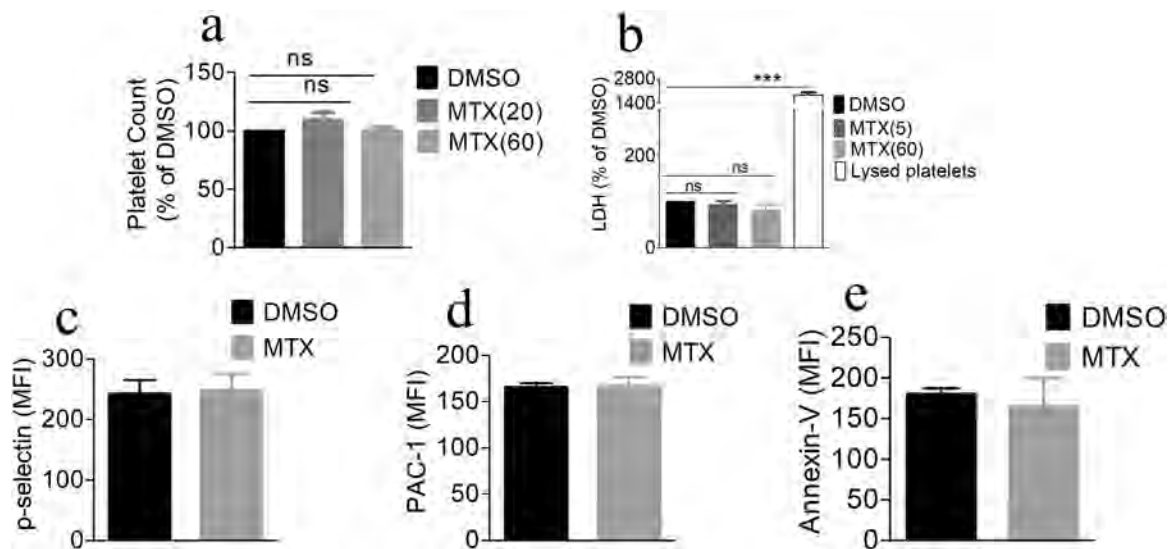

Fig. 1 MTX treatment did not influence platelet viability. Platelets were treated with either DMSO or MTX for 20 and 60 min in trypan blue assay (**a**), and 5 or 60 min in LDH release assay (**b**). Mean florescence intensity (MFI) of p-selectin (**c**), PAC-1 (**d**) and Annexin-V (**e**) is shown after pre-treatment of platelets with MTX or DMSO for 5 min. The data are presented as mean ± SEM and statistically analyzed with one-way ANOVA using Tuckey's multigroup comparison post hoc test and one tailed T-test, n = 3, ***p < 0.001, ns = non-significant whereas MTX (20) = platelets treated with 20 µM MTX for 20 min, MTX (60) = 20 µM MTX for 60 min

MTX attenuated ADP-evoked platelet aggregation in a dose-dependent manner

The contribution of mitochondrial Ca^{2+} influx and efflux pathways in ADP-induced platelet responses remains incompletely explored. Therefore, we started with the validation of the expression of MCU and NCLX in human platelet cDNA library. Our results confirmed the presence of MCU and NCLX in human platelets (Fig. 2a) with a relatively low abundance of NCLX as compared to MCU mRNA (Fig. 2b). The functional investigation of mitochondrial Ca^{2+} uptake pathway in ADP-induced platelet aggregation was carried out by using a combination of pharmacological blocker and microplate-based spectrophotometry. Our data demonstrated a strong drop in the absorbance of platelet rich plasma (PRP) upon ADP-stimulation validating the utility of this method for platelet aggregation profiling (Fig. 2c). The function of

mitochondrial Ca^{2+} influx pathway was examined by using a recently reported MCU inhibitor i.e. mitoxantrone (MTX). Although ADP generated a fast aggregation response, platelet pre-incubation with 20 µM MTX for 5 min yielded a remarkable decline of the ADP-evoked response (Fig. 2c & 2d). However, a prolonged (60 min) pre-treatment of platelets with MTX did not further enhance the inhibitory effect; thus, ruling out the time-dependent impact of MTX on ADP-induced aggregation (Fig. 2c & 2d). To further delineate the influence of MTX on ADP-induced aggregation, platelets were pre-incubated with 10 µM and 5 µM MTX for a period of 5 min that resulted in a diminution of the inhibitory response (Fig. 2e-h). A comparative analysis of the inhibitory response of three different concentrations of MTX revealed a significant dose-dependent effect of this compound on ADP-stimulated platelet aggregation (Fig. 2i).
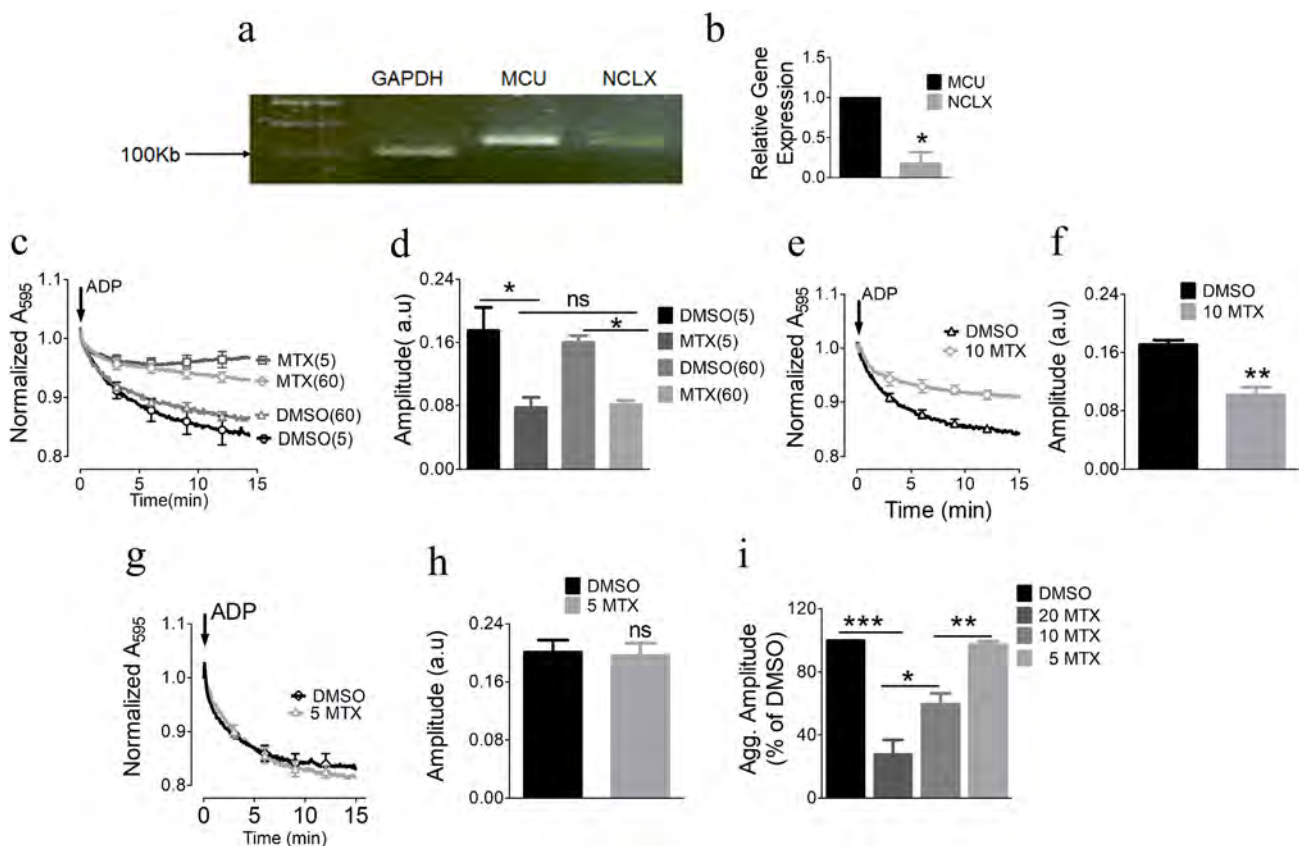
Fig. 2 MTX attenuated ADP-induced platelet aggregation. Agarose gel image of PCR products confirming the presence of MCU and NCLX mRNAs in human platelets. GAPDH was used as a process control (**a**). Relative mRNA quantification of MCU and NCLX as determined by Real Time PCR (**b**), Platelet aggregation curve (**c**) and amplitude (**d**) upon stimulation with 20 µM ADP after pre-treatment with 20 µM MTX or vehicle (DMSO) for 5 min or 60 min. Platelet aggregation was also tested at 10 µM (**e** and **f**) and 5 µM (**g** and **h**) MTX and combined concentration-dependent effect of MTX was calculated (**i**). Data is presented as mean ± SEM and analyzed using one tailed unpaired T test and One-way ANOVA with Tuckey's multigroup comparison post hoc test. n = 3, ***p < 0.001, **p < 0.01, and *p < 0.05. DMSO = Platelets + DMSO + ADP, MTX (5) = platelets + 20 µM MTX for 5 min, MTX (60) = platelets + 20 µM MTX for 60 min, 10MTX = platelets + 10 µM MTX for 5 min and 5 MTX = platelets + 5 µM MTX + ADP, ns = non-significant, NCLX1 and NCLX2 depict two different primers pairs for amplifying NCLX cDNA

MTX inhibited ADP-induced degranulation and integrin αIIbβ3 activation

The degranulation of alpha granules and activation of integrin αIIbβ3 are pivotal events for platelet activation leading to subsequent aggregation and clot formation. Therefore, we ascertained the ADP-induced platelet activation by measuring p-selectin externalization (a marker of degranulation) and integrin αIIbβ3 activation using fluorescently-labeled antibodies. As expected, ADP stimulation caused a significant increase in the mean fluorescent intensity (MFI) of p-selectin labeled platelets confirming the secretion of alpha granules (Fig. 3a & 3b). Similarly, the PAC-1 binding was also substantially elevated in ADP-induced platelets indicating the activation of integrin αIIbβ3 (Fig. 3c & 3d). Intriguingly, platelet pre-treatment with 20 μM MTX for a period of 5 min resulted in a significant diminution of both p-selectin surface expression (Fig. 3e & 3f) and αIIbβ3 activation (Fig. 3g & 3h) as

demonstrated by a marked drop in platelet MFI. Notably, the MTX-dependent inhibition of ADP-induced αIIbβ3 activation appeared to be more pronounced as compared to the p-selectin externalization (84.6% vs 40.9%) (Fig. 3f & h).

To further substantiate this data, we determined the dose-dependent effect of MTX on ADP-induced p-selectin externalization and integrin αIIbβ3 activation. To this end, platelets were incubated with 7 different concentrations of MTX ranging from 0.1 μM–30 μM for 5 min. In concordance with previous results, we observed a dose-dependent inhibitory effect of MTX on ADP-induced platelet activation as monitored by p-selectin surface expression (Fig. 3i) and αIIbβ3 activation (Fig. 3j). Interestingly, MTX demonstrated a stronger effect at inhibiting αIIbβ3 activation as compared to the inhibition of p-selectin surface expression (Fig. 3i & 3j). However, half maximal inhibitory concentration value (IC50) of MTX with p-selectin is 3.259 μM and with PAC-1 is 2.828 μM.
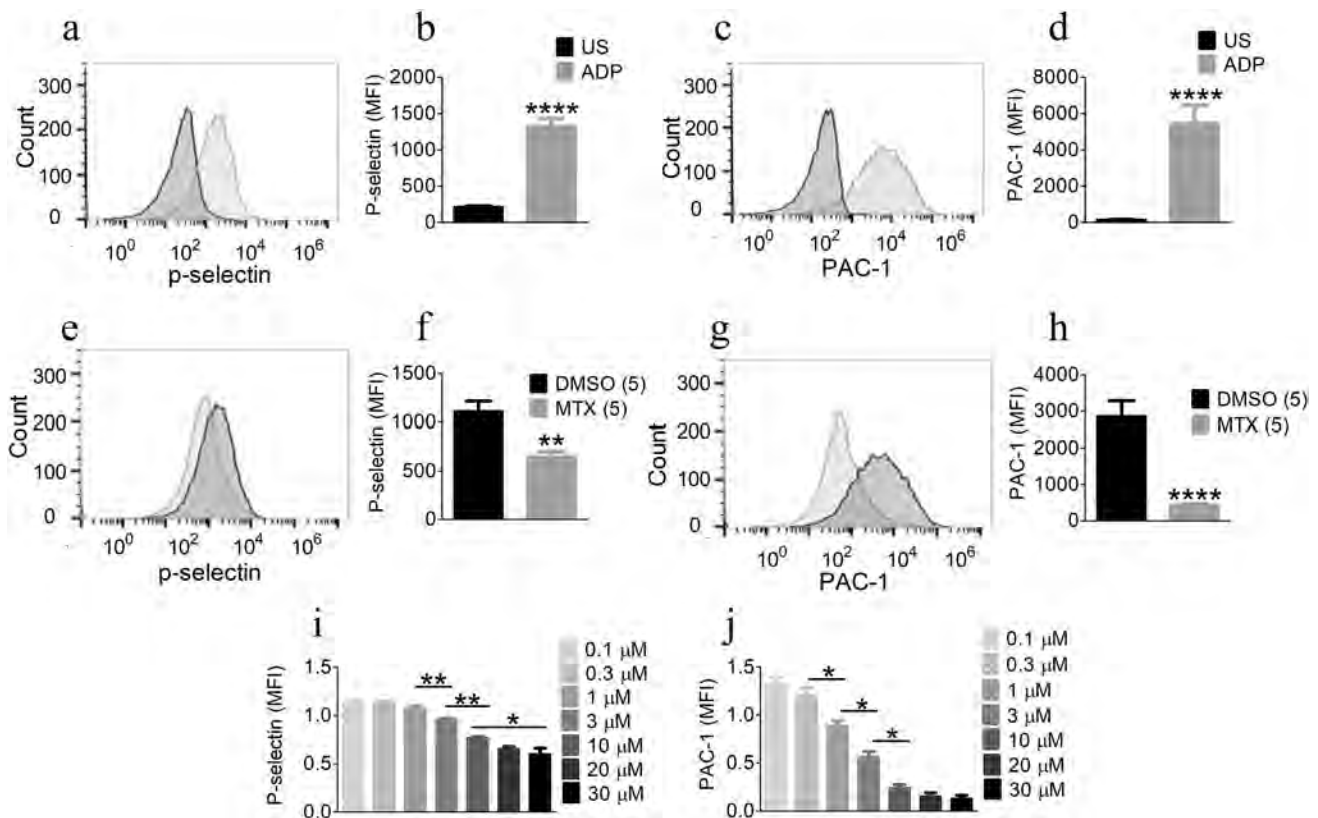
Fig. 3 MTX inhibited ADP-stimulated p-selectin externalization and αIIbβ3 activation. Representative histogram showing mean florescence intensity (MFI) of unstimulated (US = dark grey) vs ADP-stimulated platelets (light grey) of p-selectin (**a** and **b**) and PAC-1 (**c** and **d**). Histograms showing MFI of p-selectin (**e** and **f**) and PAC-1 (**g** and **h**) upon stimulation with 20 μM ADP after pre-incubation with 20 μM MTX (light grey) for 5 min in comparison to DMSO (vehicle) (dark grey).(**i** and **j**) ADP-induced p-selectin and PAC-1 positive platelets at 7 different MTX concentrations. Data represents mean ± SEM, n = 4–7, *p < 0.05, **p < 0.01, ***p < 0.001, ****p < 0.0001. DMSO (5) = platelets + DMSO incubated for 5 min, MTX (5) = platelets + MTX incubated for 5 min

Inhibition of NCLX with CGP37157 increased ADP-induced platelet aggregation without effecting the cell viability and platelet pre-activation

7-Chloro-5-(2-chlorophenyl)-1,5-dihydro-4,1-benzothiaze-pin-2(3H)-one [CGP37157 (CGP)] is a benzodiazepine, which has been reported to protect neurons from excitotoxicity, but it is also commonly used as a blocker of mitochondrial Na^{2+}/Ca^{2+} exchanger [21]. Therefore, we determined the cytotoxic effect of CGP on platelets by assessing platelets viability using trypan blue exclusion, LDH release and Annexin-V binding assays. As expected, there was no significant alteration in number of trypan blue positive platelets and release of LDH after treatment of platelets with CGP for 5, 60 and 120 min (Fig. 4a & 4b). Likewise, there was no notable change in externalization of PS after CGP treatment for 60 min (Fig. 4e). We also addressed platelet pre-activation by measuring alpha granule release (p-selectin exposure) and $\alpha IIb\beta3$ activation (PAC-1 binding) in CGP treated resting platelets. Hence, in line with our previous data platelets remained unaffected in the presence of CGP as determined by p-selectin exposure and PAC-1 binding (Fig. 4c & 4d).

Furthermore, mitochondrial Ca^{2+} handling in platelets was investigated by exploring the contribution of mitochondrial Ca^{2+} efflux pathway. To this end the involvement of NCLX in ADP-evoked aggregation response was elucidated by employing the well-known pharmacological blocker, CGP37157 (CGP). We started with assessing the effect of 0.1 μM CGP on ADP-stimulated platelet aggregation with a shorter (5 min) incubation time, which did not yield a considerable impact (Fig. 5a & b). Remarkably, an increase in the platelet pre-treatment time from 5 to 60 and 120 min resulted in a substantial enhancement of ADP-evoked platelet aggregation (Fig. 5c-f). However, there was no apparent difference in platelet aggregation between 60- and 120 min time-points indicating a maximal impact of CGP at 1 h. We also explored the dose dependent effect of CGP on platelet aggregation and our data revealed a dose independent impact of CGP on ADP-stimulated platelet aggregation (Supplementary Fig. 1a-1f). To conclude, these results corroborate the available evidence about the contribution of mitochondrial Ca^{2+} in ADP-induced platelet aggregation.

CGP enhanced the p-selectin exposure and αIIbβ3 activation in ADP-stimulated platelets

To further signify the role of mitochondrial Ca^{2+} efflux pathway in platelet activation, we measured the ADP-induced p-selectin externalization and $\alpha IIb\beta3$ activation upon blocking NCLX with CGP. Interestingly, platelet pre-treatment with 0.1 μM CGP for 60 min yielded a remarkable increase in the surface expression of p-selectin after stimulation with ADP (Fig. 6a & 6b). Likewise, pre-incubation with CGP resulted in a significantly elevated binding of PAC-1 highlighting an accelerated ADP-induced activation of $\alpha IIb\beta3$ (Fig. 6c & 6d). This data complemented the previous results and persuaded us to propose a hitherto uncharacterized involvement of mitochondrial Ca^{2+} efflux in ADP-induced platelet activation. Furthermore, in correspondence to the
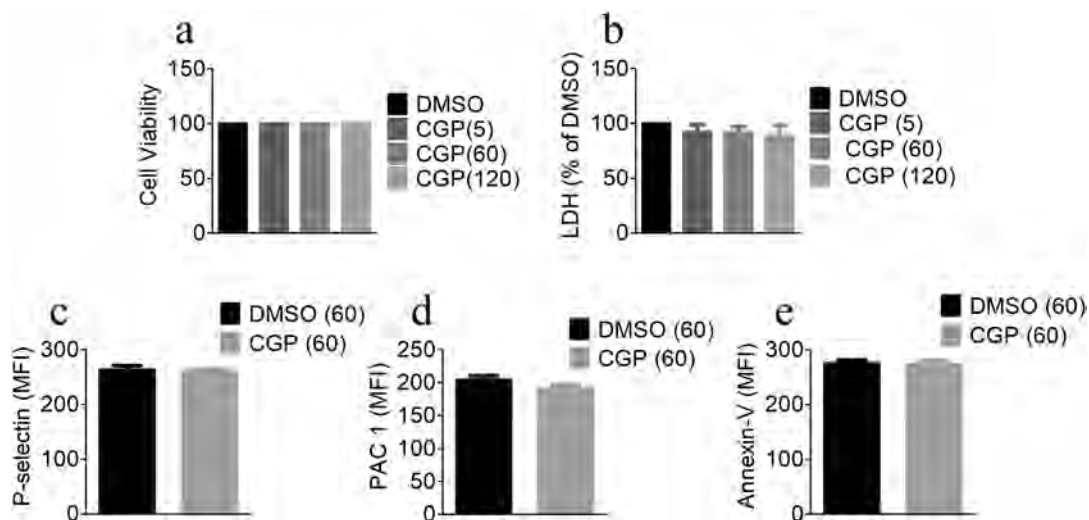

Fig. 4 CGP did not effect platelet cell viability and pre-activation: Platelets were pre-treated with DMSO or CGP for 5,10 and 60 min in Trypan blue assay (**a**) and LDH assay (**b**). Mean florescence intensity (MFI) of p-selectin (**c**), PAC-1(**d**) and Annexin-V (**e**) is shown after pre-treatment of platelets with DMSO or CGP for 60 min. The data are presented as mean ± SEM and statistically analyzed with one-way ANOVA using Tuckey's multigroup comparison post hoc test and one tailed T-test, n = 3–4. CGP (5) = platelets treated with 0.1 μM for 5 min, CGP (60) = 0.1 μM CGP for 60 min, CGP (120) = 0.1 μM CGP for 120 min
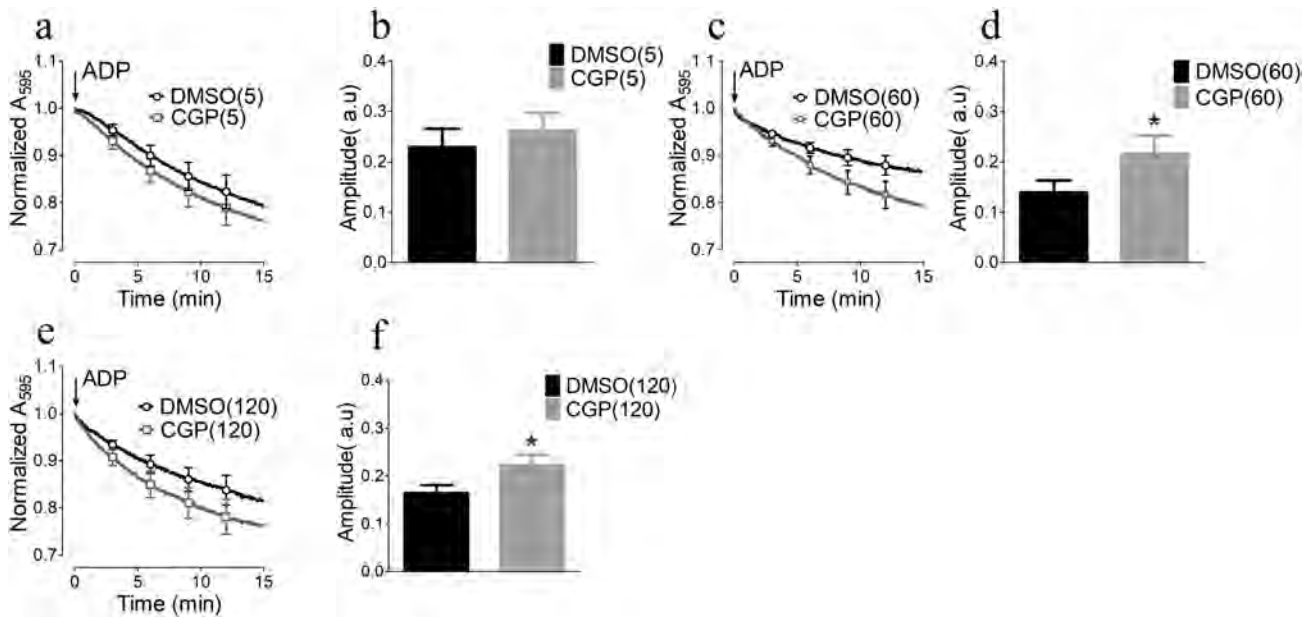
Fig. 5 CGP enhanced the ADP-induced platelet aggregatory response. Platelets were treated with either DMSO or 0.1 μM CGP for 5 min (**a** and **b**), 60 min (**c** and **d**) and 120 min (**e** and **f**) before stimulation with ADP. Data are presented as mean ± SEM and statistically analyzed using one-tailed unpaired T-test, n = 7, *p < 0.05., CGP (5) = platelets treated with CGP for 5 min before stimulation with ADP, CGP (60) = platelets treated with CGP for 60 min, CGP (120) = platelets treated with CGP for 120 min
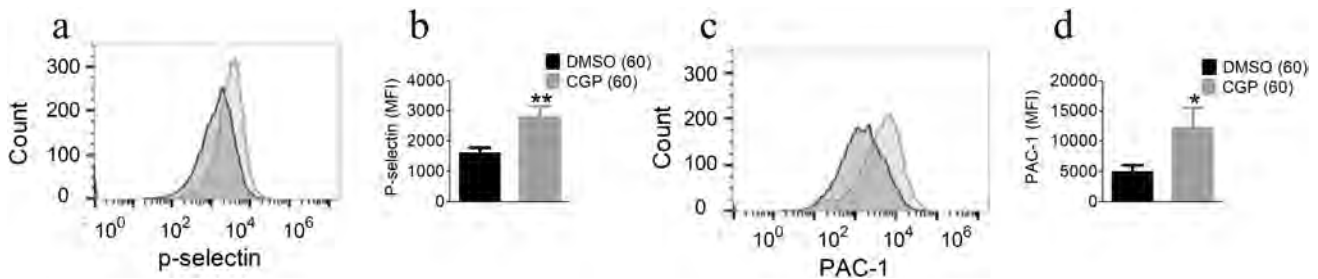
Fig. 6 CGP increased ADP-induced platelet degranulation and αIIbβ3 activation. Representative histogram showing mean florescence intensity (MFI) of p-selectin (**a** and **b**) and PAC-1 (**c** and **d**) in the presence of 0.1 μM CGP (light grey) for 60 min in comparison to DMSO (vehicle) (dark grey) after stimulation with 20 μM ADP. Data represents mean ± SEM and analyzed by using one tailed T-test. n = 7, *p < 0.05, **p < 0.01. CGP (60) = platelets treated with CGP for 60 min

above mentioned results of platelet aggregation, we also investigated the effect of different doses of CGP on platelet activation. However, there was no notable difference observed on ADP-induced platelet activation (Supplementary Fig. 1 g & 1 h).

MTX and CGP distinctly affected ADP-induced mitochondrial membrane potential without any changes in cytosolic Ca²⁺ dynamics

The contribution of mitochondrial Ca^{2+} transporters in platelets physiology was further investigated by assessing the mitochondrial membrane potential ($\Delta\Psi_m$) that indirectly reflects changes in mitochondrial bioenergetics. Interestingly, our results demonstrated an elevation of $\Delta\Psi_m$ in ADP-stimulated platelets compared to unstimulated group (US) as indicated by a significant increase in the MFI (Fig. 7a). In line with our findings, the ADP-induced mitochondrial hyperpolarization was remarkably reduced by platelet pretreatment with MTX as highlighted by a significant drop in MFI (Fig. 7b). On the contrary and in line with our hypothesis, CGP pre-incubation yielded a small increasing tendency of $\Delta\Psi_m$ upon ADP-stimulation at 30 and 60 min (Fig. 7c & 7d).

The changes in cytosolic Ca^{2+} may alter the agonist-induced platelet activation. Therefore, we further explored
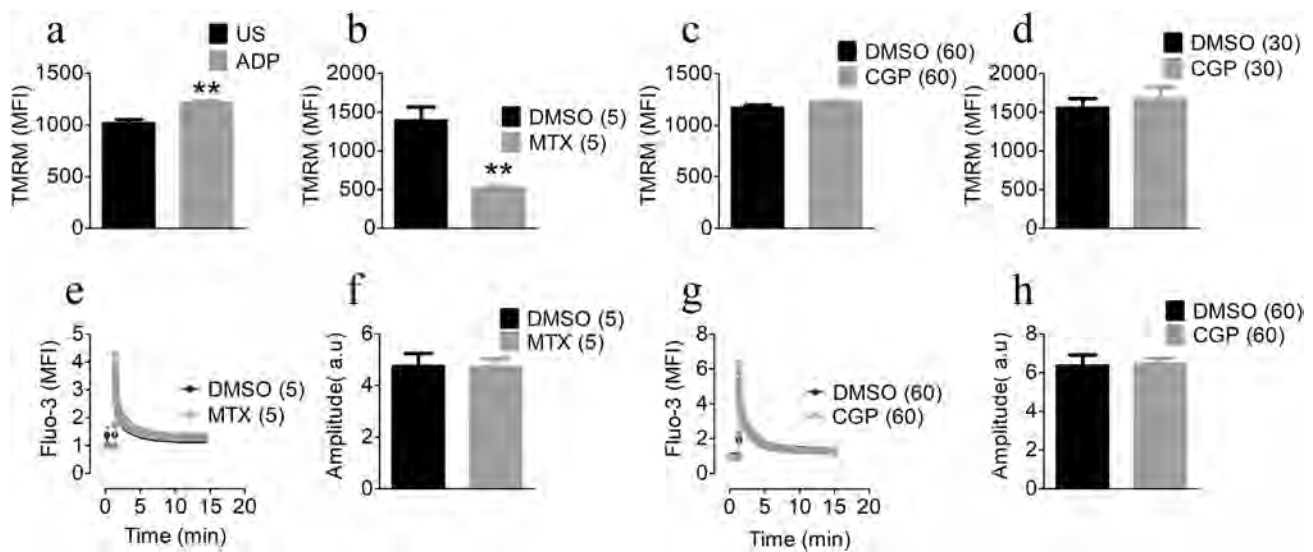
Fig. 7 Effect of MTX and CGP on mitochondrial membrane potential and cytosolic Ca^{2+}. Platelets were loaded with 5 µM TMRM and 2 µM Fluo-3 for 15 and 60 min respectively. Representative graphs showing the mean fluorescence intensity (MFI) of TMRM of unstimulated (US) and ADP stimulated platelets (ADP) (**a**). 20 µM MTX treated platelets for 5 min after stimulation with 20 µM ADP in comparison to DMSO (vehicle) (**b**). 0.1 µM CGP treated platelets for 60 and 30 min after stimulation with 20 µM ADP as compared to DMSO (vehicle) (**c** and **d**). MFI of Fluo-3 in the presence of MTX (grey) as compared to DMSO (vehicle) (black) (**e** and **f**). MFI of Fluo-3 in the presence of CGP (grey) in comparison to DMSO (vehicle) (black) (**g** and **h**). Data represents mean ± SEM and analyzed by using one tailed T-test., **p < 0.01, DMSO(5)/MTX(5) = platelets treated with DMSO/MTX for 5 min, CGP (60) and CGP (30) = platelets treated with CGP for 60 and 30 min

the ADP-induced kinetics of platelet cytosolic Ca^{2+} using a combination of Fluo-3 and flow cytometry using already established protocols. Although we observed a rapid increase in platelet cytosolic Ca^{2+} upon stimulation with ADP, the pre-treatment of platelets with MTX or CGP did not influence the Ca^{2+} kinetics (Fig. 7e & g). A quantitative analysis of the peak amplitude also revealed no significant difference between MTX/CGP treated platelets as compared to DMSO (Fig. 7f & 7h).

Discussion

Agonist-induced elevation of cytosolic Ca^{2+} contributes to a plethora of platelet functions including its uptake by mitochondria that is particularly important in the generation of procoagulant platelets with strong stimulation [22]. However, the participation of mitochondrial Ca^{2+} fluxes in case of stimulation with weak agonists like ADP remains incompletely explored. In this study we uncovered the so far elusive role of mitochondrial Ca^{2+} influx and efflux pathways by inhibiting MCU and NCLX, which are major mitochondrial Ca^{2+} transporters. Our data highlights a distinct contribution of MCU and NCLX in ADP-induced activation and aggregation responses. We unveiled the interesting fact that mitoxantrone (MTX), a FDA approved drug recently reported to inhibit MCU [23], reduced ADP-induced aggregation and

activation. These findings are complemented by inhibition of NCLX with CGP that increased ADP-induced platelet responses. Together, these data tempted us to speculate a positive role of mitochondrial Ca^{2+} uptake in ADP-induced platelet responses.

MTX is an anti-neoplastic drug that has been demonstrated to cause the demise of actively proliferating cells by inhibition of Topoisomerase A2 [24]. One study has reported the transport of Topoisomerase A2 from nucleus to mitochondria [25], while others have challenged this idea [26, 27]. However, the absence of a nucleus in platelets along with evidence coming from our unpublished data ruled out the presence of Topoisomerase A2 expression in platelets. Nevertheless, to exclude the possibility of MTX-dependent platelet cytotoxicity, we used a combination of cell death assays that assisted to establish the fact that MTX does not result in loss of platelet integrity at least for shorter incubation times (5–60 min). Similarly, MTX was also not responsible for any pre-activation as determined by p-selectin expression and αIIbβ3 integrin activation under unstimulated conditions. Therefore, based on recently proposed role of MTX as MCU inhibitor [17, 23] besides proposed lack of Topoisomerase A2 in platelets [28], it can be hypothesized that MTX most likely inhibited platelet stimulation by reducing MCU-mediated mitochondrial Ca^{2+} uptake. Moreover, a much shorter exposure time (5 min) of platelets to MTX in our experiments is also unlikely to cause cytotoxicity as

required for in vivo chemotherapy [23, 29]. The MTX-based inhibition of ADP-dependent platelet aggregation may be due to energy deficit created by reduced mitochondrial Ca^{2+} uptake thus lowering energy availability as platelet activation, aggregation, and secretion are highly energy intensive processes [30, 31]. In a very old study MTX has been linked with a decreased collagen-stimulated platelet aggregation without an exploration of the exact molecular mechanism [32].

Genetic silencing of MCU in rodent platelets has been demonstrated to reduce the generation of thrombin/collagen-induced procoagulant platelets with no report on ADP-evoked responses [12]. Similarly, Ru-360, a well-established MCU inhibitor, has also been documented to attenuate platelet activation with no impact on ATP-induced responses [10]. However, it is pertinent to mention that Ru-360 is notorious for its poor membrane permeability and authors have only seen a small drop in thrombin-induced mitochondrial Ca^{2+} uptake despite using a very high dose of Ru-360 [10]. On the contrary, we have seen a much faster impact of MTX on ADP-induced platelet aggregation at low micromolar concentration corroborating the previous reports about the dose of MTX known for inhibiting mitochondrial Ca^{2+} uptake in other cell types.[17, 23].

Although MCU expression in platelets is already known, to the best of our knowledge there is no available study showing the presence of NCLX or its functional contribution in platelets. Therefore, we reported the presence of NCLX in human platelets in addition to confirming the expression of MCU. In our study, besides inhibiting the ADP-induced platelet aggregation, MTX strikingly reduced the alpha granule secretion and integrin αIIbβ3 activation at a concentration (20 μM) that is previously reported to block MCU in yeast mitochondria [23]. Mitochondrial Ca^{2+} entry occurs in all the activated platelets, which is an essential regulator of cellular metabolism and crucial for granule release [22]. Agonist-induced platelet responses are energy demanding processes; therefore, we reasoned that inhibition of mitochondrial Ca^{2+} fluxes may affect the overall cellular energetics that may ultimately change the platelet activation. This could particularly affect energy intensive processes such as alpha granule release. Additionally, ATP generation has been reported to yield no influence on integrin αIIbβ3 activation in stimulated platelets with a probable involvement of mitochondrial ROS [33]. Thus, mitochondrial Ca^{2+} uptake induces the mitochondrial respiration and hyperpolarization of mitochondria that is in concordance with our results, which could increase the probability of mitochondrial ROS production [34] that has been recently reported to play pivotal role in platelet activation and aggregation [35]. However, as a limitation of our study we could not eliminate the fact that the decrease in $\Delta\Psi_m$ after treatment with MTX may also be a consequence of other factors in addition to MCU

blockage. Interestingly, selective inhibition of mitochondrial ROS with mitoTEMPO has been reported to substantially reduce platelet aggregation along with a reduction of integrin αIIbβ3 activation [36]. On the contrary, in a recent study deletion of MCUb (a negative regulator of MCU) in mice platelets has been shown to reduce ADP-triggered platelet aggregation. However, unexpectedly MCUb deletion did not only alter the mitochondrial Ca^{2+} but also influenced the glucose uptake and aerobic glycolysis in activated platelets [37], which could be speculated to be the result of compensatory changes in MCUb knockout mouse model. Surprisingly, this study also reported no impact of increased mitochondrial Ca^{2+} on $\Delta\Psi_m$ in MCUb KO platelets.

Along with MCU, the mitochondrial Ca^{2+} buffering capacity is credited to the presence of NCLX as the main pathway for Ca^{2+} extrusion from matrix [38]. However, there is no experimental evidence for the presence and function of NCLX in human platelets particularly in ADP-induced responses. We blocked NCLX-mediated Ca^{2+} flux by using well established pharmacological blocker, CGP37157 (CGP) to support our data generated with MTX in ADP-elicited platelet responses. CGP itself is a neuroprotector benzothiazepine, and is an effective blocker of NCLX. Our data revealed no effect of CGP on platelet integrity and pre-activation. However, it significantly increased ADP-induced platelet aggregation after longer incubation (60–120 min) possibly by increasing the mitochondrial matrix Ca^{2+} concentration and increased cellular energetics. Likewise, it also displayed a remarkable increase in ADP-induced platelet degranulation and integrin αIIbβ3 activation. In previous studies CGP has been identified to induce pyroptosis in Jukrat cells via mitochondrial Ca^{2+} overload and decreased mitochondrial and cytosolic vacuolization [39]. In our study the effect of CGP may be speculated to be a consequence of elevated activity of several Ca^{2+}-dependent mitochondrial dehydrogenases that are eventually involved in cellular respiration. NCLX inhibition by CGP in mouse astrocytes has been reported to increase ATP production [40], which may potentiate energy-dependent process like aggregation and cellular secretion. Moreover, in some cases accumulation of matrix Ca^{2+} in platelet mitochondria may trigger mPTP opening that contributes to generation of procoagulant platelets [6]. Contrary to this, mitochondrial matrix Ca^{2+} which is sustained by inhibition of NCLX might be below the threshold for mPTP opening in ADP-stimulated platelets, which could maintain αIIbβ3 activation resulting in a pro-aggregatory response probably via ROS modulation [33]. Literature reports the interaction of CGP with various Ca^{2+} channels including L-type Ca^{2+} channel and Ryanodine Receptors [15], which are not present in platelets [41]. The nanomolar concentration of CGP used in the study weakens the possibility of any interaction with

plasma membrane NCX or any other off target effects [15]. Thus, our results explain that CGP increased ADP-stimulated platelet aggregation most likely via an acceleration of Ca^{2+}-dependent mitochondrial metabolism.

In conclusion, the current study reports the presence of NCLX in platelets along with highlighting the effect of MTX and CGP on ADP-induced platelet responses. Our results revealed that MTX inhibited platelet aggregation and activation whereas CGP elevated ADP-elicited platelet responses. Taken together, the data presented in this article provided novel evidence for the involvement of mitochondrial Ca^{2+} homeostasis in ADP-induced platelet responses.

Declarations

Competing interests The authors have no relevant financial or non-financial interests to disclose.

Ethical approval This study was performed in line with the principles of the Declaration of Helsinki. Approval was granted by the Bioethics Committee of the Quaid-i-Azam University, Islamabad.

Consent to participate Informed consent was obtained from all individual participants included in the study.

References

1. van der Meijden PE, Heemskerk JW (2019) Platelet biology and functions: new concepts and clinical perspectives. Nat Rev Cardiol 16(3):166–179

2. Koupenova M et al (2017) Thrombosis and platelets: An update. Eur Heart J 38(11):785–791

3. Nishimura A et al (2017) Purinergic P2Y receptors: molecular diversity and implications for treatment of cardiovascular diseases. Pharmacol Ther 180:113–128

4. Obydennyy SI et al (2016) Dynamics of calcium spiking, mitochondrial collapse and phosphatidylserine exposure in platelet subpopulations during activation. J Thromb Haemost 14(9):1867–1881

5. Podoplelova N et al (2021) Procoagulant platelets: Mechanisms of generation and action. Hamost 41(02):146–153

6. Veuthey L et al (2022) Mechanisms underlying dichotomous procoagulant coat platelet generation—a conceptual review summarizing current knowledge. Int J Mol Sci 23(5):2536

7. Melchinger H et al (2019) Role of platelet mitochondria: life in a nucleus-free zone. Front in cardiovascular med 6:153

8. Hayashi T et al (2011) Role of mitochondria in the maintenance of platelet function during in vitro storage. Transfus Med 21(3):166–174

9. Ravera S et al (2018) Extramitochondrial energy production in platelets. Biol Cell 110(5):97–108

10. Choo H-J et al (2012) Mitochondrial calcium and reactive oxygen species regulate agonist-initiated platelet phosphatidylserine exposure. Arterioscler Thromb Vasc Biol 32(12):2946–2955

11. Kholmukhamedov A et al (2016) Mitochondrial calcium entry is essential in agonist-induced procoagulant platelet formation. Blood 128(22):3721

12. Kholmukhamedov A et al (2018) The mitochondrial calcium uniporter regulates procoagulant platelet formation. J Thromb Haemost 16(11):2315–2321

13. Jobe SM et al (2008) Critical role for the mitochondrial permeability transition pore and cyclophilin D in platelet activation and thrombosis Blood. The J American Soc Hematol 111(3):1257–1265

14. Figueira TR et al (2013) Mitochondria as a source of reactive oxygen and nitrogen species: from molecular mechanisms to human health. Antioxid Redox Signal 18(16):2029–2074

15. Palty R, Sekler I (2012) The mitochondrial Na(+)/Ca(2+) exchanger. Cell Calcium 52(1):9–15

16. Lu P-H et al (2022) Coumarin derivatives Inhibit ADP-induced platelet activation and aggregatIon. Mol 27(13):4054

17. Bermont F et al (2020) Targeting mitochondrial calcium uptake with the natural flavonol kaempferol, to promote metabolism/secretion coupling in pancreatic β-cells. Nutr 12(2):538

18. Zhang Z et al (2022) Ruthenium 360 and mitoxantrone inhibit mitochondrial calcium uniporter channel to prevent liver steatosis induced by high-fat diet. Br J Pharmacol 179(11):2678–2696

19. Rysted JE et al (2021) Distinct properties of Ca2+ efflux from brain, heart and liver mitochondria: The effects of Na+, Li+ and the mitochondrial Na+/Ca2+ exchange inhibitor CGP37157. Cell Calcium 96:102382

20. Dhivya S et al (2016) Impact of anthocyanidins on mitoxantrone-induced cytotoxicity and genotoxicity: an in vitro and in vivo analysis. Integr Cancer Ther 15(4):525–534

21. Ruiz A, Alberdi E, Matute C (2014) CGP37157, an inhibitor of the mitochondrial Na+/Ca2+ exchanger, protects neurons from excitotoxicity by blocking voltage-gated Ca2+ channels. Cell Death Dis 5(4):e1156–e1156

22. Millington-Burgess SL, Harper MT (2021) Cytosolic and mitochondrial Ca2+ signaling in procoagulant platelets. Platelets 32(7):855–862

23. Arduino DM et al (2017) Systematic identification of MCU modulators by orthogonal interspecies chemical screening. Mol cell. https://doi.org/10.1016/j.molcel.2017.07.019

24. Topcu Z (2001) DNA topoisomerases as targets for anticancer drugs. J Clin Pharm Ther 26(6):405–416

25. Zhang H et al (2014) Increased negative supercoiling of mtDNA in TOP1mt knockout mice and presence of topoisomerases IIα and IIβ in vertebrate mitochondria. Nucleic Acids Res 42(11):7259–7267

26. Goffart S, Hangas A, Pohjoismäki JL (2019) Twist and turn—topoisomerase functions in mitochondrial DNA maintenance. Int J Mol Sci 20(8):2041

27. Nicholls TJ et al (2018) Topoisomerase 3α is required for decatenation and segregation of human mtDNA. Mol Cell 69(1):9-23.e6

28. Kosovsky MJ, Soslau G (1991) Mitochondrial DNA topoisomerase I from human platelets. Biochim et Biophys Acta (BBA)-Protein Struct and Mol Enzymol 1078(1):56–62

29. Yang J et al (2014) Phase I clinical trial of pegylated liposomal mitoxantrone plm60-s: Pharmacokinetics, toxicity and preliminary efficacy. Cancer Chemother Pharmacol 74(3):637–646

30. de la Corona Peña N et al (2017) Glycoprotein Ib activation by thrombin stimulates the energy metabolism in human platelets. PLoS ONE 12(8):e0182374

31. Bisbach CM et al (2020) Mitochondrial Calcium Uniporter (MCU) deficiency reveals an alternate path for Ca 2+ uptake in photoreceptor mitochondria. Sci Rep 10(1):1–19

32. Frank P, Novak R (1986) Effects of mitoxantrone and bisantrene on platelet aggregation and prostaglandin/thromboxane biosynthesis in vitro. Anticancer Res 6(5):941–947

33. Kulkarni PP et al (2022) Mitochondrial ATP generation in stimulated platelets is essential for granule secretion but dispensable for aggregation and procoagulant activity. Haematologica 107(5):1209

34. Baev AY et al (2022) Interaction of mitochondrial calcium and ROS in neurodegeneration. Cells 11(4):706

35. Masselli E et al (2020) ROS in platelet biology: functional aspects and methodological insights. Int J Mol Sci 21(14):4866

36. Sonkar VK et al (2019) Nox2 NADPH oxidase is dispensable for platelet activation or arterial thrombosis in mice. Blood Adv 3(8):1272–1284

37. Ghatge M et al (2023) Mitochondrial calcium uniporter b deletion inhibits platelet function and reduces susceptibility to arterial thrombosis. J Thromb Haemost 21(8):2163–2174

38. Blomeyer CA et al (2013) Dynamic buffering of mitochondrial Ca 2+ during Ca 2+ uptake and Na+-induced Ca 2+ release. J Bioenerg Biomembr 45:189–202

39. Yokoi K et al (2022) Induction of paraptosis by cyclometalated iridium complex-peptide hybrids and CGP37157 via a mitochondrial Ca2+ overload triggered by membrane fusion between mitochondria and the endoplasmic reticulum. Biochem 61(8):639–655

40. Cabral-Costa JV et al (2022) Mitochondrial sodium/calcium exchanger NCLX regulates glycolysis in astrocytes, impacting on cognitive performance. J Neurochem 165(4):521–535

41. Boyanova D et al (2012) PlateletWeb: a systems biologic analysis of signaling networks in human platelets Blood. J American Soc Hematol 119(3):e22–e34

Authors and Affiliations

Durre Shehwar[1] · Saima Barki[1] · Alessandro Aliotta[2] · Lucas Veuthey[2] · Debora Bertaggia Calderara[2] · Lorenzo Alberio[2] · Muhammad Rizwan Alam[1]

✉ Muhammad Rizwan Alam
mralam@qau.edu.pk

1   Department of Biochemistry, Quaid-I-Azam University, Islamabad 45320, Pakistan

2   Hemostasis and Platelet Research Laboratory, Division of Hematology and Central Hematology Laboratory, Lausanne University Hospital (CHUV) and University of Lausanne (UNIL), CH-1010 Lausanne, Switzerland